ORNL/CON-80/R1

ornl

OAK
RIDGE
NATIONAL
LABORATORY

UNION
CARBIDE

The Oak Ridge Heat Pump Models: I. A Steady-State Computer Design Model for Air-to-Air Heat Pumps

S. K. Fischer C. K. Rice

OPERATED BY
UNION CARBIDE CORPORATION
FOR THE UNITED STATES
DEPARTMENT OF ENERGY

Printed in the United States of America. Available from
National Technical Information Service
U.S. Department of Commerce
5285 Port Royal Road, Springfield, Virginia 22161
NTIS price codes—Printed Copy: A10 Microfiche A01

ORNL/CON-80/R1

Contract No. W-7405-eng-26

Energy Division

The Oak Ridge Heat Pump Models: I. A Steady-State Computer Design Model for Air-to-Air Heat Pumps

S. K. Fischer
C. K. Rice

DEPARTMENT OF ENERGY

Division of Building Equipment

Date Published: August 1983

OAK RIDGE NATIONAL LABORATORY
Oak Ridge, Tennessee 37830
operated by
UNION CARBIDE CORPORATION
for the
DEPARTMENT OF ENERGY

TABLE OF CONTENTS

LIST OF FIGURES

LIST OF TABLES

The Oak Ridge Heat Pump Models: I. A Steady-State Computer Design Model for Air-to-Air Heat Pumps*

S. K. Fischer
C. K. Rice
Energy Division
Oak Ridge National Laboratory
Oak Ridge, Tennessee 37830

ABSTRACT

The ORNL Heat Pump Design Model† is a FORTRAN-IV computer program to predict the steady-state performance of conventional, vapor compression, electrically-driven, air-to-air heat pumps in both heating and cooling modes. This model is intended to serve as an analytical design tool for use by heat pump manufacturers, consulting engineers, research institutions, and universities in studies directed toward the improvement of heat pump performance. The Heat Pump Design Model allows the user to specify:

- system operating conditions,
- compressor characteristics,
- refrigerant flow control devices,
- fin-and-tube heat exchanger parameters,
- fan and indoor duct characteristics, and
- any of ten refrigerants.

The model will compute:

- system capacity and COP (or EER),
- compressor and fan motor power consumptions,
- coil outlet air dry- and wet-bulb temperatures,
- air- and refrigerant-side pressure drops,
- a summary of the refrigerant-side states throughout the cycle, and
- overall compressor efficiencies and heat exchanger effectiveness.

This report provides thorough documentation of how to use and/or modify the model. This is a revision of an earlier report containing miscellaneous corrections and information on availability and distribution of the model — including an interactive version.

---

*Research sponsored by the Office of Buildings and Community Systems, U.S. Department of Energy under contract W-7405-eng-26 with the Union Carbide Corporation.

†The ORNL Heat Pump Design Model was developed at Oak Ridge National Laboratory.

1. INTRODUCTION AND BACKGROUND

The ORNL Heat Pump Design Model is a Fortran-IV computer program developed to predict the steady-state performance of conventional, vapor compression, electrically-driven, air-to-air heat pumps in both heating and cooling modes. The purpose for the development of this model is to provide an analytical design tool for use by heat pump manufacturers, consulting engineers, research institutions, and universities in studies directed toward the improvement of heat pump efficiency.

The current model has evolved from programs written at ORNL [1,2] and at the Massachusettes Institute of Technology [3] and also makes use of selected routines by Kartsounes and Erth [4], Flower [5], and Kusuda [6]. The MIT model served as the starting point for heat pump modeling at ORNL, where in 1978, the original program was modified and documented in Ref. 1 as a preliminary version of the ORNL Heat Pump Model. An improved version of this code was made available in 1979 with limited, informal documentation. These two versions have been distributed to a number of manufacturing and research institutions.

Our own use of the previous programs [7,8] as well as the experiences of other users indicated the need for additional capabilities in the model. Many of these needs were incorporated between 1979 and 1981. This report is a revision of an earlier version with miscellaneous corrections and additions. The places where corrections or additions have been made are identified by vertical bars in the left margin.

The philosophy of the model development has been to base the program on underlying physical principles and generalized correlations to the greatest extent possible, so as to avoid the limitations of empirical correlations derived from manufacturers' literature. The correlations and algorithms used in the previous releases of the model have been critically reviewed and improved or replaced to include more recent or appropriate correlations and more accurate and efficient algorithms. The model has thus been significantly improved and expanded from the earlier versions from an engineering standpoint. Furthermore, it has been reorganized into a more modular format so that reseachers will be able to readily adapt it to their specific needs.

The ORNL Heat Pump Design Model allows the user to specify:

- System Operating Conditions
  1. the desired indoor and outdoor air temperatures and relative humidities,
  2. the arrangement of the compressor and fans in the air flow stream, i.e., up or downstream of the heat exchangers;
- Compressor Characteristics
  1. either a map-based model for designs with available equipment,
  2. or an efficiency and loss model for advanced reciprocating compressors;
- Refrigerant Flow Control Devices
  1. a capillary tube, thermostatic expansion valve (TXV), or a short-tube orifice, or
  2. a specified value of refrigerant subcooling (or quality) at the condenser exit (in this case the program calculates the equivalent capillary tube, TXV, and short-tube orifice parameters);
- Fin-and-Tube Heat Exchanger Parameters
  1. tube size, spacing, and number of rows, and number of parallel circuits,
  2. fin pitch, thickness, and thermal conductivity; type of fins (smooth, wavy, or louvered),
  3. air flow rates;
- Fan and Indoor Duct Characteristics
  1. overall fan efficiency values for indoor and outdoor fans, or
  2. a specified fan efficiency curve for the outdoor fan,
  3. the diameter of one of six equivalent ducts;
- Refrigerants
  1. either R12, R22, R114, or R502 as a standard option,
  2. one of six additional refrigerants (R11, R13, R21, R23, R113, and C318) by adding the appropriate thermodynamic constants given by Downing [9];

- Refrigerant Lines
  1. lengths and diameters of interconnecting pipes,
  2. pipe specifications independent of heating or cooling mode,
  3. heat losses from suction, discharge, and liquid lines.

The user cannot specify the system refrigerant charge; instead, it is implicity assumed that the system is charged with the proper amount of refrigerant for the specified operating conditions. This is a satisfactory model for heat pump systems having a suction line accumulator (charge-insensitive systems) which can store excess refrigerant and maintain a low level of evaporator superheat.

For charge-sensitive systems, the performance with a given refrigerant charge over a range of ambient temperatures cannot be accurately modeled unless the level of evaporator superheat at each ambient temperature is known. For such systems, however, single design point studies can still be made.

The input and output of the program are in English units. (The model has evolved from computer codes that were based on the British system of measurement and it would have been a major effort to convert them to SI units). The specific units used for each input and output parameter are given in Appendices A and B. Four output options allow the user to control the amount of printed output. The basic program output includes (as appropriate):

- Capacity and COP
- Compressor and fan motor power consumption
- Sensible to total heat transfer ratio
- Outlet dry- and wet-bulb temperatures
- Air- and refrigerant-side pressure drops
- Overall isentropic and volumetric compressor efficiencies
- Heat exchanger effectiveness and UA values
- Equivalent capillary tube, TXV, and short-tube orifice parameters
- Summary of the refrigerant-side states throughout the cycle

Other levels of program output are discussed in Section 3.2 and Appendix A.

This second generation heat pump model contains significant changes from its predecessors and many additional capabilities. This report is intended:

- to serve as a rigorous documentation (where appropriate) of the assumptions, correlations, and algorithms that are used by the program,
- to provide a complete list of references from which data and equations were obtained, and
- to serve as a user's manual for those who will use the code intact and to aid those who will need to add new capabilities.

A basic understanding of vapor-compression air-to-air heat pumps has been presumed for this report.

2. UTILIZATION

The physical specification of the heat pump and the indoor and outdoor operating conditions are read from a single data file, as described in Appendix A; tape drives and other peripherals are not required. The program requires 56 K words of memory and typically executes in less than 5 seconds on the IBM 3033 computer at ORNL. A complete listing of the program is provided in Appendix K.

Although the Heat Pump Design Model is generally run as a stand-alone program, it has been used in conjunction with other computer software. An earlier version of the model has been used at ORNL with numerical analysis and graphical display programs in heat pump design optimization and parametric studies [7,8].

3. CALCULATIONAL PROCEDURE AND ORGANIZATION

3.1 Modeling Procedure for the Vapor Compression Cycle

The heat pump model is organized functionally into two major sections. The first section combines the compressor, condenser, and flow control device routines into an interrelated high-side unit. The second section, the low-side unit, contains the evaporator model. Calculations proceed iteratively between these two sections until the desired overall balance is obtained. The calculational scheme is independent of whether the unit is operating in the heating or cooling mode.

Figure 3.1 represents the basic vapor compression cycle, shown on an exaggerated pressure-enthalpy diagram, that is modeled by the program. The user is required to specify:

- the level of evaporator exit superheat (or quality),
- design parameters for a flow-control device or the level of condenser exit subcooling (or quality),
- condenser and evaporator inlet air temperatures,
- dimensions of components and interconnecting pipes, and
- heat losses from interconnecting pipes.

The user must also provide estimates for:

- the refrigerant saturation temperature at the evaporator exit,
- the refrigerant saturation temperature at the condenser inlet, and
- the refrigerant mass flow rate.

These three estimates are used as starting points for iterations. The final results of the model do not depend on how well or how poorly these values are chosen; however, better guesses will yield shorter running times.

High-Side Computations

The computations for the high-side system balance begin with the refrigerant state at the exit of the evaporator (point a in Fig. 3.1), which is defined by the specified superheat and the estimate of the

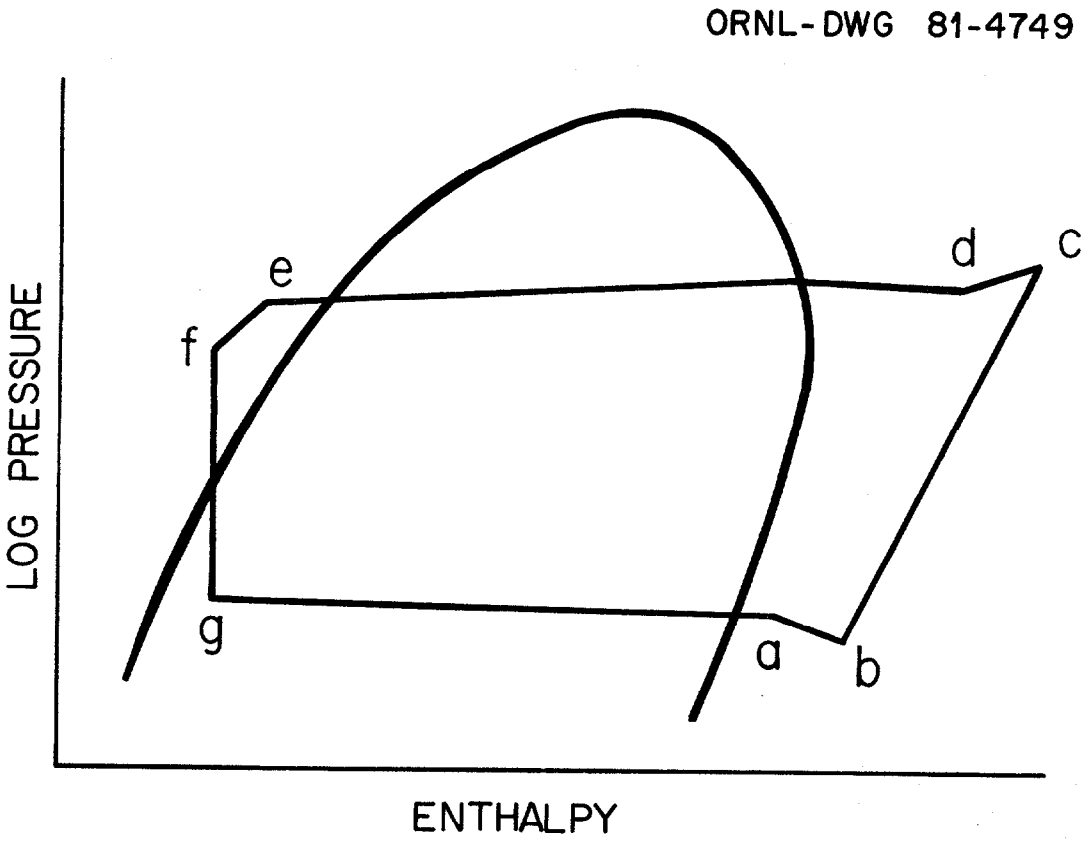

a EVAPORATOR EXIT
b COMPRESSOR SHELL INLET
c COMPRESSOR SHELL OUTLET
d CONDENSER INLET
e CONDENSER OUTLET
f INLET TO EXPANSION DEVICE
g EVAPORATOR INLET

Fig. 3.1 Pressure vs. Enthalpy Diagram for the Heat Pump Cycle

saturation temperature. This point remains fixed for one iteration of the compressor, condenser, expansion device, and evaporator calculations. The compressor model uses state point a along with:

- the estimates of the refrigerant mass flow rate and saturation temperature at the condenser inlet, and
- the specification of the dimensions and heat losses for the suction and discharge lines

to calculate the state at the shell inlet, b, shell outlet, c, and the condenser inlet, d, as well as a new estimate of the mass flow rate.

Fixed Condenser Subcooling

The remainder of the high-side calculations depend on whether a flow control device has been chosen or if a desired value of condenser exit subcooling (or quality) has been specified. The latter case is described first since it is simpler. The condenser submodel uses:

- the physical description of the heat exchanger,
- the calculated refrigerant mass flow rate,
- the condenser inlet air temperature and relative humidity, and
- the refrigerant state at the condenser inlet, point d,

to evaluate the refrigerant state at the condenser outlet, e. The level of condenser subcooling is computed from knowledge of state e, and compared to the specified value. If the two values do not agree within a fixed tolerance (see Appendix C), the saturation temperature at point d, is changed (in effect specifying a new condenser entrance pressure), and the compressor and condenser calculations are repeated.

Each time the condenser saturation temperature is changed, the compressor model calculates a new refrigerant mass flow rate and new states b, c, and d and the condenser model updates state e. Once the desired condenser subcooling is achieved, the state at the flow control device, f, is computed using:

- the state at the condenser exit, e,
- the dimensions and heat loss for the liquid line, and
- the most recent calculation of the refrigerant mass flow rate.

Refrigerant state f and the mass flow rate are then used to calculate the equivalent capillary tube, TXV, and short-tube orifice parameters that would produce the specified subcooling.

Specified Flow Control Device

When condenser subcooling is specified, the system acts as if it has a flow control device with an infinitely variable opening, that is, the high-side system pressure is completely determined by the balance between the heat rejection capability of the condenser (constrained by the exit subcooling), and the refrigerant pumping capability of the compressor. When a flow control device is specified, the high-side pressure is controlled by the pressure drop characteristics of the expansion device, so the flow control model must be coupled with the compressor and condenser routines to achieve the proper high-side balance. This balance must be found iteratively since the mass flow rate characteristic of the flow-control device is dependent on the refrigerant state at the entrance to flow control device which, in turn, is found from the condenser model using the refrigerant mass flow rate obtained from the compressor model.

The calculations to achieve a high-side balance with a specified flow control device are similar to the case where condenser subcooling is fixed. The states at the compressor shell outlet and condenser inlet and outlet, states c, d, and e, are computed for the estimate of the saturation temperature at the condenser inlet. Since the condenser subcooling has not been specified, the calculations proceed to the flow control device entrance where state f is evaluated using:

- the state at the condenser exit, e,
- liquid line dimensions and heat loss, and
- the computed compressor mass flow rate.

The refrigerant mass flow rate which the flow control device will pass based on its entrance conditions is calculated using state f and, in the case of a thermostatic expansion valve or short-tube orifice, the low-side pressure at the evaporator entrance, point g. If the latter is required, the pressure at point g is initially assumed to be equal

to that at point a (i.e., no pressure drop in the evaporator), and then later calculations in the evaporator model are used to improve the estimate. If the refrigerant mass flow rates of the compressor and flow control device do not agree within a specified tolerance the compressor, condenser, and expansion device calculations are repeated with a new estimate of the saturation temperature at the condenser entrance. Once the two mass flow rates are in agreement, a high-side balance has been obtained. One cycle analysis can now be completed by computing the evaporator performance.

Low-Side Computations

The evaporator, or low-side, computations are based on:

- the refrigerant condition at the evaporator exit, state a,
- the refrigerant enthalpy at the evaporator inlet, point g, and
- the refrigerant mass flow rate.

These values have all been computed based on the estimated saturation temperature and specified superheat (or quality) at the evaporator exit. The saturation pressure at the evaporator inlet, point g, and the inlet air temperature which would yield the specified superheat at the assumed exit saturation temperature are still unknown. The evaporator model is executed iteratively, varying the inlet air temperature from one execution to the next, to calculate a value of superheat at the evaporator exit and a pressure drop across the heat exchanger (and hence a saturation pressure at the inlet since the exit conditions are fixed).

A system solution has been completed for some evaporator inlet air temperature, though not necessarily the desired one, when the calculated exit superheat agrees with the specified value within a given tolerance. (The high- and low-side loops are repeated once if a thermostatic expansion valve or a short-tube orifice is specified as the flow control device to ensure that an accurate evaporator inlet pressure is used during the high-side calculations.) The system solution is found for the desired evaporator inlet air temperature by changing the saturation temperature at the evaporator exit, point a,

and repeating the entire calculational process. This iteration on state point a continues until the computed inlet air temperature agrees with the desired value within a specified tolerance. The sequence of calculations is summarized in Fig. 3.2. The evaporator inlet air temperature is nearly a linear function of the exit refrigerant saturation temperature so that usually only one or two iterations over the outermost loop in Fig. 3.2 are required.

3.2 Organization of the Computer Program

Just as the calculations shown in Fig. 3.2 are divided into distinct sections, subroutines to perform these computations are divided into distinct modules. The calculation of the system high-side balance, for example, requires computing the performance of the compressor, condenser, and (optionally) the flow control device and then balancing the output of these components and the interconnecting pipes with each other. This is accomplished in the heat pump model using individual subroutines, one for each task:

- modeling the compressor
- modeling the condenser
- modeling the flow control device
- iterating on condenser saturation temperature

In addition each of these subroutines calls other *service* routines to perform inner iterations and calculate thermodynamic and thermophysical properties, pressure drops, and heat transfer coefficients, etc. (Appendix F contains a cross-reference of all subroutines called from each subroutine.)

The advantages to this program structure are that:

- separate and identifiable tasks are performed by each subroutine,
- modules can be easily modified to make improvements, replaced to use models for a different component type, or added to increase system analysis capability
- familiarization with the code can be done at different levels, depending upon the needs of a specific user.

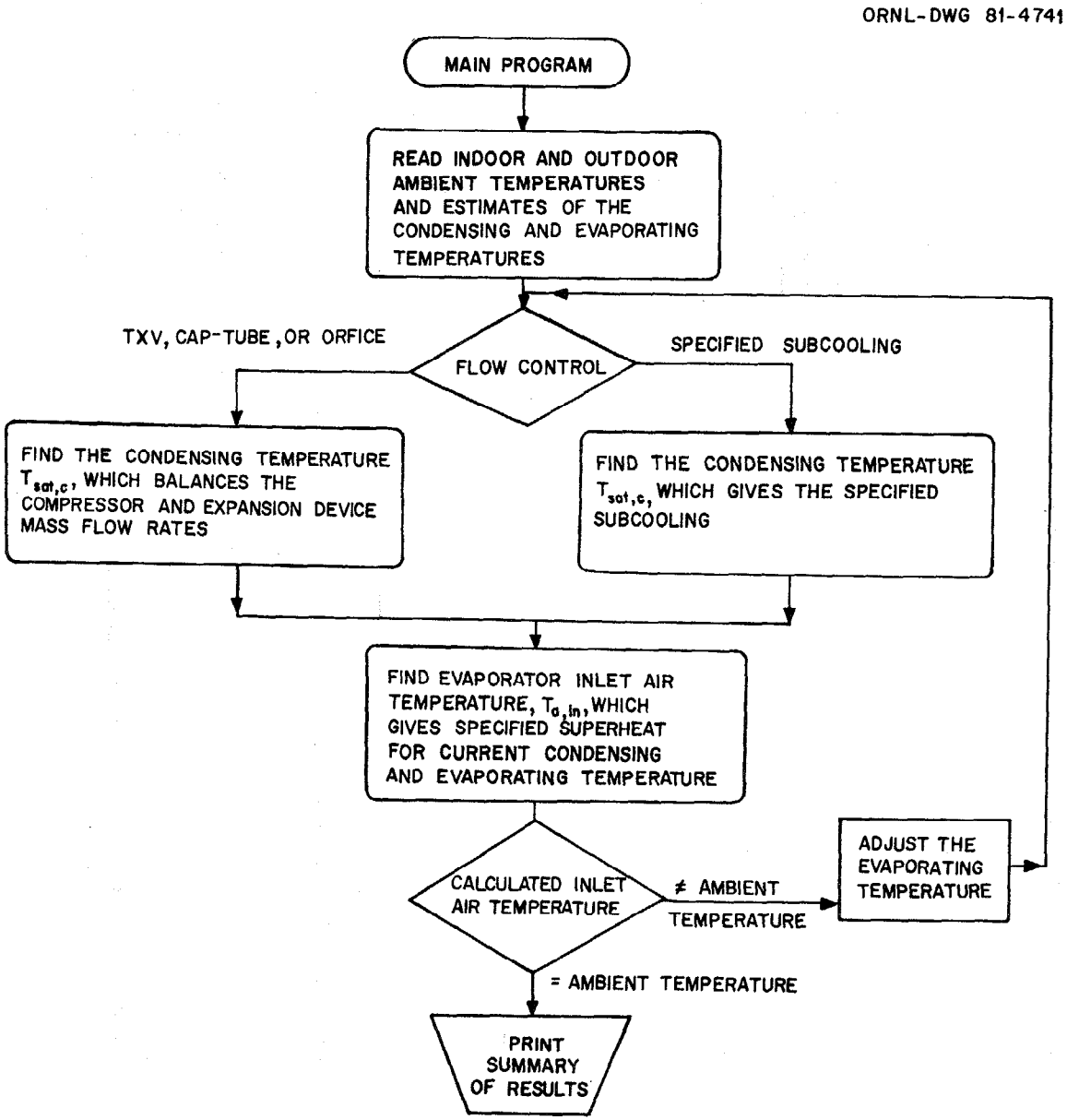

Fig. 3.2 Block Diagram of Iterative Loops in the Main Program

One consequence of this modular approach, however, is that a single large program becomes many short subprograms with a large number of variables passed between them through common blocks. Appendices D and E are included as aides to identify variables used in common blocks and to identify which common blocks are used to pass data between which subroutines.

3.3 Input and Output Description

As part of the modularization of the program, almost all of the data input and output are done by two subroutines. Appendix A contains definitions of the input data and Appendix B contains sample input and output. There are, however, other constants used by the model which are not read as input data, and there are other levels of printed output than that shown in Appendix B.

Parameters and physical constants (e.g., tolerance parameters, refrigerant number, atmospheric pressure) which are unlikely to be changed frequently from one use of the program to another are assigned values in a single subroutine (BLOCK DATA) in order to reduce the amount of data that the user must specify for each run. These parameters are described in Appendix C so that the user can change them as necessary.

The printed output shown in Appendix B is a system summary and contains results computed after the outermost loop in Fig. 3.2 has converged. The program has three other output options, as defined in Appendix A. The first option limits the output to only one page of computed results which gives the COP and capacity of the heat pump and a brief energy summary. The other two options are for diagnostic purposes in cases where an iterative loop fails to converge or for use in checking out the proper operation of the program after changes have been made. Intermediate results in the computations are printed out with either of these two options. An input variable, as defined in Appendix A, is used to specify whether to print the abbreviated output, the standard output summary as in Appendix B, a summary after completion of each major iteration in Fig. 3.2, or continuous output throughout the entire sequence of computations. Further, the output statements

in most of the subroutines are arranged so that detailed, diagnostic output from a particular subroutine can be obtained by removing one or two print control statements in that routine.

4. COMPRESSOR MODELS

4.1 Introduction

Since the compressor is the heart of a heat pump system and the primary user of electrical power, accurate compressor modeling is important to good system performance prediction. This criterion, however, must be tempered by consideration of the type of information available to most potential users of the program and of the different types of heat pump studies in which the program may be used. For these reasons the ORNL Heat Pump Design Model does not incorporate a subroutine which rigorously models compressor performance using detailed hardware design parameters. Instead, users can choose between two simpler models depending upon their specific needs.

The first compressor model is based on the use of compressor manufacturers' data (compressor maps) for a specific compressor or compressor type; the model has built-in corrections to adjust for levels of refrigerant superheat in reciprocating compressors which are different from those for which the maps were generated. Although this model was written for reciprocating compressors, it should be easy to modify for use with rotary, screw, or centrifugal compressors. Accurate simulation of existing compressors is possible with this model.

The second model, a loss and efficiency-based compressor model, is intended for use in heat pump design studies, e.g., to predict how changes in compressor loss and efficiency terms affect system performance. It can also be used to model compressor performance with a new refrigerant. This more general routine models the internal energy balances in a reciprocating compressor using user-supplied heat loss and internal efficiency values. This model cannot predict compressor performance as accurately over the same range of operating conditions as the map-based model without local adjustment of some of the input efficiency and loss values. It is well suited, however, for studying internal compressor improvements and interactions and their effect on system performance about a particular design point.

4.2 General Calculational Scheme

Both compressor models have a number of calculations in common and interact with the rest of the system model in the same way. The general calculational scheme is discussed first, followed by descriptions of those sections of the two routines which are different.

Both models are functionally dependent on the refrigerant saturation temperature at the condenser entrance and the evaporator exit and on the refrigerant superheat at the evaporator exit. Figure 4.1 shows the sequence of calculations for either method of compressor simulation. The current estimates of the condenser inlet and evaporator outlet refrigerant saturation temperatures are used to calculate the corresponding refrigerant pressures at the evaporator exit and the condenser entrance. The refrigerant state at the evaporator exit is identified using the specified degree of evaporator superheat or quality and the calculated evaporator exit pressure (from the estimated refrigerant saturation temperature), from which the refrigerant temperature, enthalpy, entropy, and specific volume are computed.

The pressure drops in the suction and discharge lines are computed as described in Section 8 using the current estimates for the refrigerant mass flow rate and average refrigerant temperatures in the lines. The refrigerant state at the compressor shell inlet is then identified using the calculated suction line pressure drop and the specified (input) value of heat gain in the suction line.

From this point, each of the compressor models use different procedures to calculate:

- the refrigerant mass flow rate,
- the compressor motor input power,
- the compressor shell heat loss (optional), and
- the refrigerant state at the compressor shell exit.

Finally the refrigerant state at condenser entrance is computed using the previously calculated discharge line pressure drop and the specified (input) value of discharge line heat loss.

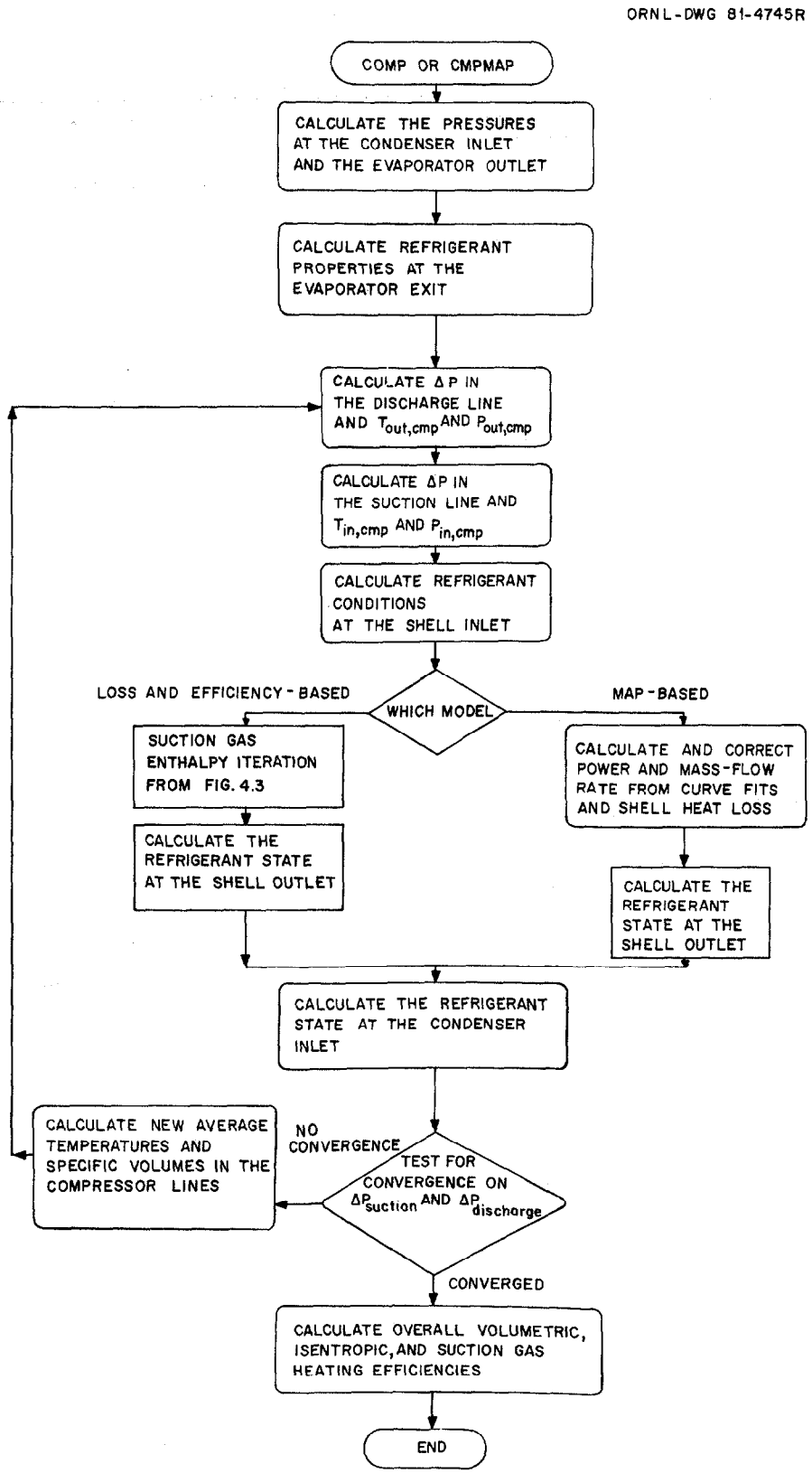

Fig. 4.1 Computational Sequence in the Compressor Models

Upon completion of these calculations, new average temperatures and specific volumes in the suction and discharge lines are computed. These are used with the latest calculation of the refrigerant mass flow rate to recalculate the suction and discharge line pressure drops. The entire process is repeated, as shown in Fig. 4.1, until the pressure drops agree within tolerances from one iteration to the next.

After completion of the pressure drop iteration, compressor efficiency indices are computed. In both compressor models, two basic efficiency indices are calculated — the overall isentropic compression efficiency and the overall volumetric efficiency. The term "overall" is used to refer to a value based on compressor shell inlet and (when appropriate) shell outlet conditions.

The overall isentropic compression efficiency, η_{cm} is given by the equation

$$\eta_{cm} = \frac{\dot{W}_{cm,ideal}}{\dot{W}_{cm,actual}} = \frac{\dot{m}_{r,actual}\,(h_{outlet,isen} - h_{inlet})}{\dot{W}_{cm,actual}} \qquad (4.1)$$

where $\dot{W}_{cm}$ and $\dot{m}_r$ represent compressor *motor* power and refrigerant mass flow rate and h represents specific enthalpy. The term $h_{outlet,isen}$ represents the outlet specific enthalpy that would be obtained from an (ideal) isentropic compression process based on the refrigerant entropy at compressor shell inlet and the refrigerant pressure at shell outlet. Thus η_{cm} represents the ratio of the minimum power required (to compress a given refrigerant mass per unit time) to the actual required power. It should be emphasized that the actual refrigerant enthalpy at shell outlet, h_{outlet}, is not used in Eq. 4.1; were this the case, any completely insulated compressor would have an η_{cm} value of 1.0.

The overall volumetric efficiency, η_{vol}, is given by

$$\eta_{vol} = \frac{\dot{m}_{r,actual}}{\dot{m}_{r,ideal}} = \frac{\dot{m}_{r,actual}\,v_{inlet}}{DS} \qquad (4.2)$$

where v_{inlet} is the refrigerant specific volume at compressor shell inlet, D is the total compressor displacement, and S is either the rated compressor motor speed for the map-based model (e.g., 3450 or 3500 rpm) or the actual motor speed for the loss and efficiency model.

These two efficiency indices, η_{cm} and η_{vol} should not be confused with similarly defined internal compressor efficiencies for the loss and efficiency compressor model based on suction and discharge port conditions as discussed in Section 4.4.

The next two sections describe the differences between the two compressor models — differences in input requirements, calculational methods, and resulting output.

4.3 Map-Based Compressor Model

The map-based compressor model uses empirical performance curves for reciprocating compressors obtained from compressor calorimeter measurements performed by the manufacturers. These performance curves provide compressor motor power input, refrigerant mass flow rate and/or refrigerating capacity as functions of "evaporator" saturation temperature (i.e., at compressor shell inlet) for four to six "condenser" saturation temperatures (i.e., at the compressor shell outlet).

Usually each performance map is generated for fixed values of condenser exit subcooling and compressor inlet superheat. For some maps, however, the superheat is allowed to vary with changes in "evaporator" saturation temperature while the suction gas temperature at compressor shell inlet is held constant. Given the condenser exit subcooling and compressor inlet superheat or fixed suction gas temperature, refrigerant mass flow rate values can be derived from refrigerating capacity data. A routine for performing these calculations is given in Appendix N.

The map-based routine uses curve fits to the compressor motor power input (kW) and the refrigerant mass flow rate (lbm/h) as functions of compressor shell inlet and outlet saturation temperatures to model the published performance data. The user must provide sets of coefficients; C_1, C_2, ..., for bi-quadratic functions of the form given by Eq. 4.3

for the power input and mass flow rate as functions of the inlet and outlet saturation temperatures.

$$f(T_{outlet}, T_{inlet}) = C_1 T_{outlet}^2 + C_2 T_{outlet} + C_3 T_{inlet}^2 + C_4 T_{inlet} + C_5 T_{outlet} T_{inlet} + C_6 \qquad (4.3)$$

A short computer program which uses a least squares algorithm to compute these coefficients is listed in Appendix N. Except as noted below, these coefficients will apply for only one particular compressor.

The user must also specify the total *actual* compressor displacement, the rated compressor motor speed, and the fixed refrigerant superheat or temperature at the compressor shell inlet (upon which the map is based) for the compressor which is being modeled. The *desired* compressor displacement is also an input parameter; this value is used by the map-based model to scale the compressor performance curves linearly to represent a compressor with the same general performance characteristics as the original compressor but of a different capacity.

As noted earlier, the compressor maps and the biquadiatic fits to them are strictly applicable only for the superheat level or suction gas temperature for which they were generated. The map-based model applies correction factors to the empirical curve fits to model the compressor at actual operating conditions.

Dabiri and Rice [10] presented a technique for correcting the compressor motor power input, $\dot{W}_{cm,map}$, and the refrigerant mass flow rate, $\dot{m}_{r,map}$ for values of superheat or suction gas temperature other than those for which the maps were generated. Equations 4.4 and 4.5 give their correction factors to account for non-standard superheat values,

$$\dot{m}_{r,actual} = [1 + F_v(\frac{\nu_{map}}{\nu_{actual}} - 1)]\, \dot{m}_{r,map} \qquad (4.4)$$

and

$$\dot{W}_{cm,actual} = \left(\frac{\dot{m}_{r,actual}}{\dot{m}_{r,map}}\right)\left(\frac{\Delta h_{isen,actual}}{\Delta h_{isen,map}}\right)\dot{W}_{cm,map} \qquad (4.5)$$

where ν and Δh represent specific volume and enthalpy change, respectively, of the refrigerant based on *estimated suction port conditions*. The subscripts "actual", "map", and "isen" represent actual superheat conditions, map superheat conditions, and an isentropic process from *estimated suction port conditions* to compressor shell outlet pressure, respectively, and F_v is a volumetric efficiency correction factor (assigned a value of 0.75 in the Block Data subroutine, see Appendix C).

Dabiri and Rice *estimated the suction port conditions* from the shell inlet conditions using the assumption of a constant enthalpy gain to the suction gas between compressor shell inlet and suction port, $\Delta h_{inlet,suction\ port}$, of 21 kJ/kg (9 Btu/lbm), due to motor and compressor cooling by the suction gas [10]. This assumption has been improved upon in our map-based model by assuming instead that

$$\Delta h_{inlet,suction\ port} = F_{sh}\frac{\dot{W}_{cm,map}}{\dot{m}_{r,map}} \qquad (4.6)$$

where F_{sh} is an appropriate suction gas heating factor. F_{sh} is assigned a value of 0.33 in the Block Data subroutine (see Appendix C). Use of Eq. 4.6 assumes that the *suction gas temperature change* (from shell inlet to suction port) will increase at lower evaporating saturation temperatures and higher condensing saturation temperatures as the compressor work input per unit mass flow rate increases. Such a trend has been observed in typical reciprocating compressors [11].

Once the corrections for actual superheat level have been applied to the values of $\dot{W}_{cm,map}$ and $\dot{m}_{r,map}$, the enthalpy at the compressor shell outlet, h_{outlet}, is computed from Eq. 4.7

$$h_{outlet} = (\dot{W}_{cm,actual} - \dot{Q}_{can})/\dot{m}_{r,actual} + h_{inlet} \qquad (4.7)$$

where $\dot{Q}_{can}$ is the heat loss rate from the compressor shell. $\dot{Q}_{can}$ is specified by the user as either a fixed input value or as a specified fraction of actual compressor power, $\dot{W}_{cm,actual}$. (Values of $\dot{Q}_{can}$ are not usually provided by the compressor manufacturers.)

The state at the compressor exit has been identified at this point in the calculations and all the relevant thermodynamic properties at the shell exit and condenser entrance are computed next. The calculations then proceed to the outer pressure drop convergence loop as described in Section 4.2.

4.4 Loss and Efficiency-Based Compressor Model

The loss and efficiency-based compressor routine models the internal energy balances in a reciprocating compressor from user-supplied design, internal efficiency, and heat-loss values. A conceptual representation of the loss and efficiency-based compressor model is shown in Fig. 4-2. The user is required to specify the following values:

- D - total compressor displacement,
- C - actual clearance volume ratio,
- S_{input} - synchronous or actual compressor motor speed (as appropriate),
- $\dot{W}_{s,fl}$ - compressor motor full load shaft power (optional),
- $\eta_{mot,max}$ - maximum compressor motor efficiency,
- η_{mech} - compressor mechanical efficiency, and
- η_{isen} - isentropic compression efficiency from suction to discharge port.

The *internal* heat loss from the compressor discharge tube to the low-side refrigerant gas, $\dot{Q}_{hilo}$, and the compressor shell heat loss, $\dot{Q}_{can}$, are also specified by the user according to the choices in Eqs. 4.8 and 4.9.

$$\dot{Q}_{hilo} = \begin{cases} \text{specified directly,} \\ \alpha_{hilo}\,\dot{W}_{cm,actual}, \text{ or} \\ 0.03\,\dot{W}_{cm,actual} \end{cases} \qquad \text{(see Appendix A)} \qquad (4.8)$$

ORNL-DWG 77-19443R

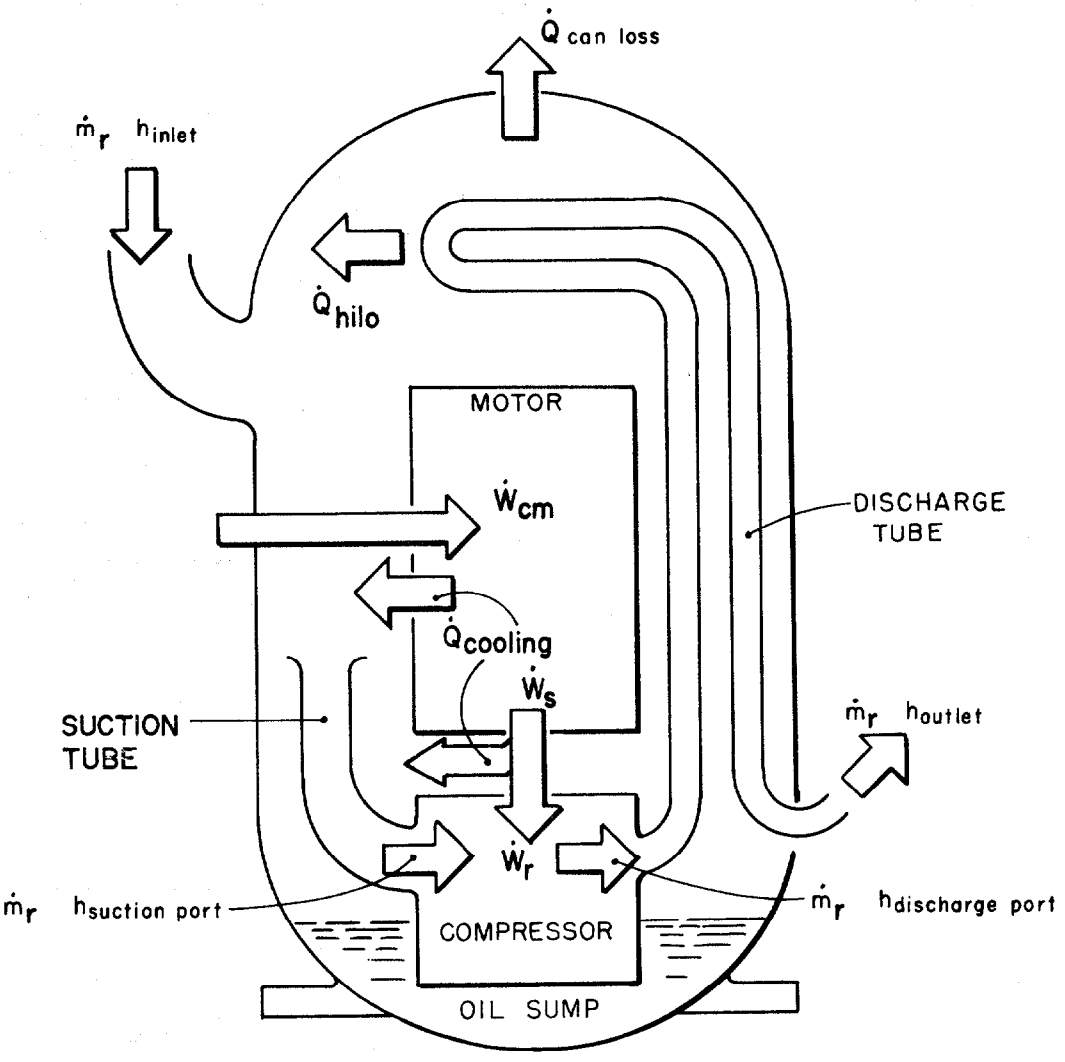

Fig. 4.2 Components of Compressor Energy Balance

$$\dot{Q}_{can} = \begin{cases} \text{specified directly,} \\ \alpha_{can}\, \dot{W}_{cm,actual}, \text{ or} \\ 0.9\ (1.0 - \eta_{motor}\, \eta_{mech})\ \dot{W}_{cm,actual} \end{cases} \qquad \text{(see Appendix A)} \qquad (4.9)$$

The explicit losses, $\dot{Q}$, or fractions, α, are part of the input data to the program as described in Appendix A.

The unknowns which need to be calculated are:

$\dot{m}_r$	refrigerant mass flow rate
$h_{suction\ port}$	enthalpy at the suction port
$h_{discharge\ port}$	enthalpy at the discharge port
h_{outlet}	enthalpy at the shell outlet
$\dot{W}_r$	work done on the refrigerant
$\dot{W}_s$	work done on the shaft
$\dot{W}_{cm}$	work input to the compressor
$\dot{Q}_{cooling}$	rate of heat loss due to cooling of compressor and motor

and if they are not specified explicitly, the:

$\dot{Q}_{can}$	rate of compressor shell heat loss, and
$\dot{Q}_{hilo}$	rate of heat transfer from the discharge gas to the suction gas

These *ten unknowns* are calculated from the *three energy balance equations* in Eqs. 4.10 – 4.12,

$$\dot{m}_r\ (h_{suction\ port} - h_{inlet}) = \dot{Q}_{hilo} + \dot{Q}_{cooling} - \dot{Q}_{can}\ , \qquad (4.10)$$

$$\dot{m}_r\ (h_{discharge\ port} - h_{suction\ port}) = \dot{W}_r\ , \qquad (4.11)$$

and

$$\dot{m}_r \, (h_{\text{outlet}} - h_{\text{discharge port}}) = -\dot{Q}_{\text{hilo}} \quad , \tag{4.12}$$

and the *seven defining equations* given in Eqs. 4.8 and 4.9 and Eqs. 4.13 through 4.17.

$$\dot{W}_r = \dot{m}_r \, (h_{\text{isen,discharge port}} - h_{\text{suction port}})/(3413 \, \eta_{\text{isen}}) \quad , \tag{4.13}$$

$$\dot{W}_s = \dot{W}_r/\eta_{\text{mech}} \quad , \tag{4.14}$$

$$\dot{W}_{cm} = \dot{W}_s/\eta_{\text{motor}} \quad , \tag{4.15}$$

$$\dot{Q}_{\text{cooling}} = (1 - \eta_{\text{mech}} \eta_{\text{motor}}) W_{cm} \quad , \tag{4.16}$$

and

$$\dot{m}_r = \eta_{\text{vol,suction port}} \, S_{\text{oper}} \, D/v_{\text{suction port}} \tag{4.17}$$

The combination of Eqs. 4.10 – 4.16 yields Eq. 4.18 for the overall compressor energy balance,

$$\dot{W}_{cm} = [\dot{m}_r(h_{\text{outlet}} - h_{\text{inlet}}) + \dot{Q}_{\text{can}}]/3413 \tag{4.18}$$

which is identical to Eq. 4.7, the corresponding expression for the map-based model. Equations 4.8 – 4.15 form a non-linear (through the refrigerant properties), coupled set of equations where $\dot{W}_r$ and $\dot{m}_r$ are dependent on $h_{\text{suction port}}$. The enthalpy at the suction port is

dependent on $\dot{m}_r$ and on the heat losses, $\dot{Q}_{cooling}$, $\dot{Q}_{hilo}$, and $\dot{Q}_{can}$, all of which can be dependent of $\dot{W}_r$.

The iterative calculational scheme used to solve this system of equations is shown in Fig. 4.3. In order to begin the calculations, $h_{suction\ port}$ is assumed to be equal to h_{inlet}. Thereafter $h_{suction\ port}$ is calculated from the rearranged form of Eq. 4.10, given by Eq. 4.19.

$$h_{suction\ port} = h_{inlet} + (\dot{Q}_{hilo} + \dot{Q}_{cooling} - \dot{Q}_{can})/\dot{m}_r \qquad (4.19)$$

The refrigerant conditions at the suction port are computed using the values of $h_{suction\ port}$ and the refrigerant pressure at the shell inlet. Next, the refrigerant enthalpy at the discharge port is computed using Eq. 4.20 (which combines Eq. 4.11 and 4.13),

$$h_{discharge\ port} = h_{suction\ port} + \frac{h_{isen,discharge\ port} - h_{suction\ port}}{\eta_{isen}} \qquad (4.20)$$

where $h_{isen,discharge\ port}$ is the enthalpy after an isentropic compression from the suction port conditions to discharge port pressure (assumed equal to the shell outlet pressure).

Equation 4.20 contains the assumption that all the inefficiencies in the compression process result in additional enthalpy gain for the refrigerant gas. This is, of course, not theoretically correct since the actual compression process is nonadiabatic (and is more properly modeled as sequence of polytropic processes). There is heat transfer from the compressor body to the refrigerant gas inside the compressor shell. This extra heat loss is handled in a manner similar to that of Davis and Scott [12], through an artifical increase in the mechanical efficiency term in Eq. 4.16 above that which might be expected due to frictional sources.

Once $h_{discharge\ port}$ has been calculated, the remaining refrigerant conditions at the discharge port are computed assuming the refrigerant pressure at the discharge port is equal to that at the shell outlet.

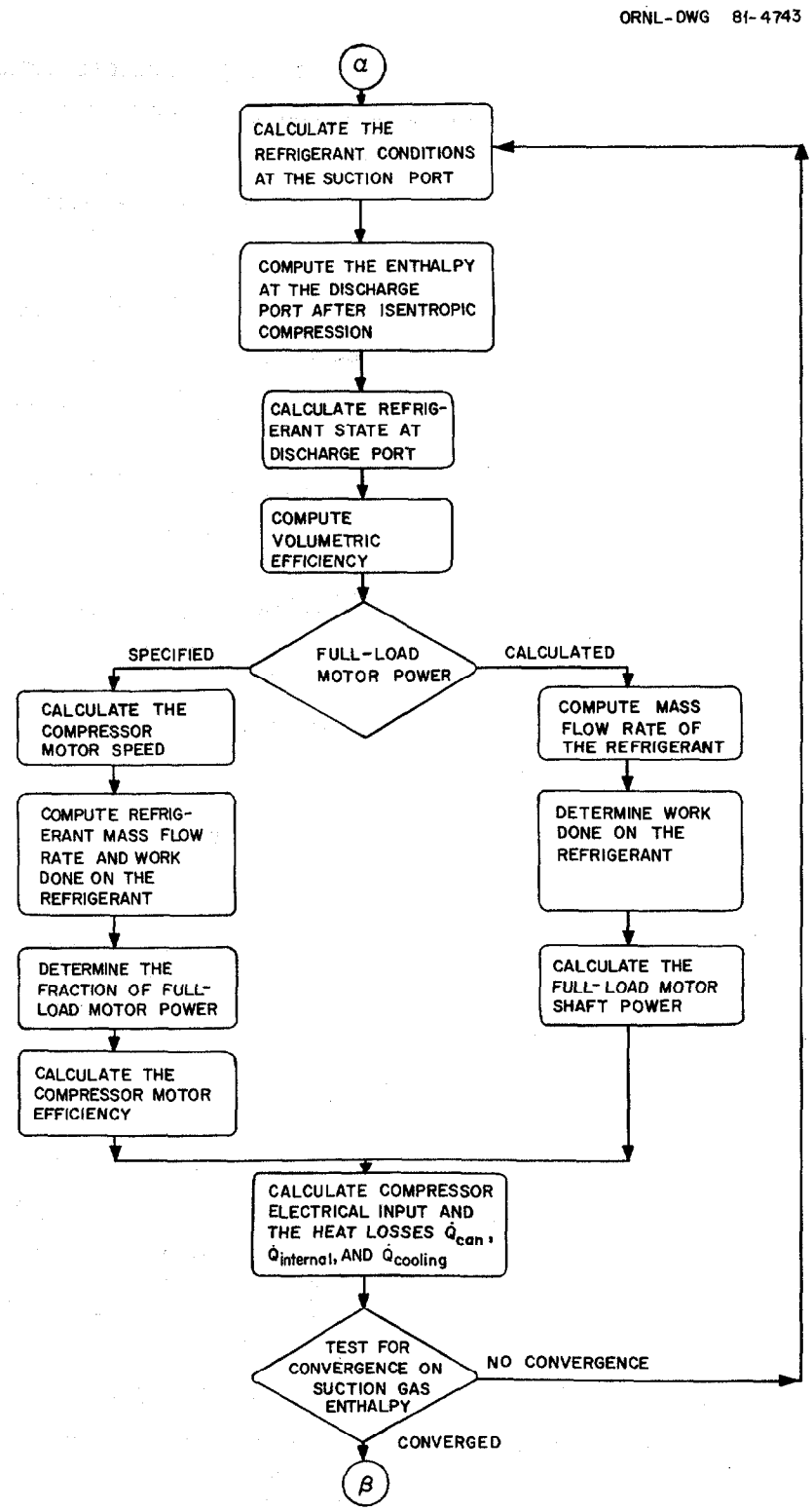

Fig. 4.3 Iteration on Internal Energy Balance for the Loss and Efficiency-Based Compressor Model

The volumetric efficiency based on suction port conditions is computed from Eq. 4.21 given by Davis and Scott [12].

$$\eta_{vol,\text{suction port,actual}} = \eta_{vol,\text{suction port,theoretical}} - a\left(\frac{\gamma-1}{\gamma}\frac{P_{\text{discharge port}}}{P_{\text{suction port}}}\right) - b \qquad (4.21)$$

where

$$\eta_{vol,\text{suction port,theoretical}} = 1 - C\left[\left(\frac{P_{\text{discharge port}}}{P_{\text{suction port}}}\right)^{1/\gamma} - 1\right] \qquad (4.22)$$

$P_{\text{discharge port}}$ - refrigerant pressure at discharge port

$P_{\text{suction port}}$ - refrigerant pressure at suction port

γ - specific heat ratio for the specific refrigerant evaluated at suction port conditions

C - actual clearance volume ratio,

and "a" and "b" are empirical constants derived from test data for compressors of different capacities but of the same series (defined in Block Data). Davis and Scott [12] note that their equation should be valid for "basically similar units which differ only in stroke or clearance volume."

Once the volumetric efficiency has been evaluated, a decision point is reached in Fig. 4.3. If the compressor-motor full load shaft power, $\dot{W}_{s,fl}$, has not been specified as input data, the input values of compressor motor speed and efficiency are taken to be the *actual operating* values, i.e., $S_{oper} = S_{input}$ and $\eta_{motor} = \eta_{motor,max}$, respectively. The refrigerant mass flow rate, $\dot{m}_r$, the work input to the refrigerant, $\dot{W}_r$, and the required full load motor power, $\dot{W}_{s,fl}$ are then computed from Eqs. 4.17, 4.13, and 4.14, respectively. The computed value for $\dot{W}_{s,fl}$ is the rated (full) load that must be imposed on the compressor motor to achieve the assumed maximum rated motor efficiency.

Alternatively, if $\dot{W}_{s,f1}$ is specified as input data, the motor speed, S_{oper}, and efficiency, η_{mot}, are computed as built-in functions of fractional rated (full) load, f_{f1}, as defined in Eq. 4.23.

$$f_{f1} = \dot{W}_r/(\eta_{mech}\ \dot{W}_{s,f1}) \tag{4.23}$$

The operating motor speed, S_{oper}, is assumed to be a linear function of f_{f1}, i.e.,

$$S_{oper} = (1.0 + a_{f1}\ f_{f1})\ S_{sync} \tag{4.24}$$

where S_{sync} is the synchronous motor speed (e.g. 3600 or 1800 rpm) as specified in the input data, i.e., $S_{sync} = S_{input}$.

The value of a_{f1} is determined by solving Eq. 4.24 under full-load conditions ($f_{f1} = 1.0$) using known values of synchronous and full-load motor speeds (i.e., $a_{f1} = \frac{S_{f1} - S_{sync}}{S_{sync}}$).

Since S_{oper} is a function of $\dot{m}_r$ (through Eqs. 4.24, 4.23, and 4.13), and since $\dot{m}_r$ is dependent on S_{oper} (from Eq. 4.17), Eq. 4.24 is not directly solvable for S_{oper}. However, Eqs. 4.23 and 4.24 can be used with Eqs. 4.13 and 4.17 to solve for S_{oper} algebraically. This results in Eq. 4.25,

$$S_{oper} = \frac{1.0}{\frac{1}{S_{sync}} - a_{f1}\left(\frac{\dot{m}_r}{S_{oper}}\right)\left(\frac{\dot{W}_r}{\dot{m}_r}\right)\left(\frac{f_{f1}}{\dot{W}_r}\right)} \tag{4.25}$$

where

$$\left(\frac{\dot{m}_r}{S_{oper}}\right) = 60\eta_{vol,\text{suction port}}\ D(1728\nu_{\text{suction port}}) \quad , \tag{4.26}$$

$$\left(\frac{\dot{W}_r}{\dot{m}_r}\right) = h_{\text{discharge port}} - h_{\text{suction port}} \tag{4.27}$$

and

$$\left(\frac{f_{fl}}{\dot{W}_r}\right) = 1/(3413\ \eta_{mech}\ \dot{W}_{s,fl}) \tag{4.28}$$

and the constants 1728 and 3413 are used to maintain consistent units. Once S_{oper} has been evaluated from Eq. 4.25, values for $\dot{m}_r$, $\dot{W}_r$, and f_{fl} are calculated from Eqs. 4.26, 4.27, and 4.28.

After f_{fl} has been computed, the compressor motor efficiency can be calculated from the fit of motor efficiency to f_{fl}, given by Eq. 4.29.

$$\eta_{motor} = \eta_{motor,max} \sum_{i=0}^{5} \eta_{motor,i}\ (f_{fl})^i \tag{4.29}$$

The coefficients $\eta_{motor,i}$ in Eq. 4.29 are assigned values in the Block Data subroutine (see Appendix C). These coefficients were obtained from a fit to data published by Johnson [13] for a motor with "medium" slot size and maximum motor efficiency of 86% at a load of 6.8 N-m (80 oz-ft).

The next step in the calculations, after the compressor motor speed and efficiency have been computed by one of these two methods and a value has been calculated for $\dot{W}_r$, is to calculate the compressor power input from Eq. 4.30.

$$\dot{W}_{cm} = \dot{W}_r/(\eta_{mech}\eta_{motor}) \tag{4.30}$$

The computed value of $\dot{W}_{cm}$ is then used to evaluate $\dot{Q}_{cooling}$ and (optionally) $\dot{Q}_{hilo}$ and $\dot{Q}_{can}$ using Eqs. 4.16, 4.8, and 4.9.

A new refrigerant enthalpy at the compressor suction port is calculated using Eq. 4.19 and the sequence shown in Fig. 4.3 is repeated until the change in the value of $h_{suction\ port}$ from one iteration to the next is smaller than a specified tolerance. The refrigerant enthalpy at

compressor shell exit, h_{outlet}, is then computed using Eq. 4.31 (a rearranged form of Eq. 4.12),

$$h_{outlet} = h_{discharge\ port} - \frac{\dot{Q}_{hilo}}{\dot{m}_r} \tag{4.31}$$

After the associated refrigerant properties at the compressor shell outlet and the refrigerant state and properties at condenser inlet have been computed, the calculations proceed to the outer pressure drop convergence loop described earlier in Section 4.2.

Once all of these iterative loops have converged, the loss and efficiency-based model calculates a suction gas heating efficiency in addition to the values of overall isentropic and volumetric efficiency described in Section 4.2. The suction gas heating efficiency, η_{sh}, is defined by Shaffer and Lee [14] as

$$\eta_{sh} = \frac{\Delta h_{isen,inlet}}{\Delta h_{isen,suction\ port}} \tag{4.32}$$

where

$\Delta h_{isen,inlet}$ = specific enthalpy change for an isentropic compression from *shell inlet* conditions to shell outlet pressure

and

$\Delta h_{isen,suction\ port}$ = specific enthalpy change for an isentropic compression from *suction port* conditions to shell outlet pressure

The overall isentropic compression efficiency, η_{cm}, is related to η_{sh} by Eq. 4.33 [7,14].

$$\eta_{cm} = \eta_{sh}\ \eta_{isen}\ \eta_{mech}\ \eta_{motor} \tag{4.33}$$

The terms on each side of Eq. 4.33 are thus computed independently. All five efficiency terms in Eq. 4.33 are printed in the output for the loss and efficiency-based model. These values serve as an independent check on the compressor calculations and also to identify the relative magnitude of the various compressor inefficiencies.

As a final note, the user must exercise caution in selecting input values for η_{mech}, η_{motor}, $\dot{Q}_{hilo}$ (or α_{hilo}), and $\dot{Q}_{can}$ (or α_{can}) in the loss- and efficiency-based model. This is because certain combinations of the four parameters can result in suction gas cooling rather than heating between the compressor shell inlet and suction port. This is an unrealistic situation and results in termination of the program with a message "Inconsistent Data Set." Such a situation can be checked for by the use of Eq. 4.10 and the requirement that the suction gas enthalpy change be positive or zero, i.e.,

$$\dot{Q}_{hilo} + \dot{Q}_{cooling} - \dot{Q}_{can} \geq 0 \tag{4.34}$$

Using Eq. 4.16 this gives

$$\dot{Q}_{hilo} + (1 - \eta_{mech}\eta_{motor})\,\dot{W}_{cm} - \dot{Q}_{can} \geq 0 \tag{4.35}$$

or, dividing through by $\dot{W}_{cm}$, an alternative expression is

$$\alpha_{hilo} + (1 - \eta_{mech}\eta_{motor}) - \alpha_{can} \geq 0 \tag{4.36}$$

5. FLOW CONTROL DEVICES

5.1 Introduction

The ORNL Heat Pump Design Model allows the user to specify a fixed level of condenser subcooling or design parameters for a particular expansion device in order to control the refrigerant flow between the high and low sides of the system. The program contains subroutines which employ correlations for capillary tubes, thermostatic expansion valves (TXV), and short-tube orifices so that any of these three devices can be modeled. In the event that condenser subcooling is held fixed, each of these three submodels is called in such a way as to compute the design parameters for an equivalent capillary tube, TXV, and orifice that would produce the specified subcooling (this involves using some assumed operating characteristics from BLOCK DATA). When a flow control device is specified, the corresponding model is used with the compressor and condenser models in an iterative loop to obtain a balance between the calculated refrigerant mass flow rate from the compressor and that through the expansion device as described in Section 3.1.

5.2 Capillary Tube Model

One of the options in the Heat Pump Model is to simulate the operation of one, or more, capillary tubes in parallel. The capillary tube model requires the refrigerant pressure and degree of subcooling at the inlet of the capillary tube or tubes. The model consists of empirical fits to curves given in the ASHRAE Equipment Handbook [15] for a standardized capillary tube flow rate as a function of inlet pressure and subcooling for R-12 and R-22. The actual mass flow rate through the capillary tube is given by

$$\dot{m}_r = \phi N_{cap} \dot{m}'_r \qquad (5.1)$$

where

$\dot{m}_r'$ - standardized mass flow rate,

N_{cap} - number of capillary tubes in parallel,

ϕ - flow factor.

The capillary tube flow factor, ϕ, must be obtained from the ASHRAE Equipment Handbook [15] for each particular combination of length and inside tube diameter. The value of N_{cap} is also required as input. The standardized mass flow rate $\dot{m}_r'$ is given by Eq. 5.2 in terms of inlet pressure, P, and two functions of the degree of subcooling, m_o and k.

$$\dot{m}_r' = m_o \left(\frac{P}{1500}\right)^k \tag{5.2}$$

The coefficient, m_o, and exponent, k, have been fit as functions of subcooling, ΔT, as given by Eq. 5.3 and 5.4, such that $\dot{m}_r'$ agrees to within 1.5% of the curves across the range of Fig. 40 in Ref. 15

$$m_o = 356 + 0.641 \left|\frac{\Delta T - 31}{10}\right|^{3.56} \tag{5.3}$$

$$k = 0.4035 + 0.4175\ e^{-0.04\Delta T} \tag{5.4}$$

In the situation where the Design Model is used with a specified level of condenser subcooling in lieu of a specific flow control device, the capillary tube correlations are used in such a way as to compute the flow factor, ϕ, which would give the desired subcooling. The capillary tube model used in the program assumes that the downstream pressure is at or below critical pressure. However, Smith [16] has fit additional curves in the ASHRAE Equipment Handbook [15] which could be added by the user to predict capillary tube performance under non-critical conditions.

The current model cannot handle incomplete condensation at the capillary tube entrance. For all cases of incomplete condensation, the subcooling is set to zero and calculations continue assuming that the final conditions will have zero degrees of condenser subcooling. If error messages are printed concerning "flashing in the liquid line," the final results should be checked to make sure that the refrigerant is not in a two-phase state at the capillary tube entrance. If incomplete condensation is specified as input, the required value for the flow factor ϕ is set to zero.

5.3 Thermostatic Expansion Valve Model

The TXV subroutine contains:

- a general model of a cross-charged thermostatic expansion valve,
- specific empirical correlations for one size of distributor nozzle and tubes, and
- additional empirical equations to correct for nonstandard liquid line temperatures, tube lengths, and nozzle and tube loadings.

The general model of a cross-charged TXV is a form of the equation used by Smith [16]:

$$\dot{m}_{r,TXV} = C_{TXV}(\Delta T_{oper} - \Delta T_{static})(\rho_r \Delta P_{TXV})^{1/2} \qquad (5.5)$$

where a dependence on the refrigerant liquid line density, ρ_r, has been added, in keeping with the general form of the standard orifice equation. The remaining parameters in Eq. 5.5 are defined as follows:

$\dot{m}_{r,TXV}$ - mass flow rate that TXV will pass,

C_{TXV} - general orifice flow area coefficient,

ΔT_{oper} - actual operating superheat,

ΔT_{static} - static superheat (superheat at which the valve is just barely open), and

ΔP_{TXV} - available pressure drop from TXV_{inlet} to TXV_{exit}.

The assumption of a cross-charged TXV valve implies that a given ΔT_{oper}, at a given ρ_r and ΔP_{TXV}, will provide a certain valve opening that is independent of evaporator pressure. Most TXV valves used in the higher efficiency heat pumps are of the type described above since such valves tend to maintain a relatively constant superheat over a range of operating conditions.

If the actual operating superheat is greater than the maximum effective superheat, $\Delta T_{max\ eff}$, where

$$\Delta T_{max,eff} = \Delta T_{static} + 1.33\ (\Delta T_{rated} - \Delta T_{static}) \tag{5.6}$$

then $\Delta T_{max,eff}$ is used in place of ΔT_{oper} in Eq. 5.5.

The flow area coefficient, C_{TXV}, and the available pressure drop across the TXV valve, ΔP_{TXV}, have to be calculated before Eq. 5.5 can be used to compute a refrigerant mass flow rate. The value of C_{TXV} depends on four variables from the input data [17]:

$\dot{Q}_{rated}$, the capacity rating of the TXV valve (tons),

ΔT_{rated}, the rated operating superheat of the valve (at 75% of the maximum valve opening),

ΔT_{static}, defined earlier, and

b_{fac}, the valve bleed factor.

The given capacity rating is used in conjunction with the bleed factor and standard TXV rating conditions for a specific refrigerant (specified in the Block Data routine) to calculate the rated refrigerant mass flow rate:

$$\dot{m}_{r,rated} = \frac{12{,}000\ \dot{Q}_{rated}\ b_{fac}}{h_{evap\ out,rated} - h_{liquid\ line,rated}} \tag{5.7}$$

where

the constant 12,000 is used to convert from tons of capacity to Btu/hr.

$h_{evap\ out,rated}$ is the evaporator outlet refrigerant enthalpy at rated evaporator pressure and superheat,

and

$h_{liquid\ line,rated}$ is the refrigerant enthalpy at rated liquid line temperature.

C_{TXV} is calculated from Eq. 5.8 using $\dot{m}_{r,rated}$:

$$C_{TXV} = \frac{\dot{m}_{r,rated}}{(\Delta T_{rated} - \Delta T_{static})(\rho_{r,rated} \Delta P_{rated})^{1/2}} \tag{5.8}$$

where

$\rho_{r,rated}$ = refrigerant density at rated liquid line temperature

and

ΔP_{rated} = rated pressure drop across expansion device.

The available pressure drop across the TXV valve, ΔP_{TXV}, is the remaining unknown in Eq. 5.5. This is computed using the pressures at the TXV inlet and evaporator inlet and the pressure drops in the distributor nozzle and tubes, i.e.,

$$\Delta P_{TXV} = P_{in,TXV} - P_{in,evap} - \Delta P_{noz} - \Delta P_{tube} \tag{5.9}$$

The pressures $P_{in,TXV}$ and $P_{in,evap}$ are computed elsewhere in the heat pump model and are input data for the TXV routine. The nozzle and tube pressure drops are calculated using *specific empirical fits* for *one set of* distributor nozzle and tube *sizes for R-22 flow* and *additional empirical equations* to correct for non-standard liquid line temperature, tube lengths, and distributor loading *for R-12, 22, and 502*. All the equations were obtained from fits to published performance data [18].

Distributor nozzles and tubes are often used with TXV's to equalize the refrigerant flow in each evaporator circuit and to assure proper

TXV operation. At standard rating conditions the distributor nozzle will have a pressure drop of 172 kPa (25 psi) for R-22 and R502 [103 kPa (15 psi) for R-12] and the distributor tubes will each have 69 kPa (10 psi) drop. An input option has been provided which allows the user to omit the nozzle and distributor tube computations for specific applications to systems which do not have these components.

The first step in the evaluation of ΔP_{noz} and ΔP_{tube} is the calculation of the actual capacity of the nozzle, $\dot{Q}_{noz}$, and of each tube, $\dot{Q}_{tube}$, i.e.,

$$\dot{Q}_{noz} = \dot{m}_r(h_{evap\ out,rated} - h_{liquid\ line,actual}) \qquad (5.10)$$

$$\dot{Q}_{tube} = \dot{Q}_{noz}/N_{circuits} \qquad (5.11)$$

where $\dot{m}_r$ is the mass flow rate calculated by the compressor model and $N_{circuits}$ is the number of circuits in the evaporator.

Next, the capacities are computed which yield the rated pressure drops across the nozzles and tubes, i.e.,

$$\dot{Q}_{noz,rated} = (3)\,12000\ \alpha_{cor}\ 10^{(T_{sat,evap} - 40)/201.0} \qquad (5.12)$$

and

$$\dot{Q}_{tube,rated} = (1.1)12000\ \alpha_{cor}\ \beta_{cor}\ 10^{(T_{sat,evap} - 40)/177.64} \qquad (5.13)$$

where

the constants 3 and 1.1 are tonnage ratings from the equipment specifications [18],

α_{cor} = correction factor for liquid line temperature other than 100°F, i.e.,

$$\alpha_{cor} = \begin{cases} 10^{(100 - T_{in,TXV})/155.18} & T_{in,TXV} \leq 100 \\ 10^{(100 - T_{in,TXV})/140.19} & T_{in,TXV} > 100 \end{cases} \quad (5.14)$$

and

β_{cor} = correction factor for tube lengths other than 30 inches, i.e.,

$$\beta_{cor} = (30/\ell_{tube})^{1/3} \quad (5.15)$$

Equations 5.12 and 5.13, respectively, represent the R-22 capacity of a Sporlan [17] nozzle No. 2.5 and 1/4 inch OD copper tubes. *For any other nozzle or tube, or refrigerant, Eqs. 5.12 and 5.13 must be replaced* (the correction terms α_{cor} and β_{cor}, Eq. 5.14 and 5.15, do not need to be replaced).

Given the actual nozzle and tube capacities from Eqs. 5.10 and 5.11 and the rated capacities from Eqs. 5.12 and 5.13, the nozzle and tube loadings L_{noz} and L_{tube}, defined as $\dot{Q}_{noz}/\dot{Q}_{noz,rated}$ and $\dot{Q}_{tube}/\dot{Q}_{tube,rated}$ respectively, and the nozzle and tube pressure drops, ΔP_{noz} and ΔP_{tube}, can be found.

For R-22 or R-502

$$\Delta P_{noz} = \begin{cases} 25.0\ (L_{noz})^{1.838} & L_{noz} \leq 1.2 \\ 29.4\ (L_{noz})^{0.9547} & L_{noz} > 1.2 \end{cases} \quad (5.16)$$

$$\Delta P_{tube} = 10.0(L_{tube})^{1.8122} \quad (5.17)$$

For R-12

$$\Delta P_{noz} = \begin{cases} 15.0(L_{noz})^{1.817} & L_{noz} \leq 1.1 \\ 15.81(L_{noz})^{1.265} & L_{noz} > 1.1 \end{cases} \quad (5.18)$$

$$\Delta P_{tube} = \begin{cases} 10.0(L_{tube})^{1.772} & L_{tube} \leq 1.6 \\ 12.265(L_{tube})^{1.3377} & L_{tube} > 1.6 \end{cases} \quad (5.19)$$

Equation 5.9 is then used to obtain ΔP_{TXV} which, in turn, is used in Eq. 5.5 to evaluated $\dot{m}_{r,TXV}$.

In a case where a fixed level of condenser subcooling is specified, the subroutine calculates the required rated capacity of the TXV valve from the equations

$$C_{TXV} = \frac{\dot{m}_r}{(\Delta T_{oper} - \Delta T_{static})(\rho_r \Delta P_{TXV})^{1/2}} \quad (5.20)$$

$$\dot{m}_{r,rated} = C_{TXV}(\Delta T_{rated} - \Delta T_{static})(\rho_{r,rated} \Delta P_{rated})^{1/2} \quad (5.21)$$

$$\dot{Q}_{rated} = \frac{\dot{m}_{r,rated}(h_{evap\ out,rated} - h_{liquid\ line,rated})}{12000\ b_{fac}} \quad (5.22)$$

where ΔT_{oper} is replaced by $\Delta T_{max,eff}$ from Eq. 5.6 if $\Delta T_{oper} > \Delta T_{max,eff}$ or by ΔT_{rated} if $\Delta T_{oper} \leq \Delta T_{static}$. The option to omit the nozzle and tube pressure drop computations is also available when condenser subcooling is specified.

The current model is not intended to handle incomplete condensation at the TXV entrance. In such cases, the subcooling is set to zero and calculations continue as described in the capillary tube case. If incomplete condensation is specified, the program will set the TXV rating values to zero.

5.4 Short Tube Orifice Model

The short-tube orifice subroutine which is included in the ORNL Heat Pump Design Model uses correlations developed by Mei [19]. He obtained data for five 0.127 m (0.5 in.) long Carrier Accurators with diameters from 1.067 to 1.694 mm (0.0420 to 0.0667 inches) (L/D ratios from 7.5 to 11.9) using R-22. He observed pressure drops

between 620 and 1515 kPa (90 and 220 psi) across the restrictor and levels of subcooling from 0 to 28 C° (0 to 50 F°) at the inlet. The observed refrigerant mass flow rates ranged from 68.0 to 213 kg/h (150 to 470 lbm/h). The standard orifice relation in Eq. 5.23,

$$G_r = \dot{m}_r / A_{orifice} = C(2g_c \rho \Delta P)^{1/2} \quad , \tag{5.23}$$

was solved for the orifice coefficient C which was then correlated with both the pressure drop across the short tube orifice, ΔP, and the level of subcooling at the inlet, ΔT. Equation 5.24,

$$\dot{m}_r = \begin{cases} \frac{\pi D^2}{4} \left[0.63683 - 0.019337 \, (P_{in} - P_{in,evap})^{1/2} + 0.006\Delta T \right] \\ \qquad \times \left[2\rho_r g_c (P_{in} - P_{in,evap}) \right]^{1/2} \\ \qquad \textit{for } \Delta T \leq 40 \\ \frac{\pi D^2}{4} \left[0.9175 - 0.00325\Delta T \right] \left[2\rho_r g_c (P_{in} - P_{in,sat}) \right]^{1/2} \\ \qquad \textit{for } \Delta T > 40 \quad , \end{cases} \tag{5.24}$$

was found to correlate the data to within 7.5% (with the maximum difference occuring at low subcooling levels), where P_{in}, $P_{in,evap}$, and $P_{in,sat}$ are the pressures at the inlet to the orifice, the inlet to the evaporator, and the saturation pressure at the inlet to the orifice, respectively.

If the user has specified a fixed level of *condenser* subcooling rather than selecting a particular flow control device Eq. 5.24 is solved for the orifice diameter that would provide that subcooling. As in the case of the other two models, if incomplete condensation is specified, the corresponding orifice diameter is set to zero.

The user should always check that the computed refrigerant quality at the flow control device entrance is equal to zero when using any of the three flow control device models. If it is not, the calculated results should not be used because the flow control models have been extended beyond their intended range.

6. CONDENSER AND EVAPORATOR MODELS

6.1 Introduction

The ORNL Heat Pump Design Model calculates the performance of air-to-refrigerant condensers and evaporators by using:

- effectiveness vs. N_{tu} correlations for heat transfer for a dry coil,
- a modified version of the effective surface temperature approach when there is dehumidification,
- the Thom correlation for two-phase refrigerant pressure drops and the Moody friction factor chart plus momentum terms for the single-phase refrigerant pressure drop, and
- friction factor equations for the air-side pressure drop for dry, partially wetted, or fully wetted coils.

Although the models for the condenser and evaporator are not identical, the principal differences center around the dehumidification algorithm. Since there are many similarities, the condenser and evaporator are discussed together and the differences are pointed out where they occur. The calculational methods which have been used assume that the heat exchangers consist of equivalent, parallel refrigerant circuits with unmixed flow on both the air and refrigerant sides [3]. The refrigerant-side calculations are separated into computations for the superheated and two-phase regions for the evaporator and for the superheated, two-phase, and subcooled regions for the condenser.

Figure 6.1 is a general block diagram, or flow chart, outlining the organization and iterative loops for the condenser model. Figure 6.2 is a similar diagram for the evaporator calculations.

The air-side mass flow rate for each heat exchanger is calculated from the volumetric air flow rate specified in the input data and the air density calculated from the ideal gas equation using atmospheric pressure, the Universal gas constant for air (given in BLOCK DATA), and the inlet air temperature. Since the heat exchangers are modeled as several equivalent parallel refrigerant circuits (the actual number being specified with the input data), the air-side mass flow rate and the estimated refrigerant mass flow rate from the compressor model are divided by the number of circuits to obtain values for each circuit.

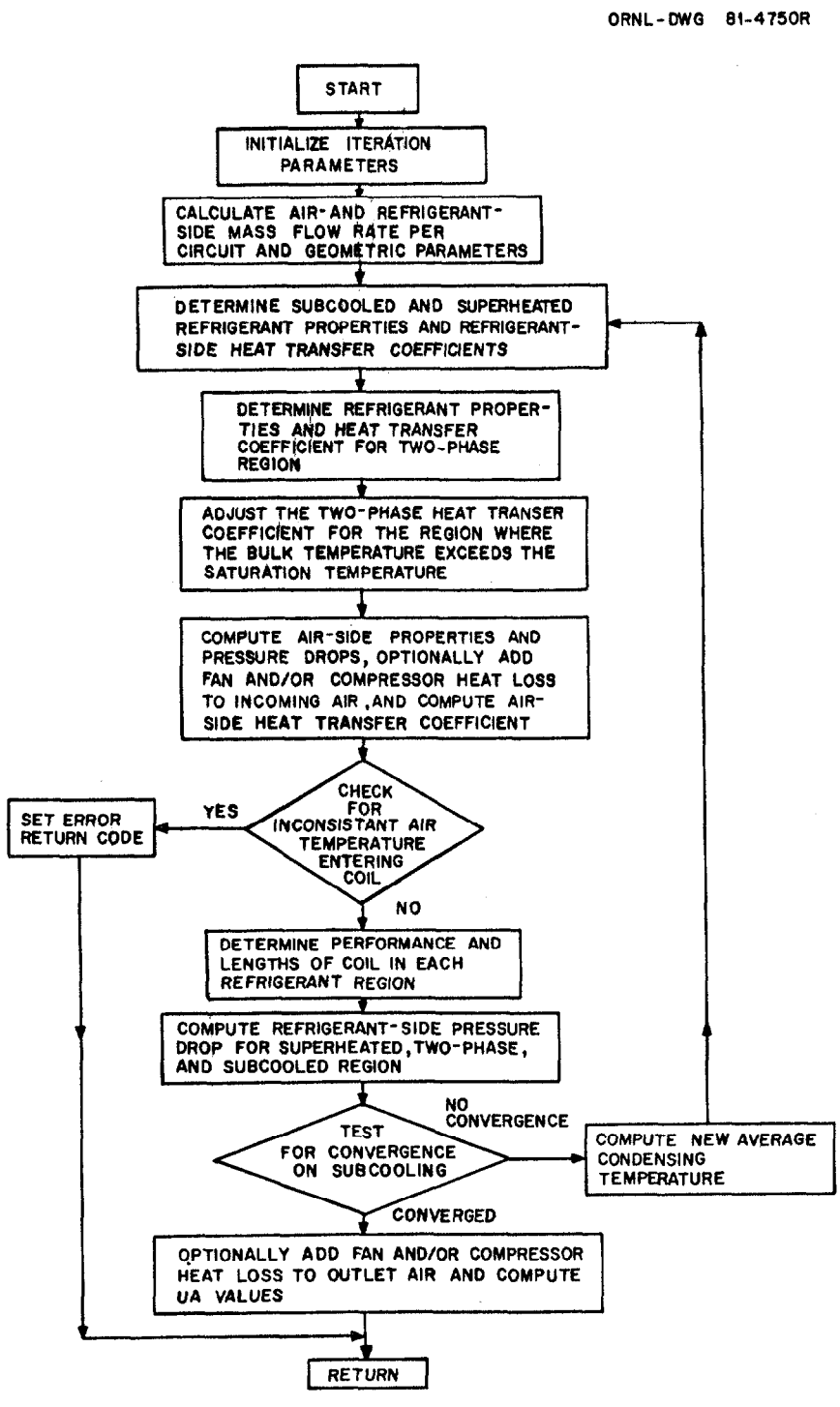

Fig. 6.1 General Structure of the Condenser Model

ORNL-DWG 81-4751

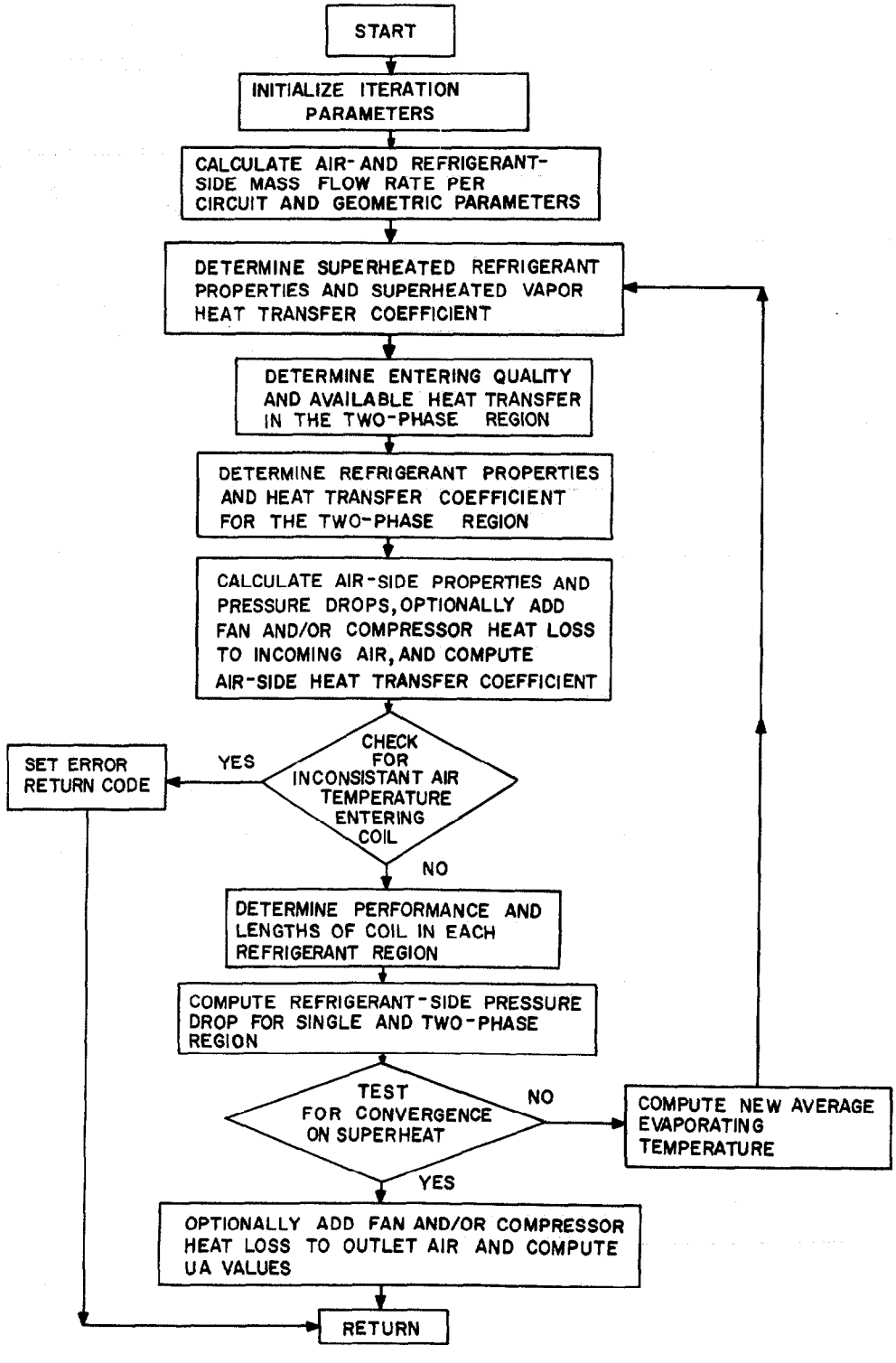

Fig. 6.2 General Structure of the Evaporator Model

The average densities of the refrigerant liquid and vapor in the two-phase region of each coil and the latent heat of vaporization are calculated from the current estimates of the average saturation temperatures in the heat exchangers. The thermophysical properties for the single-phase refrigerant (subcooled and superheated for the condenser and superheated for the evaporator), i.e., the viscosity, thermal conductivity, and liquid specific heat, are calculated according to a routine written by Flower [5]. The specific heat for the vapor region, $c_{p,v}$, is determined by a routine developed by Kartsounes and Erth [4] which computes the local value of $\left.\frac{\partial h}{\partial t}\right|_p = c_{p,v}$.

6.2 Single-Phase Heat Transfer Coefficients in Heat Exchanger Tubes

The refrigerant heat transfer coefficient for the superheated region in the condenser is calculated (as reported in the MIT Model [3]) by Eq. 6.1 for gas flow from an abrupt contraction entrance [20] (h is used throughout this report for heat transfer coefficients and h for enthalpy variables).

$$h = C_1 G_r c_{p,v} N_{Pr}^{-2/3} N_{Re}^{C_2} \qquad (6.1)$$

where $N_{Re} = G_r D/\mu$ and,

$$C_1 = \begin{cases} 1.10647 & \text{for } N_{Re} < 3500 \\ 3.5194 \times 10^{-7} & \text{for } 3500 \le N_{Re} < 6000 \\ 0.01080 & \text{for } N_{Re} \ge 6000 \end{cases} \qquad (6.2)$$

$$C_2 = \begin{cases} -0.78992 & \text{for } N_{Re} < 3500 \\ 1.03804 & \text{for } 3500 \le N_{Re} < 6000 \\ -0.13750 & \text{for } N_{Re} \ge 6000 \end{cases} \qquad (6.3)$$

The constants used to define the step functions C_1 and C_2 defined in Eqs. 6.2 and 6.3 are assigned in the BLOCK DATA subroutine (see Appendix C).

The heat transfer coefficients for the subcooled region of the condenser and the superheated region in the evaporator are computed using the Dittus-Boelter correlation for fully developed flow [21]:

$$h = 0.023\, G_r\, c_p\, N_{Pr}^{(C-1)}\, N_{Re}^{-0.20} \qquad (6.4)$$

where "C" is 0.3 when the refrigerant is being cooling and 0.4 when being heated.

6.3 Two-Phase Refrigerant Heat Transfer Coefficients in Heat Exchanger Tubes

The two-phase heat transfer coefficients for the condenser and the evaporator are average values obtained by effectively integrating local values over the length of the two-phase region. The actual integration is performed over the range of refrigerant quality [3] where a length of tube dz is related to a change in quality of dx by

$$dz \propto \frac{dx}{h(x)\Delta T}$$

and ΔT is the change in temperature between the refrigerant and the tube wall. Assuming that ΔT remains practically constant (as opposed to assuming a constant heat flux) [3,22], the average heat transfer coefficient, h_{ave}, is given by

$$h_{ave} = \frac{\int_{z_i}^{z_o} h(x)\,dz}{\int_{z_i}^{z_o} dz} = \frac{\int_{x_i}^{x_o} dx}{\int_{x_i}^{x_o} \frac{dx}{h(x)}} \quad ,$$

which reduced to

$$\frac{1}{h_{ave}} = \frac{\int_{x_i}^{x_o} \frac{dx}{h(x)}}{x_i - x_o}$$

The local heat transfer coefficient, $h(x)$, for the condenser is calculated as a function of the quality according to a correlation by Travis [22].

$$h(x) = \begin{cases} k_\ell \, N_{Pr} \, N_{Re}^{0.9} \, \dfrac{F(X_{tt})}{DF_2} & F(X_{tt}) < 1.0 \\ k_\ell \, N_{Pr} \, N_{Re}^{0.9} \, \dfrac{F(X_{tt})^{1.15}}{DF_2} & 1.0 < F(X_{tt}) < 15 \end{cases} \tag{6.5}$$

where

$$X_{tt} = \left(\frac{\mu_\ell}{\mu_v}\right)^{0.1} \left(\frac{\rho_v}{\rho_\ell}\right)^{0.5} \left(\frac{1 - x}{x}\right)^{0.9} , \tag{6.6}$$

$$N_{Re} = \frac{G_r \, D \, (1 - x)}{\mu_\ell} , \tag{6.7}$$

$$F(X_{tt}) = 0.15 \left(\frac{1}{X_{tt}} + 2.85 X_{tt}^{-0.476}\right) , \text{ and} \tag{6.8}$$

$$F_2 = \begin{cases} 0.707 \, N_{Pr} \, N_{Re}^{0.5} & N_{Re} < 50 \\ 5.0 \, N_{Pr} + 5.0 \, \ell n[1.0 + N_{Pr}(0.09636 \, N_{Re}^{0.585} - 1.0)] & 50 < N_{Re} < 1125 \\ 5.0 \, N_{Pr} + 5.0 \, \ell n[1.0 + 5.0 \, N_{Pr}] + 2.5 \, \ell n[0.00313 \, N_{Re}^{0.812}] & N_{Re} > 1125 \end{cases} \tag{6.9}$$

The integration is carried out by a summation over steps of a constant Δx and has been changed slightly from that in the Hiller and Glicksman MIT Model [3]. The modifications pertain to the manner of extrapolating to liquid and vapor heat transfer coefficients at the end points of the integration. The average two-phase heat transfer coefficient is adjusted using a correlation given by Rohsenow [23] for the region where condensation (desuperheating) is occurring at the wall but the bulk refrigerant temperature exceeds the saturation temperature. The equation is

$$h_{tp} = h_{ave}\left(1 + c_{p,v}\frac{T_{v,ds} - T_{sat,in}}{h_{fg}}\right)^{1/4} \qquad (6.10)$$

The bulk refrigerant temperature, $T_{v,ds}$, where refrigerant condensation begins at the tube wall is calculated from Eqs. 6.11 and 6.12 where

$$T_{v,ds} = \frac{rT_{tp,in} - T_{a,in}}{r - 1} \qquad (6.11)$$

and

$$r = 1 + \frac{h_v A_r}{h_a A_a \eta_d} \quad , \qquad (6.12)$$

$T_{tp,in}$ and $T_{a,in}$ are the refrigerant temperature entering the two-phase region and the inlet air temperature, respectively.

The average heat-transfer coefficient for the two-phase region of the evaporator is derived from a correlation developed by Chaddock and Noerager [24] for evaporation of refrigerant 12 in horizontal tubes and from the general observations of Sthapak [25] for the dry-out region. Equation 6.13 expresses the heat transfer coefficient in terms of the local heat transfer coefficients as functions of refrigerant

quality from the inlet to the dry-out point, $h_1(x)$ from x_i to x_{do}, and from dry-out to exit quality, $h_2(x)$ between x_{do} and x_o.

$$\frac{1}{h_{tp}} = \frac{\int_{x_i}^{x_{do}} \frac{dx}{h_1(x)} + \int_{x_{do}}^{x_o} \frac{dx}{h_2(x)}}{\int_{x_i}^{x_o} dx} \tag{6.13}$$

Examining the two integrals separately, $h_1(x)$ is given by Eq. 6.14

$$h_1(x) = 3.0\, h_\ell \left(\frac{1}{X_{tt}}\right)^{2/3} \tag{6.14}$$

where X_{tt} is as defined in Eq. 6.6 and h_ℓ is the heat transfer coefficient for liquid refrigerant obtained from Eq. 6.4. Thus

$$h_1(x) = 3.0 h_\ell \left(\frac{\rho_\ell}{\rho_v}\right)^{1/3} \left(\frac{\mu_v}{\mu_\ell}\right)^{0.0667} \left(\frac{x}{1-x}\right)^{0.6}$$

and

$$\int_{x_i}^{x_{do}} \frac{dx}{h_1(x)} = \frac{1}{c} \int_{x_i}^{x_{do}} \frac{(1-x)^{0.6}\, dx}{x^{0.6}} \tag{6.15}$$

where

$$c = 3.0 h_\ell \left(\frac{\rho_\ell}{\rho_v}\right)^{1/3} \left(\frac{\mu_v}{\mu_\ell}\right)^{0.0667}$$

Equation 6.15 can be expanded, truncated, and integrated term by term to yield

$$\int_{x_i}^{x_{do}} \frac{dx}{h_1(x)} = \frac{1}{c} \left\{ \frac{1}{0.4} \left[\left(x_{do}^{0.4} - x_i^{0.4}\right) - \frac{0.6}{1.4} \left(x_{do}^{1.4} - x_i^{1.4}\right) - \frac{0.12}{2.4} \times \left(x_{do}^{2.4} - x_i^{2.4}\right) - \frac{0.056}{3.4} \left(x_{do}^{3.4} - x_i^{3.4}\right) - \frac{0.034}{4.4} \left(x_{do}^{4.4} - x_i^{4.4}\right) \right] \right\} \tag{6.16}$$

The second integral in the numerator of Eq. 6.13 is based on a nonlinear interpolation of the heat transfer coefficient from the two-phase value at the dry-out point, $h_1(x_{do})$, from Eq. 6.14 to value of pure vapor, h_v, from Eq. 6.4, i.e.,

$$h_2(x) = h_1(x_{do}) - \left(\frac{x - x_{do}}{x_o - x_{do}}\right)^2 (h_1(x_{do}) - h_v) \tag{6.17}$$

where x_{do} and x_o are refrigerant qualities at the dry-out point and the outlet of the evaporator or the two-phase region (whichever comes first). The second integral in Eq. 6.13 can be evaluated in closed form using Eq. 6.17, i.e.,

$$\int_{x_{do}}^{x_o} \frac{dx}{h_2(x)} = \frac{\{h_1(x_{do})[h(x_{do}) - h_v]\}^{-1/2}}{2(x_o - x_{do})} \times \ell n \left\{ \frac{h_1(x_{do}) + \left\{h_1(x_{do})[h_1(x_{do}) - h_v]\right\}}{h_1(x_{do}) - \left\{h_1(x_{do})[h_1(x_{do}) - h_v]\right\}} \right\} \tag{6.18}$$

A value of 0.65 is assumed for x_{do} in the model [25].

6.4 Air-Side Heat Transfer Coefficients

The air-side heat transfer coefficients are based on the work of McQuiston [26,27], Yoshii [28], and Senshu [29] and are calculated by the correlation given by Eq. 6.19.

$$h_a = C_o G_a c_{pa} N_{Pr}^{-2/3} j \left[\frac{1 - 1280\, N_T\, N_{Re}^{-1.2}}{1 - 5120\, N_{Re}^{-1.2}}\right] \tag{6.19}$$

where

$$j = 0.0014 + 0.2618 \left(\frac{1}{1 - F_a}\right)^{-0.15} \left(\frac{G_a D}{\mu}\right)^{-0.4},$$

$$N_{Re} = \frac{G_a W_T}{\mu},$$

and

C_o = 1.0, 1.45, or 1.75 depending on whether the fins are smooth, wavy, or louvered (see Appendix G for parameter definitions).

Equation 6.19 was obtained from extensive test data on smooth fins over the Reynolds number range of $3{,}000 \leq N_{Re} \leq 15{,}000$. The heat transfer coefficients for wavy and louvered fins are assumed to be predicted approximately by the use of the smooth fin equation increased by the multiplicative constant C_o. Data to verify this assumption for a number of fin-and-tube geometries, however, are not available. The heat transfer coefficients so calculated for wavy and louvered fin surfaces are assumed to be referenced to smooth-fin surface area; thus the C_o values for wavy and louvered fins are intended to account for increases in both heat transfer coefficient and surface area from smooth fin values. Equation 6.19 includes terms to adjust for a number of geometric effects such as the number of tube rows, the fin spacing, and the transverse tube spacing. The air-side properties are calculated using a modified version of a subroutine by Flower [5] which is based on correlations published by the American Society of Heating, Refrigeration, and Air Conditioning Engineers [30].

The air-side heat transfer coefficient for the portion of the evaporator which is wetted due to dehumidification is calculated from the dry coefficient, h_a, by Eq. 6.20 from Myers [31].

$$h_{a,w} = 0.626 \left(\frac{\dot{Q}}{A}\right)^{0.101} h_a \qquad (6.20)$$

The fin efficiency and overall surface effectiveness for the condenser and for the dry region of the evaporator are calculated based on the work of Schmidt [32] as reported by McQuiston and Tree [33] for a tube surrounded by a hexagonal fin segment of a sheet fin (the representative fin shape surrounding each tube in a staggered tube arrangement). This work has been generalized to properly handle orientation changes that occur as the longitudinal and transverse tube spacings are varied.

6.5 Heat Exchanger Performance

Figures 6.3 and 6.4 are block diagrams for the subroutines which calculate the performance of the condenser and evaporator, respectively.

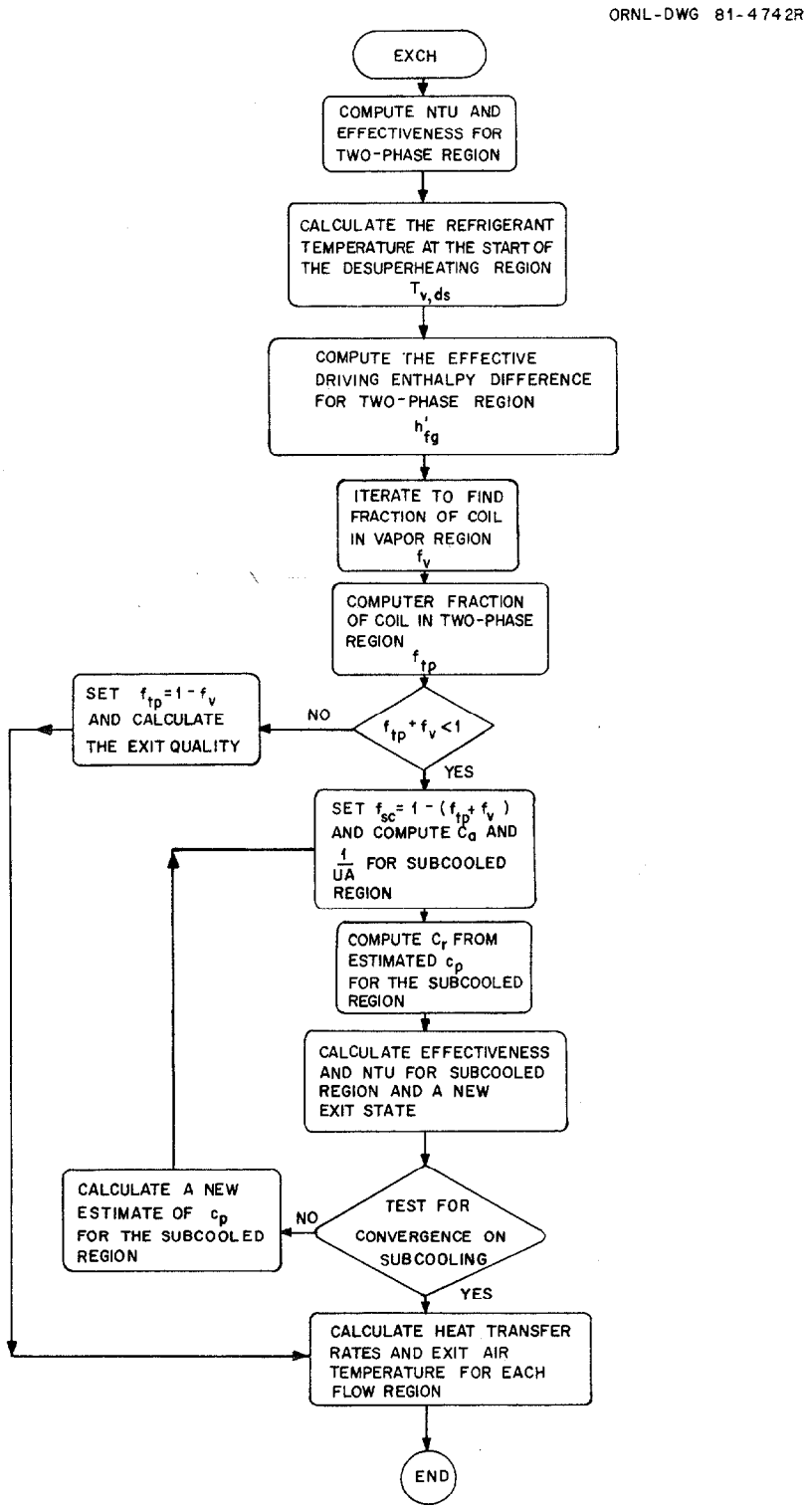

Fig. 6.3 Computational Sequence in the Condenser Model

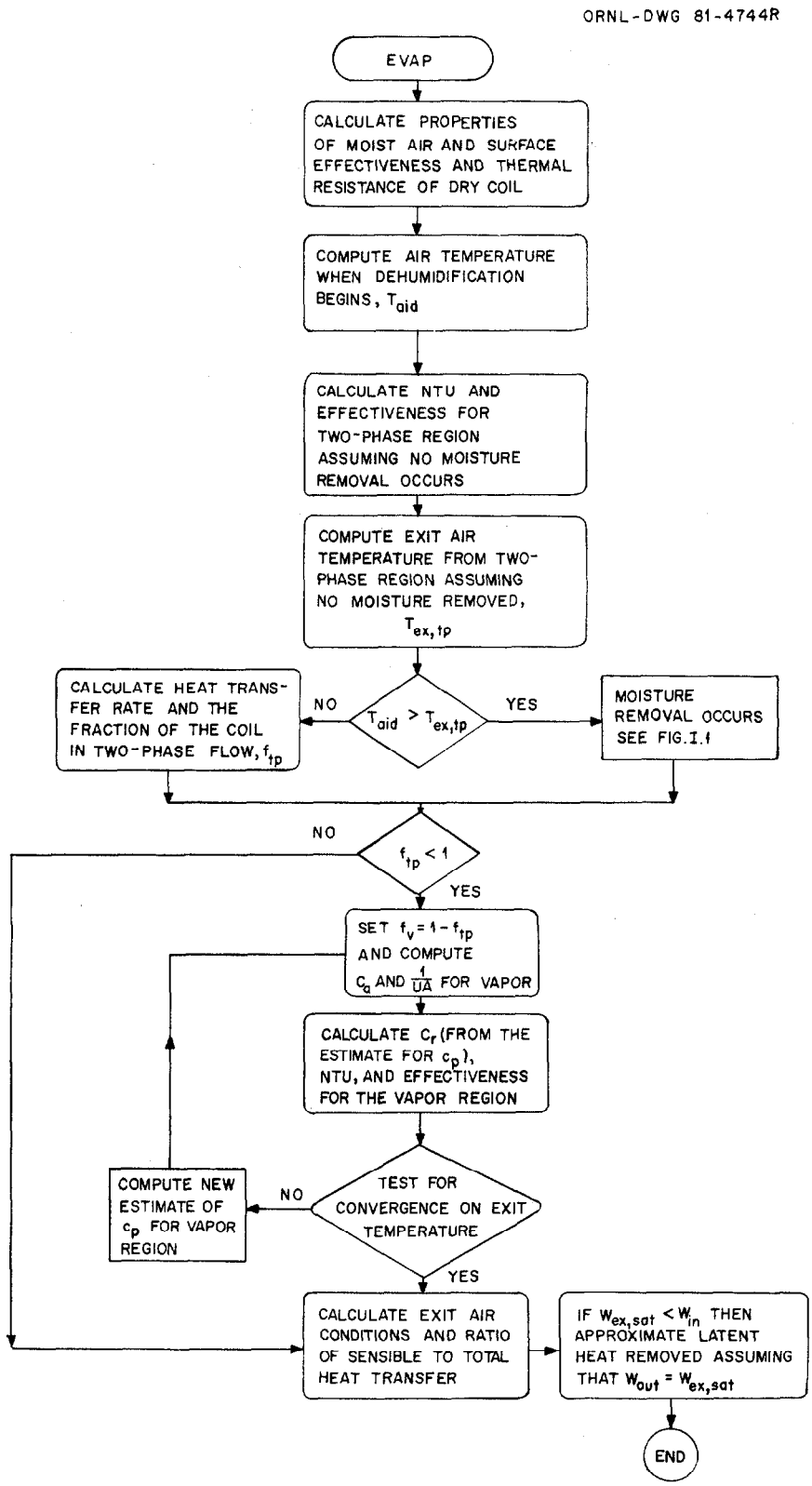

Fig. 6.4 Computational Sequence in the Evaporator Model

In each case, the heat transfer for the liquid, vapor, and two-phase refrigerant regions of the heat exchanger are computed using effectiveness vs. N_{tu} correlations, except for the two-phase refrigerant region of an evaporator with dehumidification. If there is dehumidification along the two-phase region of the evaporator, an effective surface temperature approach is used as described in Appendices H and I. Except for this case, the number of heat transfer units for the two-phase region (condenser or evaporator) is given by Eq. 6.21,

$$N_{tu} = \frac{UA}{C_{min}} = \left(\frac{A_o}{c_{pm}\left[\frac{A_r}{\eta_d \bar{h}_a A_a} + \frac{1}{\bar{h}_{tp}} \right]} \right), \tag{6.21}$$

where c_{pm} is corrected for moist air conditions (i.e., $c_{pm} = c_{pa} + 0.444*W$ where W is the air humidity ratio), and the effectiveness is given by Eq. 6.22,

$$\varepsilon_{tp} = 1 - e^{-N_{tu}} \tag{6.22}$$

The numerator in Eq. 6.21, A_o, is the refrigerant-side heat transfer area per unit of air mass flow rate (see Appendix J).

When there is moisture removal on the evaporator, it is assumed to occur only on the two-phase region of the coil. There is a check, however, to ensure that the air leaving the superheated region of the evaporator is not super-saturated. If this situation were to occur, the humidity ratio and related values are changed to the appropriate saturation values. Heat transfer in the case of dehumidification is calculated using algorithms as described in Appendices H and I.

The air temperature for which dehumidification would occur at the finned tube surface, T_{aid}, is computed from the dew-point and saturation temperatures, T_{dp} and T_{sat}, using Eq. 6.23,

$$T_{aid} = \frac{T_{dp}\, r_1 - T_{sat}}{r_1 - 1}, \tag{6.23}$$

where r_1 is given by Eq. 6.24

$$r_1 = \frac{1}{\eta_d} + \frac{h_a A_a}{h_{tp} A_r} \quad . \tag{6.24}$$

T_{aid} is used to determine whether or not dehumidification will occur as is shown in Fig. 6.4.

The fraction of each coil with two-phase, superheated, and subcooled refrigerant is needed to calculate the pressure drop and heat transfer rate for each region. The computation of the fraction of the condenser or evaporator containing two-phase refrigerant is based on the heat transfer rate necessary to condense or evaporate all of the refrigerant, which is given by Eq.6.25,

$$\dot{Q}_{tp} = \begin{cases} \dot{m}_r h'_{fg} & \text{for the condenser} \\ \dot{m}_r h_{fg} & \text{for the evaporator} \end{cases} \tag{6.25}$$

where

$$h_{fg} = h_{tp,out} - h_{tp,in}.$$

The *driving enthalpy difference*, h'_{fg}, for the condenser calculations in Eq. 6.25 is given by Eq. 6.26,

$$h'_{fg} = h_{fg} + c_{p,v} (T_{v,ds} - T_{tp,in}) \tag{6.26}$$

where the bulk refrigerant temperature at which refrigerant condensation begins at the tube wall [3], $T_{v,ds}$, is computed from Eq. 6.11. The mass flow rate of air necessary to achieve $\dot{Q}_{tp}$ is then given by Eq. 6.27

$$\dot{m}_{a,tp} = \frac{\dot{Q}_{tp}}{\varepsilon_{tp} c_{pm} \left| T_{r,tp,avg} - T_{a,in} \right|} \tag{6.27}$$

and the fraction of the coil with two-phase refrigerant by Eq. 6.28

$$f_{tp} = \dot{m}_{a,tp}/\dot{m}_a \tag{6.28}$$

If f_{tp} for the evaporator is greater than 1, the entire coil contains two-phase refrigerant. If $f_{tp} + f_v$ is greater than 1 for the condenser, where f_v is the fraction of the coil which is superheated (as described later), then f_{tp} is set equal to $1 - f_v$.

The effectiveness of the superheated and subcooled regions is calculated for a cross-flow heat exchanger with both fluids unmixed. Since the exact solution is not in closed form, an approximate solution developed by Hiller [3] is used.

The approximate solution uses equations for a counterflow heat exchanger, i.e., Eq. 6.29,

$$\varepsilon_{cf} = \begin{cases} \dfrac{1 - e^{-N_{tu}(1 - C_{min}/C_{max})}}{\left(1 - \dfrac{C_{min}}{C_{max}}\right) e^{-N_{tu}(1 - C_{min}/C_{max})}} & C_{min} < C_{max} \\ \dfrac{N_{tu}}{1 + N_{tu}} & C_{min} = C_{max} \end{cases} \tag{6.29}$$

in conjunction with Eq. 6.30 to correct for a cross-flow orientation.

$$\varepsilon_v = \varepsilon_{cf} \frac{1}{(1 + 0.047 \frac{C_{min}}{C_{max}})(N_{tu})^{0.036\, C_{min}/C_{max}}} \tag{6.30}$$

The parameters C_{min} and C_{max} are the minimum and maximum capacity rates ($\dot{m}c_p$), respectively. The number of transfer units for the superheated region is given by Eq. 6.31

$$N_{tu} = \frac{1}{RC_{min}} \tag{6.31}$$

where the thermal resistance, R, is given by Eq. 6.32

where

$$R = \frac{1}{f_v}\,\frac{1}{A_{rh}}\left[\frac{A_r}{\eta_d \bar{h}_a A_a} + \frac{1}{h_v}\right] \tag{6.32}$$

The fraction of the evaporator in the superheated region is simply whatever is not in two-phase, i.e.,

$$f_v = 1 - f_{tp} \tag{6.33}$$

However, the average specific heat of the vapor, and thus the capacity rate of the refrigerant vapor, C_r, depends on the unknown exit refrigerant temperature. Thus, the effectiveness and fraction of the coil in the vapor region of the evaporator must be found as the result of an iteration on the exit state.

The fraction of the coil in the superheated region of the condenser requires one further iteration. Since all three refrigerant regions can occur in the condenser, f_v cannot be calculated from Eqs. 6.28 and 6.33. The fraction of the condenser which is superheated is found by iterating on f_v, and thus C_{max}/C_{min}, until Eq. 6.34 is satisfied, i.e.,

$$\frac{C_{max}\left|T_{in} - T_{out}\right|_{max}}{C_{min}\left(T_{r,in} - T_{a,in}\right)} = \varepsilon_v\left(\frac{C_{max}}{C_{min}},\ N_{tu}\right) \tag{6.34}$$

where

$$C_a = \dot{m}_a c_{pm} f_v = C_{min} \text{ or } C_{max} \ . \tag{6.35}$$

The single-phase effectiveness vs. N_{tu} relations, Eqs. 6.29-6.32, are also used to calculate the effectiveness of the subcooled fraction of the condenser, ε_ℓ, (f_ℓ is necessarily used in place of

f_v). If there is liquid refrigerant at the condenser exit, f_ℓ can be calculated from the previously determined values of f_v and f_{tp} using Eq. 6.36

$$f_\ell = 1 - f_{tp} - f_v \tag{6.36}$$

and C_a calculated as in Eq. 6.35 with f_v replaced by f_ℓ.

The refrigerant capacity rate, C_r, depends on the average specific heat for the subcooled region and hence on the unknown exit temperature. Thus, the effectiveness and heat transfer rate for the subcooled region are found by iterating on the exit temperature and average specific heat for the liquid refrigerant.

The heat transfer rate for the entire coil is calculated as the sum of the rates for the two-phase, subcooled, and superheated regions. The heat transfer rate for the two-phase region is calculated according to Eq. 6.25 while those for the single-phase regions are computed using Eq. 6.37,

$$\dot{Q} = \dot{m}_r \, c_p \Delta T_r \quad . \tag{6.37}$$

The air-side temperature change for each of the three regions is determined using Eq. 6.38,

$$\Delta T_a = \frac{\dot{Q}}{C_a} \quad . \tag{6.38}$$

where $\dot{Q}$ is sensible heat transfer only and both $\dot{Q}$ and C_a pertain to the particular region of the coil. The outlet air temperature from either heat exchanger is calculated by Eq. 6.39,

$$T_{a,out} = T_{a,in} + \frac{\sum \dot{Q}_i}{\dot{m}_a c_{pm}} \tag{6.39}$$

where the summation is over the two or three refrigerant regions of evaporator or condenser, respectively.

6.6 Fan Motor and Compressor Shell Heat Losses

Section 7 contains a discussion of the air-side pressure drops and fan motor power consumption. The Heat Pump Design Model has an option (specified with the input data) which allows the user to determine whether or not fan motor or compressor-shell heat losses are added to the incoming or exiting air for each heat exchanger. For blow-through units, the fan heat is added to the air before it crosses the coil, and hence before coil performance is computed. Alternatively, the fan heat can be added after the air has crossed the coil for draw-through units so that only the exit air temperature is affected. The compressor placement in the air stream, i.e., before or after the heat exchanger, can also be specified. If desired, the compressor shell and/or fan heat losses can be omitted from the air temperature calculations.

7. AIR-SIDE PRESSURE DROPS AND FAN POWERS

The air-side pressure drop for the indoor unit is calculated as the sum of pressure drops due to the ducts, filter, supplemental heaters, and the coil and cabinet:

$$\Delta P_{indoor} = \Delta P_{ducts} + \Delta P_{filter} + \Delta P_{heaters} + \Delta P_{coil\ and\ cabinet}$$

The first three components are computed using the correlations given in Eqs. 7.1 – 7.3 [34,35,36],

$$\Delta P_{ducts} = 2.035 \times 10^{-8}(0.03613)\frac{\dot{Q}^{1.84}}{D^{5}_{ducts}} \tag{7.1}$$

$$\Delta P_{filter} = 6.75 \times 10^{-7}\,(0.03613)\left(\frac{\dot{Q}}{A_{filter}}\right)^{2} \tag{7.2}$$

$$\Delta P_{heaters} = 1.027 \times 10^{-7}\,(0.03613)\;\alpha_{racks}\left(\frac{\dot{Q}}{A_{heater}}\right)^{2} \tag{7.3}$$

where

$\dot{Q}$ - the volumetric air-flow rate

A_{filter} - the frontal area of the filter, and

A_{heater} - the cross-sectional area of the resistance heater section.

The constant α_{racks} depends on the number of racks of heater elements and is 1.0 for one or two racks, 2.0 for three racks, and 2.4 for four racks.

The correlation [34] for the pressure drop across dry, wavy- or louvered-fin coils depends on the fin type, the number of tube rows, N_T,

the fin pitch, F_p, and the air face velocity, represented as the ratio of the volumetric air flow rate to the frontal area, $\dot{Q}/A$, i.e.,

$$\Delta P_{\text{coil \& cabinet,dry}} = 1.10(0.03613)\left[3.84 \times 10^{-6}\left(\frac{N_T}{2}\right)^{0.7}\right] \times \left[0.235 + 0.0638F_p\right]\left[\frac{\dot{Q}}{A}\right]^{1.7} \quad . \quad (7.4)$$

The value of ΔP given from Eq. 7.4 is increased by 10% for louvered fins as reported by Hosoda [37]. The pressure drop across the fraction of the coil which is wet due to dehumidification is increased by a factor w which is correlated to the gap (in mm) between fins [37], i.e., $[1/F_p - \delta]$.

$$w = 1.2 + 1.359\ (1/F_p - \delta)^{-0.5786}$$

Thus

$$\Delta P_{\text{coil \& cabinet}} = \Delta P_{\text{coil \& cabinet,dry}} \cdot [(1 - F_w) + F_w w] \quad (7.5)$$

where

$$F_w = F_{w,tp}\, f_{tp}$$

F_w is the fraction of the evaporator air-side area wetted by dehumidification and $F_{w,tp}$ is the fraction of the coil depth in the two-phase region that is wetted.

The coil pressure drop for smooth fins is based on Fanning friction factors for the dry and wet regions and correlating parameters FP and F(s) defined by McQuiston [26,27]:

$$f_{dry} = 0.004904 + 1.382\ (FP)^2$$

$$f_{wet} = 0.004904 + 1.382\ [F(s)\ FP]^2,$$

$$\text{where } FP = \left(\frac{D_a}{2Re_D R^*}\right)^{.25}\left(\frac{(S_t - D_a)F_p}{4(1 - F_p\delta)}\right)^{-0.4}\left(\frac{S_t}{2R^*} - 1\right)^{-0.5}$$

$$F(s) = (1 + N_{Re}^{-0.4})\left(\frac{1}{1 - F_p\delta}\right)^{1.5},$$

$$R^* = \frac{D_a}{2(1 - F_a)[(S_t - D_a)F_p + 1]}, \text{ and } Re_D = \frac{G_a D_a}{\mu_a}.$$

Using the above correlations, the value of $\Delta P_{coil\ \&\ cabinet}$ for smooth dry or wet fins is given by Eq. 7.6,

$$\Delta P_{coil\ \&\ cabinet} = \frac{1.10\ f_{tot}\ A_{min}\ G_a^2}{2\rho_a(32.174)(3600)^2\ (144)}, \tag{7.6}$$

where f_{tot} is a weighted sum of the wet and dry Fanning friction factors given by

$$f_{tot} = f_{dry}(1 - F_w) + f_{wet}\ F_w \tag{7.7}$$

The parameter A_{min} in Eq. 7.5 is the ratio of total air-side area to minimum free-flow area. Note that the effect of the number of tube rows is implicitly included in A_{min}. The 1.1 factor in Eqs. 7.4 and 7.6 is to account for cabinet pressure drop.

The air-side pressure drop for the outdoor unit contains only components for losses due to the coil and cabinet. Equation 7.5 is used to compute $\Delta P_{outdoor}$ for a coil with smooth fins and Eq. 7.4 for a coil with either wavy or louvered fins.

The fan motor power consumption, $\dot{W}_{fan}$, is computed according to Eq. 7.8,

$$\dot{W}_{fan} = 11.1\ \frac{\dot{Q}\ \Delta P_{air}}{\eta_{fan,motor}} \tag{7.8}$$

where the constant is to convert to consistent units. The combined fan and fan-motor efficiency, $\eta_{fan,motor}$, is a constant for the indoor unit and can be held constant or allowed to vary with the fan specific speed for the outdoor unit. If the built-in outdoor fan curve is

selected (see Appendix A), the static efficiency of the fan is computed according to Eqs. 7.9 and 7.10 as a function of the specific speed, S_s.

$$\eta_{static} = -3.993 + 4.266 \log_{10}\left(\frac{S_s}{1000}\right) - 1.024 \left[\log_{10}\left(\frac{S_s}{1000}\right)\right]^2 \quad (7.9)$$

where

$$S_s = S_{fan}(\dot{Q})^{0.5} (\Delta P_{H_2O})^{-0.75} \quad (7.10)$$

Equation 7.9 is for a representative propeller fan. The coefficients in Eq. 7.9 are assigned in BLOCK DATA (see Appendix C) as well as a representative fan speed of 825 rpm and fan motor efficiency of 55%. The combined fan and fan-motor efficiency is given by Eq. 7.11,

$$\eta_{fan,motor} = 0.55\ \eta_{static} \quad (7.11)$$

An outdoor fan efficiency curve is provided as an option for the outdoor coil because the outdoor coil and fan characteristics are closely coupled. The indoor fan is less affected by the indoor coil air-side pressure drop than by the rest of the indoor duct system. Therefore, an after-the-fact selection of an indoor fan will not be likely to result in any compatibility problems. Such a problem might occur, however, in the outdoor coil, i.e., fan requirements may not be easily met with current fans [8].

The various correlations for coil air-side pressure drops given here are not widely verified nor well correlated (e.g., ± 35% for smooth fins). The smooth-fin correlation (for a dry condition) predicts pressure drops some 20% higher than the wavy-fin equation. This is a contradiction of the results of Yoshii [28] and of general expectations regarding wavy fins vs. smooth fins. The wavy fin equations given by Kirshbaum and Veyo [34], however, agree well with the results given by Hosoda [37]. *The user should be aware of these inconsistencies* and should rely on experimental data specific to the application at hand whenever possible.

8. PRESSURE AND ENTHALPY CHANGES IN REFRIGERANT LINES

All of the refrigerant-side pressure losses are computed on the basis of equivalent lengths. The equivalent length and inside diameter of each section of refrigerant piping, denoted by L, and D, respectively, are specified as part of the input data (see Appendix A) for:

- the liquid line from the condenser to the flow control device,
- the line from the outdoor coil to the reversing valve,
- the line from the indoor coil to the reversing valve, and
- the suction and discharge lines from the compressor shell inlet and outlet to the reversing valve.

The rates of heat loss in the discharge and liquid lines, $\dot{Q}_{dis}$ and $\dot{Q}_{liquid\ line}$, and the heat gain in the suction line, $\dot{Q}_{suction\ line}$, can also be specified in order to allow enthalpy changes in the piping, i.e.,

$$\Delta h = \dot{Q}/\dot{m}_r$$

The line specifications are independent of operating mode. Pressure and enthalpy changes in the suction and discharge lines and lines from coils to reversing valve are calculated in the compressor subroutines, COMP and CMPMAP, while the liquid line is modeled in subroutine FLOBAL.

The Darcy incompressible flow relation, as given by Eq. 8.1, is used to compute the pressure drop of the refrigerant in both the compressor suction and discharge lines:

$$\Delta P = \frac{2f(L/D)G^2}{\rho_{ave}} \qquad (8.1)$$

where f is the Moody friction factor. Thus, it has been assumed that there are no significant density or momentum changes in these lines.

If there is two-phase flow in the suction line the pressure drop is approximated by 190% of the pure vapor value, rather than iterating to find the lengths of pipe having single-phase and two-phase flow. The Moody friction factor, f, in Eq. 8.1 is computed using a subroutine written by Hiller and Glicksman [3] and takes into account the surface roughness of the tubes (see Appendix C).

The refrigerant-side pressure drops for the evaporator and condenser are calculated separately for the superheated, two-phase, and subcooled regions of each coil. The pressure drop in the vapor region is computed as the sum of changes due to momentum and friction effects and due to losses in the return bends. The momentum component of the pressure drop is given by Eq. 8.2,

$$\Delta P_{v,mom} = \pm \frac{G^2(\nu_o - \nu_i)}{(32.174)(3600)^2\ (144)} \tag{8.2}$$

where the plus sign is used for the evaporator and the minus sign for the condenser. The Moody friction factor, f, and the equivalent length of tubing in the vapor region, L/D, are used to compute the pressure drop due to friction from Eq. 8.3.

$$\Delta P_{v,frict} = \frac{G^2\ f(L/D)\ 2\nu_{ave}}{(32.174)(3600)^2\ (144)} \tag{8.3}$$

where $\nu_{ave} = (\nu_o + \nu_i)/2$. Finally, the pressure drop in the return bends is computed using Eq. 8.4 from Ito [38] where S_T is the spacing between tube passes and N_{rb} is the number of return bends in the vapor region of the coil.

$$\Delta P_{v,rb} = \left\{0.4338\ [1 + 116\ (\frac{S_T}{D})^{-4.52}]\ (\frac{S_T}{D})^{0.84}\right\} \times \frac{N_{Re}^{-0.17}\ G^2\ N_{rb}\ \nu_{ave}}{2(32.174)(3600)^2\ (144)} \tag{8.4}$$

It has been assumed that the density changes in the subcooled region of the condenser are insignificant, so the pressure drop in the liquid region only has friction and return bend components. These factors are computed using Eqs. 8.3 and 8.4 with the properties and parameters referring to the liquid refrigerant region rather than the vapor region.

The pressure drop in the two-phase region of each heat exchanger is calculated as the sum of momentum, friction, and return bend components integrated over the two-phase region. The momentum and friction terms are computed using equations from Thom [39] as discussed by Goldstein [40], that is,

$$\Delta P_{tp,mom} = \frac{G^2}{C_o \rho_\ell} \left[r_2(x_o) - r_2(x_i) \right] \tag{8.5}$$

and

$$\Delta P_{tp,frict} = C_2 \left[x_o r_3(x_o) - x_i r_3(x_i) \right] \tag{8.6}$$

where

$C_o = (32.174)(3600)^2\ (144)$,

$C_1 = (x_o - x_i)/L_{tp}$,

$C_2 = \dfrac{0.184\ N_{Re_\ell}^{-0.2}\ G^2}{2 C_o C_1 D \rho_\ell}$,

$r_2(x)$ = acceleration multiplier tabulated by Thom as a function of quality and steam pressure,

and

$r_3(x)$ = frictional multiplier tabulated by Thom as a function of quality and steam pressure.

The values of steam pressure in Thom's tables [39] have been converted to equivalent property index values where the property index is given by Goldstein [40] as ρ_ℓ/ρ_v. Double-quadratic interpolations are used to obtain values of r_2 and r_3 as a function of quality and property index.

The total pressure drop in the return bends with two-phase flow is computed using Eq. 8.7 an equation due to Geary [41].

$$\Delta P_{tp,rb} = \frac{5.58\ 10^{-6}(N_{Re_{sat}})^{1/2} x_m (1.5708)(\frac{S_T}{D})\ G^2 e^{-0.215(S_T/D)}\ N_{rb,tp}}{2\rho_v\ (32.174)(3600)^2} \quad (8.7)$$

where

$$x_m = (x_o^{2.25} - x_i^{2.25})/[2.25(x_o - x_i)] \quad (8.8)$$

9. MODEL VALIDATION

9.1 Introduction

Earlier versions of the ORNL heat pump model have been tested [1,2,7] against data taken in our laboratory [42] to assess the accuracy of the calculations. Since a number of air and refrigerant-side correlations have been improved from the previous versions, a new validation is needed. The present version has been validated against the same data base [42] as previously used except for an important correction to the experimental data. It was recently found by Miller [43] that the rotameter used in the original experiment gave results which underestimated the refrigerant mass flow rate by 5 to 20% (with the larger errors occurring at lower mass flow rates) when compared to a more accurate turbine flow meter. This finding is consistent with the observations that

- the air-side heating capacities in the original experiment were generally 5 to 15% higher than the refrigerant-side values,
- the agreement between air and refrigerant-side values in Miller's experiment [43] using the turbine meter was within 4%, and
- the refrigerant mass flow rates measured in Miller's experiment are within $\pm$ 1% of the compressor map value [10].

Thus, in previous validations where the compressor model was "calibrated" with experimental data, values of refrigerant mass flow rate that were too low were used in the heat exchanger calculations. The geometry of the low-bid test unit as described by Domingorena [42] and given in the sample input in Appendix B is used for all validation runs discussed here.

9.2 Compressor Modeling

Previous validations have been made using a "calibrated" loss and efficiency-based compressor model. The loss and efficiency-based compressor model, as discussed in Section 4, cannot model existing compressors over a range of operating conditions as accurately as can the map-based

model. For this reason, the curves of a compressor map for the Tecumseh AH5540E compressor used in the laboratory unit were fit over the operating conditions of interest (using the program in Appendix M) to obtain coefficients for a biquadratic fit of compressor power and refrigerant mass flow rate as functions of condensing and evaporating saturation temperatures.

The predictions of the compressor map model, as reported by Dabiri and Rice [10], are shown in Table 9.1 and compared with the "corrected" experimental data at the validation points to be considered here. These tabulations show that the compressor map model slightly overpredicts refrigerant mass flow rate and more significantly underpredicts the required compressor input power.

Experimental data with which to compare the compressor map model may not be available to many users of the heat pump model. For such users, the errors of the magnitude shown in Table 9.1 and Ref. 10 must be expected. However, if experimental data are available, the compressor map equations can be refined to predict the performance of a specific compressor more accurately by the use of multiplicative correction constants.

9.3 Heat Exchanger Calibration

Such corrections to the compressor map equations were performed for validation runs at ambient temperatures of 5.4°C (41.7°F) and 10.6°C (51.0°F). By making such corrections, the accuracy of the heat exchanger predictions can be examined independently of the accuracy of the compressor model for the purpose of heat exchanger model calibration.

The heat exchangers on both the indoor and outdoor coil of the laboratory test unit have wavy fin surfaces; however, the only general air-side heat transfer correlations that are available [26,27] are for smooth fins. Thus it was decided to adjust the air-side heat transfer coefficient for smooth fins by a multiplicative factor until good agreement in heating capacity (based on refrigerant-side calculations) was reached between model and experiment.

Table 9.1

Comparison of Experimental Data with Predictions of Compressor Map Model

Ambient Temperature °C (°F)	Calculated Value	Observed Value	% Difference Calculated/Observed
	Comparison of refrigerant mass flow rates		
5.4 (41.7)	0.045 (359)	0.044 (351)	2.3
10.6 (51.0)	0.048 (379)	0.047 (371)	2.2
	Compressor Power Input (watts)		
5.4 (41.7)	3779	4090	-7.6
10.6 (51.0)	4011	4170	-3.8

9.4 Heat Pump Validation at a 5.4°C (41.7°F) Ambient

This procedure was carried out for the 5.4°C (41.7°F) ambient, heating-mode case. Table 9.2 gives the results of the final validation run with a multiplicative factor of 1.45 applied to the smooth-fin, air-side heat transfer coefficient. This validation run and the limited experimental results of Yoshii [28] form the basis for our choice of a 1.45 factor for wavy fin geometry as discussed in Section 6. The model values for indoor and outdoor fan power consumptions were set equal to the experimental values because the unit was tested in atypical duct loops. Experimental values for the compressor shell heat loss as a fraction of the compressor input power and the suction, discharge, and liquid line heat transfer rates were also specified as input data for the model. Thus, Table 9.2 is primarily a test of the accuracy of heat exchanger models and the capillary tube model. Since the air-side heat transfer coefficient was uniformly adjusted until the calculated heating capacity was in reasonably good agreement with the measured capacity, the validation check points are the refrigerant pressures and temperatures throughout the cycle and the evaporator capacity, refrigerant mass flow rate, compressor power input, and the COP (the latter four because they are functionally dependent on the condenser and evaporator saturation temperatures obtained from the heat exchanger energy balances). The calculated value of capillary tube flow factor can also be compared with the actual value.

Comparison of the calculated and observed values of refrigerant pressures and temperatures shows excellent agreement (i.e., within 0.6 C° (1.0 F°); 1.5 kpa (0.2 psi) on the low-side and 24 kpa (3.7 psi) on the high side) except for the refrigerant temperature at the evaporator inlet. At this location the measured value is 4.9 C° (8.8 F°) higher than the calculated value. However, the experimental value was measured upstream of the evaporator inlet header, and the inlet header pressure drop (which would have the largest pressure drop since the refrigerant is in a two-phase state) is not accounted for in the model. The computed evaporator capacity, refrigerant mass flow rate, compressor power input and COP are each within 1% of the experimental values.

Table 9.2

Heat Pump Model Validation at 5.4°C (41.7°F) Ambient

Compressor Performance	Observed	Calculated
Refrigerant mass flow rate, kg/h (lbm/h)	159 (351)	160 (353)
Compressor-motor power input, kW	4.09	4.11
Compressor shell heat loss, kW (Btu/h)	1.497 (5109)	1.503 (5130)
Overall isentropic efficiency, %	44.8	45.4
Refrigerant-Side Conditions		
Temperatures, °C (°F)		
Compressor shell inlet	6.00 (42.8)	5.8 (42.5)
shell outlet	107 (224.0)	107 (224.2)
Condenser inlet	94.3 (201.7)	94.4 (201.9)
outlet	26.6 (79.8)	27.1 (80.8)
subcooling, C° (F°)	24.6 (44.2)[a]	24.6 (44.2)[b]
Capillary tube inlet	24.3 (75.7)	24.8 (76.7)
Evaporator inlet	3.1 (37.6)	-1.8 (28.8)
outlet	3.7 (38.7)	3.7 (38.6)
superheat, C° (F°)	8.1 (14.5)[a]	8.1 (14.5)[b]
Pressures, kPa (psia)		
Compressor shell inlet	429 (62.2)	427 (62.0)
Capillary tube inlet	1891 (274.2)	1914 (277.8)
Air-Side Temperatures, °C (°F)		
Outdoor unit entrance	5.4 (41.7)	5.4 (41.7)[b]
Evaporator entrance	— —	6.8 (44.3)
exit	0.83 (33.5)	1.1 (34.0)
Condenser entrance	22.5 (72.5)	22.5 (72.5)[c]
exit	— —	36.8 (98.3)
Indoor unit exit	38.4 (101.2)	37.7 (99.9)
Capillary Tube Flow Factor	2.2	2.20
Evaporator Capacity, kW (Btu/h)	7.961 (27171)	7.963 (27178)
Heating Capacity, kW (Btu/h)	10.62 (36258)	10.63 (36297)
COP[d]	2.039	2.035

[a] Estimated values (saturation temperatures not known exactly)

[b] Convergence check points (required to agree with observation)

[c] Fixed input value

[d] COP includes fan power of 511 W for outdoor fan, 608 W for indoor fan

The value of capillary flow factor calculated by the program agrees with the value obtained from the curves in the ASHRAE Equipment Handbook [15], to the accuracy with which the published graph can be read. The agreement of exit air temperatures is not particularly useful for validation purposes, except to show consistency in calculated values, i.e., the predicted indoor unit exit air temperature should be lower than the measured value because the measured air-side heating capacity was slightly greater than the refrigerant-side capacity plus the indoor fan power.

The adjustments that were made to the compressor and heat exchanger models did not force agreement on all the system points but rather eliminated known model inadequacies and allowed the heat exchanger routines to be tested in a fair manner.

Table 9.3 gives results for the 5.4°C (41.7°F) ambient case with no corrections applied to the compressor map. The system COP is over-predicted by 5.8% and the heating capacity is underpredicted by 0.9%.

9.5 Heat Pump Validation at 10.6°C (51.0°F) Ambient

Another heating mode validation run was made for the 10.6°C (51.0°F) ambient test condition as reported by Domingorena [42] using the compressor correction factors given in Table 9.1. The calculations are compared to the experimental data in Table 9.4. Comparison of the calculated and observed values of refrigerant pressures and temperatures again shows good agreement except for the evaporator inlet temperature. The computed heating capacity, refrigerant mass flow rate, compressor power input, and COP are within 2.5, 3.0, 0.7, and 2.0%, respectively. The calculated capillary flow factor is again within the "accuracy" of the ASHRAE figure.

Both of the heating mode tests which were used for validation had low values of ambient relative humidity and thus no dehumidification occurred on the outdoor coil. The dehumidification routines have not been validated in either the heating or cooling modes due to a lack of experimental air-to-refrigerant heat exchanger data for simple coil geometries with a fin surface type which the program is equipped to handle.

Table 9.3

Heat Pump Model Validation at 5.4°C (41.7°F) Ambient
Without Corrections to Compressor Map

Compressor Performance	Observed	Calculated
Refrigerant mass flow rate, kg/h (lbm/h)	159 (351)	162 (357)
Compressor-motor power input, kW	4.09	3.76
Compressor shell heat loss, kW (Btu/h)	1.497 (5109)	1.377 (4701)
Overall isentropic efficiency, %	44.8	50.2
Refrigerant-Side Conditions		
Temperatures, °C (°F)		
Compressor shell inlet	6.0 (42.8)	5.6 (42.1)
shell outlet	107 (224.0)	100.2 (212.4)
Condenser inlet	94.3 (201.7)	88.1 (190.6)
outlet	26.6 (79.8)[a]	27.0 (80.6)[b]
subcooling, C° (F°)	24.6 (44.2)[a]	24.6 (44.2)[b]
Capillary tube inlet	24.3 (75.7)	24.7 (76.5)
Evaporator inlet	3.1 (37.6)	-1.9 (28.5)
outlet	3.7 (38.7)[a]	3.4 (38.2)[b]
superheat, C° (F°)	8.1 (14.5)[a]	8.1 (14.5)[b]
Pressures, kPa (psia)		
Compressor shell inlet	429 (62.2)	424 (61.5)
Capillary tube inlet	1891 (274.2)	1907 (276.8)
Air-Side Temperatures, °C (°F)		
Outdoor unit entrance	5.4 (41.7)	5.4 (41.7)[b]
Evaporator entrance	—— ——	6.8 (44.2)
exit	0.83 (33.5)	0.94 (33.7)[c]
Condenser entrance	22.5 (72.5)	22.5 (72.5)[c]
exit	—— ——	36.7 (98.1)
Indoor unit exit	38.4 (101.2)	37.6 (99.6)
Capillary Tube Flow Factor	2.2	2.23
Evaporator Capacity, kW (Btu/h)	7.961 (27171)	8.070 (27544)
Heating Capacity, kW (Btu/h)	10.62 (36258)	10.52 (35921)
COP[d]	2.039	2.156

[a] Estimated values (saturation temperatures not known exactly)

[b] Convergence check points (required to agree with observation)

[c] Fixed input value

[d] COP includes fan power of 511 W for outdoor fan, 608 W for indoor fan

Table 9.4

Heat Pump Validation at 10.6°C (51°F) Ambient

Compressor Performance	Observed	Calculated
Refrigerant mass flow rate, kg/h (lbm/h)	168 (371)	173 (382)
Compressor-motor power input, kW	4.17	4.20
Compressor shell heat loss, kW (Btu/h)	1.556 (5311)	1.565 (5341)
Overall isentropic efficiency, %	47.4	47.9
Refrigerant-Side Conditions		
Temperatures, °C (°F)		
Compressor shell inlet	12.1 (53.7)	12.4 (54.3)
shell outlet	109 (229)	108.1 (226.7)
Condenser inlet	96.4 (205.5)	95.4 (203.7)
outlet	25.4 (77.7)	25.4 (77.7)[b]
subcooling, C° (F°)	29.1 (52.3)[a]	29.1 (52.3)[b]
Capillary tube inlet	24.4 (75.9)	24.4 (76.0)
Evaporator inlet	5.8 (42.4)	0.89 (33.6)
outlet	9.7 (49.5)	10.2 (50.4)[b]
superheat, C° (F°)	11.9 (21.4)[a]	11.9 (21.4)[b]
Pressures, kPa (psia)		
Compressor shell inlet	461 (66.9)	468 (67.9)
Capillary tube inlet	2030 (294.4)	2030 (294.7)
Air-Side Temperatures, °C (°F)		
Outdoor unit entrance	10.6 (51.0)	10.5 (50.9)[b]
Evaporator entrance	— —	12.1 (53.8)
exit	5.3 (41.5)	5.2 (41.4)
Condenser entrance	20.9 (69.6)	20.9 (69.6)[c]
exit	— —	36.7 (98.1)
Indoor unit exit	38.6 (101.5)	37.6 (99.6)
Capillary Tube Flow Factor	2.2	2.24
Evaporator Capacity, kW (Btu/h)	8.577 (29272)	8.839 (30168)
Heating Capacity, kW (Btu/h)	11.25 (38407)	11.53 (39358)
COP[d]	2.140	2.182

[a] Estimated values (saturation temperatures not known exactly)

[b] Convergence check points (required to agree with observation)

[c] Fixed input value

[d] COP includes fan power of 499 W for outdoor fan, 590 W for indoor fan

9.6 Cooling Mode Results

While no cooling mode data were taken by Domingorena [42], the predictions of the ORNL heat pump model can be compared with the rated cooling-mode performance at an ambient temperature of 35°C (95°F) and indoor conditions of 26.7°C (80°F) and 51% relative humidity. The rated cooling performance of the laboratory test unit at the above conditions is:

- a total cooling capacity of 10.55 KW (36,000 Btu/h), and
- an EER of 6.3 (Btu/h)/W

In order to model the test unit in the cooling mode without test data, the capillary tube model is used (for three capillary tubes in parallel, having a flow factor of 1.42) to eliminate the need for an experimental value of condenser subcooling. Also, an assumption of 1.67 C° (3 F°) of evaporator superheat is made. Representative values for the compressor shell heat loss fraction and the refrigerant line heat transfer rates from the heating mode tests are assumed. The compressor map is used without any "calibration" adjustments. The indoor fan power consumption recommended by the Air-Conditioning and Refrigeration Institute for rating purposes [44] of 365 watts per 472 ℓ/sec (1000 cfm) was assumed [yielding a total of 438 watts for 566 ℓ/sec (1200 cfm)] along with an outdoor fan power consumption of 513 watts (obtained from the heating mode tests). The calculated results are:

- a total cooling capacity of 10.24 kW (34963 Btu/h),
- an EER of 6.40, and
- a sensible to total capacity ratio of 0.76,

for an underestimate of 2.9% in rated capacity and an overestimate of 1.6% in rated EER. The sensible to total capacity ratio of 0.76 seems to be a reasonable value; however, no manufacturer's values were available for comparison.

It can be fairly concluded that, based on the available data, the ORNL Heat Pump Model is capable of accurately predicting the performance

of existing equipment of specific types provided that minimal experimental data are available:

- to specify the evaporator superheat,
- to estimate compressor shell and refrigerant line heat transfer rates, and
- to calibrate the fan power consumption models.

Further, the generality built into the model provides the capability for good predictions in design situations different from current practice.

10. RECOMMENDATIONS

The ORNL Heat Pump Design Model has been developed to provide a general tool for the prediction of the steady-state performance of existing and new designs of electrically driven air-to-air heat pumps. As such, this program can be considered complete. There are, obviously, other modular routines, such as:

- liquid-to-suction line heat exchanger models,
- interconnecting pipe heat loss models,
- generalized or empirical desuperheater models,
- tube-by-tube condenser and evaporator models,
- correlations for thermo-electric expansion valves,
- heat transfer and pressure drop correlations for dry and wet spine-fin heat exchangers,
- water-to-refrigerant heat exchanger models, and
- fan efficiency curves for tube- and vane-axial and forward- and backward-curved centrifugal fans

which could be developed from existing information and added as the specific need arose. The model contains all of the general component calculations and interconnections that we judge significant to a broad community of users. Furthermore, the documentation in the body and appendices of this report contains sufficient information so that individuals can modify the code to accomodate their own needs and interests (such as those listed above).

Modifications and improvements will most likely need to be made as new information becomes available since assumptions and limitations have been imposed on the model due to lack of data and correlations. Improvements which could be made later include:

- extension of the flow-control device models to handle two-phase refrigerant at the inlet,
- substitution of more consistent and general air-side heat transfer and pressure drop equations for smooth, wavy, and louvered fin surfaces under wet and dry coil conditions,
- use of better refrigerant-side heat transfer and pressure drop correlations for the evaporator,

- addition of pressure drop models for the heat exchanger headers,
- addition of heat transfer, pressure drop, and leakage models of reversing valves,
- addition of a more general TXV model as described by Dhar [45],
- accounting for the effects of coil orientation (i.e., slant, A-coils) on heat exchanger performance,
- development of a wide-range efficiency and loss-based compressor model following the work of Davis and Scott [12],
- development of a map-based compressor model which can be applied for different refrigerants, and
- addition of the capability to model discrete and continuous compressor speed changes.

An important capability which is not in the Heat Pump Design Model is refrigerant charge inventory—how much refrigerant is in each heat exchanger, the compressor, and the lines. Although some information on this subject is available in the literature, it is a significant development effort to incorporate these calculations into the model and to validate the results. This capability, however, would significantly broaden the use of the model. The user would be able to:

- model a given system over a range of ambient temperatures without knowledge of the evaporator superheat level at each ambient condition,
- determine parametrically the optimum refrigerant charge for a system,
- estimate cycling losses due to pressure equilization, and
- calculate concentration and performance changes when using non-azeotropic refrigerant mixtures for capacity modulation [46].

Here again, this report contains adequate information about the structure and organization of the computer program so that this capability can be added to the model with a minimum of difficulty.

11. REFERENCES

1. R. D. Ellison and F. A. Creswick, *A Computer Simulation of Steady State Performance of Air-to-Air Heat Pumps*, ORNL/CON-16, 1978.

2. R. D. Ellison et al., "Heat Pump Modeling: A Progress Report," *Proceedings of the Fourth Annual Heat Pump Technology Conference*, Oklahoma State University, Stillwater, April 9-10, 1979.

3. C. C. Hiller and L. R. Glicksman, *Improving Heat Pump Performance via Compressor Capacity Control — Analysis and Test*, Vols. I and II, MIT Energy Laboratory Report No. MIT-EL 76-001, 1976.

4. G. T. Kartsounes and R. A. Erth, "Computer Calculation of the Thermodynamic Properties of Refrigerants 12, 22, and 502," *ASHRAE Transactions*, Vol. 77, Part II, 1971.

5. J. E. Flower, *Analytical Modeling of Heat Pump Units as a Design Aid and for Performance Prediction*, Lawrence Livermore Laboratory Report, UCRL-52618, 1978.

6. T. Kusuda, *NBSLD, the Computer Program for Heating and Cooling Loads in Buildings*, NBS Building Science Series 69, July 1976.

7. C. K. Rice et al., *Design Optimization and the Limits of Steady-State Heating Efficiency for Conventional Single-Speed Air-Source Heat Pumps*, ORNL/CON-63, 1981.

8. C. K. Rice et al., "Design Optimization of Conventional Heat Pumps: Applications to Steady-State Heating Efficiency," *ASHRAE Transactions*, Vol. 87, Part I, 1981.

9. R. C. Downing, "Refrigerant Equations," *ASHRAE Transactions*, Vol. 80, Part II, 1974.

10. A. E. Dabiri and C. K. Rice, "A Compressor Simulation Method with Corrections for the level of Suction Gas Superheat," *ASHRAE Transactions*, Vol. 87, Part II, 1981.

11. S. E. Veyo, Westinghouse Electric Corporation, Pittsburgh, PA, private communication, 1981.

12. G. L. Davis and T. C. Scott, "Component Modeling Requirements for Refrigeration System Simulation," *Proceedings of the 1976 Purdue Compressor Technology Conference*, July 3-6, 1976.

13. J. H. Johnson, "Hermetic Motor Efficiency," *Proceedings of the Conference on Improving Efficiency and Components in HVAC Equipment and Components for Residential and Small Commercial Buildings*, Purdue University, October 1974.

14. R. W. Shaffer and W. D. Lee, "Energy Consumption in Hermetic Refrigerator Compressors," *Proceedings of the 1976 Purdue Compressor Technology Conference*, Ray W. Herrick Laboratories, West Lafayette, Indiana, July 6-9, 1976.

15. American Society of Heating, Refrigerating, and Air-Conditioning Engineers, 1975 Equipment Volume, Chapter 20, pp. 20.20-20.27.

16. L. D. Smith, *Influence of the Expansion Device on the Performance of a Residential Air Conditioning Unit*, University of Illinois at Urbana-Champaign, Masters Thesis, 1978.

17. Bulletin F210-10-3, Sporlan Valve Company, July 1970.

18. Bulletin 20-10, Sporlan Valve Company, June 1975.

19. V. C. Mei, "Short Tube Refrigerant Flow Restrictors," to be published.

20. W. M. Kays and A. L. London, *Compact Heat Exchangers*, McGraw-Hill Book Company, New York, 1974, p. 182.

21. F. W. Dittus and L. M. K. Boelter, University of California (Berkeley) Pub. Eng., Vol. 2, p. 443, 1930.

22. D. P. Travis, A. B. Baron, and W. M. Rohsenow, "Forced Convection Condensation Inside Tubes: A Heat Transfer Equation for Condenser Design," *ASHRAE Transactions*, Vol. 79, Pt 1, 1973.

23. W. M. Rohsenow and J. P. Hartnett, eds., *Handbook of Heat Transfer*, McGraw-Hill Book Company, p. 12-29, 1973.

24. J. B. Chaddock and J. A. Noerager, "Evaporation of Refrigerant 12 in a Horizontal Tube with a Constant Wall Heat Flux," *ASHRAE Transactions*, Vol. 72, Pt. 1, 1966.

25. B. K. Sthapak, H. K. Varma, and C. P. Gupta, "Heat Transfer Coefficients in Dry-Out Region of Horizontal Tube," *ASHRAE Transactions*, Vol. 82, Pt. 2, 1976.

26. F. C. McQuiston, "Finned Tube Heat Exchangers; State of the Art for the Air Side," *ASHRAE Transactions*, Vol. 87, Pt. 1, 1981.

27. F. C. McQuiston, "Correlation of Heat, Mass, and Momentum Transport Coefficients for Plate-Fin-Tube Heat Transfer Surfaces with Staggered Tube," *ASHRAE Transactions*, Vol. 84, Part 1, 1978.

28. T. Yoshii, "Transient Testing Technique for Heat Exchanger Fin," *Reito*, 47:531, 1972, pp. 23-29.

29. T. Senshu, et al, "Surface Heat Transfer Coefficient of Fins Utilized in Air-Cooled Heat Exchangers," *Reito*, 54:615, 1979, pp. 11-17.

30. American Society of Heating, Refrigerating and Air-Conditioning Engineers, *Thermophysical Properties of Refrigerants*, 1976.

31. R. J. Myers, *The Effect of Dehumidification on the Air-Side Heat Transfer Coefficient for a Finned Tube Coil*, University of Minnesota, Master's Thesis, 1967.

32. T. E. Schmidt, "Heat Transfer Calculations For Extended Surfaces," *Refrigerating Engineering*, April 1949, pp. 351-357.

33. F. C. McQuiston and D. R. Tree, "Optimum Space Envelopes of the Finned Tube Heat Transfer Surface," *ASHRAE Transactions*, Vol. 79, Pt. 2, 1973.

34. H. S. Kirschbaum and S. E. Veyo, *An Investigation of Methods to Improve Heat Pump Performance in a Northern Climate*, Vol. I-III, Electric Power Research Institute, EPRI EM-319, January 1977.

35. ————————, *Energy Efficiency Program For Room Air Conditioners, Central Air Conditioners, Dehumidifiers, and Heat Pumps*, Science Applications, Inc., SAI-77-858-LJ, La Jolla, CA, March 1978.

36. ————————, "Split System Weathertron Heat Pumps," *General Electric Product Data*, Publication No. 22-1009-6, p. 7, April 1977.

37. T. Hosoda, H. Uzuhashi, and N. Kobayashi, "Louver Fin Heat Exchangers," *Heat Transfer Japanese Research*, Vol. 6, No. 2, pp. 67-77, 1977.

38. H. Ito, "Pressure Losses in Smooth Pipe Bends," *Journal of Basic Engineering, Transactions of the ASME*, March 1960, p. 135.

39. J. R. S. Thom, "Prediction of Pressure Drop During Forced Circulation Boiling of Water," *International Journal of Heat and Mass Transfer*, Vol. 7, pp. 709-724, 1964.

40. S. D. Goldstein, "On the Calculation of R-22 Pressure Drop in HVAC Evaporators," *ASHRAE Transactions*, Vol. 85, Part 2, 1979.

41. D. F. Geary, "Return Bend Pressure Drop in Refrigeration Systems," *ASHRAE Transactions*, Vol. 81, Pt. I, 1975.

42. A. A. Domingorena, *Performance Evaluation of a Low First-Cost, Three Ton, Air-to-Air Heat Pump in the Heating Mode*, ORNL/CON-18, October, 1978.

43. W. A. Miller, *The Influence of Ambient Temperature and Relative Humidity on the Heating Mode Performance of a High-Efficiency Air-to-Air Heat Pump*, University of Tennessee, Masters Thesis, 1980.

44. Air-Conditioning and Refrigeration Institute, *Standard for Air-Source Unitary Heat Pump Equipment*, ARI 240-77 (1977).

45. M. Dhar and W. Soedel, "Transient Analysis of a Vapor Compression Refrigeration System: Part I - The Mathematical Model," *XV International Congress of Refrigeration*, Venice, Italy, September 1979.

46. W. D. Cooper and H. J. Borchardt, "The Use of Refrigerant Mixtures in Air-to-Air Heat Pumps," *XV International Congress of Refrigeration*, Venice, Italy, September 1979.

Appendix A: Definitions of Input Data

MISCELLANEOUS DATA

Card 1		FORMAT(20A4)	
	ITITLE	Descriptive title for system described by this data set.	SAMPLE
Card 2		FORMAT(3F10.0)	
	FIXCAP	Value of desired heating capacity, used to calculate supplemental resistance heat (Btu/h).	40000.0
	DDUCT	Diameter of each of 6 identical air ducts with equivalent lengths of 100 ft (in).	8.00
	SUPER	Specified superheat at the outlet from the evaporator (F), use the negative of the desired quality for incomplete evaporation, i.e. -0.99 for 99% quality.	10.00
Card 3		FORMAT(6I10)	
	NCORH	Switch to specify cooling or heating mode: =1, for cooling mode, =2, for heating mode.	2
	LPRINT	Output switch to control the detail of printed results: =0, only an energy input and output summary is printed, =1, a summary of the compressor and heat exchanger operating conditions is printed as well as the energy summary, =2, the summaries are printed after each iteration converges, =3, calculated parameters are printed during each iteration.	1
	MCMPOP	Switch to control whether or not heat rejected from the compressor is added to the air flow for the outdoor coil: =0, heat rejected from the compressor is not added to the air flow for the outdoor coil, =1, heat rejected from the compressor is added to the air flow before it crosses the outdoor coil, =2, heat rejected from the compressor is added to the air flow after it crosses the outdoor coil.	1
	MFANIN	Switch to control whether or not heat rejected from the indoor fan is added to the air flow, settings are similar to those for MCMPOP.	2
	MFANOU	Switch to control whether or not heat rejected from the outdoor fan is added to the air flow, settings are similar to those for MCMPOP.	1

MFANFT	Switch to determine whether to use the outdoor fan efficiency curve fit specified in Block Data: =0, use constant fan efficiency specified on Card 19, =1, use the fan efficiency curve fit and constant fan motor efficiency from Block Data.	0

FLOW CONTROL DEVICE DATA - the variables on this card depend on the type of flow control device selected.

Fixed Condenser Subcooling:

Card 4	FORMAT(I10,6F10.0)	
IREFC	=0, for specified refrigerant subcooling at condenser exit,	1
DTROC	Desired refrigerant subcooling at condenser exit (F), use the negative of the desired quality for incomplete condensation, i.e. -0.05 for 5% quality.	45.00

Thermostatic Expansion Valve:

Card 4	Format(I10,6F10.0)	
IREFC	=1 for the thermal expansion valve.	1
TXVRAT	The capacity rating of the TXV (tons).	1.995
STATIC	The static superheat for the TXV (F).	6.00
SUPRAT	The rated operating superheat for the TXV (F).	11.00
BLEEDF	A leakage or bleed factor for the TXV.	1.15
NZTBOP	A switch to bypass the TXV nozzle and tube pressure drop calculations, =1.0, calculate the tube and nozzle pressure drops, =0.0, bypass the tube and nozzle pressure drops.	0.0

Capillary Tube:

Card 4	FORMAT(I10,6F10.0)	
IREFC	=2 for a capillary tube expansion device.	2
CAPFLO	the capillary tube flow factor, see ASHRAE Guide and Data Book, Equipment Vol. (1975), Fig. 41, p.20.25.	5.448
NCAP	the number of capillary tubes.	1.0

Short-Tube Orifice:

Card 4	FORMAT(I10,F10.0)	
IREFC	=3 for a short-tube orifice	3
ORIFD	Diameter of the orifice (in).	0.0544

REFRIGERANT LINES DATA

Card 5	FORMAT(5F10.5)	
DLL	Inside diameter of liquid line from indoor coil to outdoor coil (in).	0.1900
XLEQLL	Equivalent length of liquid line from indoor coil to outdoor coil (ft).	30.4

	QDISLN	Heat loss rate in the compressor discharge line (Btu/h)	2000.0
	QSUCLN	Rate of heat gain in the compressor suction line (Btu/h)	300.0
	QLIQLN	Heat loss rate in the liquid line from the indoor coil to the outdoor coil (Btu/h).	200.0
Card 6		FORMAT(4F10.5)	
	DLRVOC	Inside diameter of refrigerant line from the reversing valve to the outdoor coil (in).	0.68
	XLRVOC	Equivalent length of the refrigerant line from the reversing valve to the outdoor coil (ft).	6.00
	DLRVIC	Inside diameter of refrigerant line from the reversing valve to the indoor coil (in).	.5556
	XLRVIC	Equivalent length of the refrigerant line from the reversing valve to the indoor coil (ft).	30.40
Card 7		FORMAT(4F10.5)	
	DSLRV	Inside diameter of the refrigerant line from the compressor shell inlet to the reversing valve (in).	0.680
	XLEQLP	Equivalent length of the refrigerant line from the compressor suction port to the reversing valve (ft).	2.00
	DDLRV	Inside diameter of the refrigerant line from the compressor shell outlet to the reversing valve (in).	0.556
	XLEQHP	Equivalent length of the refrigerant line from the compressor discharge port to the reversing valve (ft).	2.00

INITIAL ESTIMATES TO BEGIN ITERATIONS

Card 8		FORMAT(3F10.2)	
	TSATEO	Estimate of the saturation temperature at the outlet of the evaporator (F).	30.0
	TSATCI	Estimate of the saturation temperature at the inlet of the condenser (F).	115.0
	XMR	Estimate of the refrigerant mass flow rate (lbm/h).	400.0

COMPRESSOR DATA

Card 9		FORMAT(I10,7F10.0)	
	ICOMP	switch to specify which compressor submodel is to be used, =1, for the efficiency and loss model, =2, for the map-based compressor model.	2
	DISPL	Total compressor piston displacement (cu in).	4.520
	SYNC	when ICOMP = 1, synchronous compressor motor speed when FLMOT (on card 11) is specified (rpm);	3600.0
		actual compressor motor speed when FLMOT (on card 11) is to be calculated (rpm).	3450.0
		when ICOMP = 2, rated compressor motor speed (rpm);	3450.0
	QCAN	Heat rejection rate from the compressor can, used if CANFAC = 0.0 (Btu/h).	0.0

	CANFAC	Switch to control the method of specifying QCAN =0.0, to specify QCAN explicitly, <1.0, to set QCAN = CANFAC * compressor power, =1.0, to set QCAN = 0.9*(1.0 - actual motor efficiency * mechanical efficiency)*compressor power (not used with the map-based model).	0.350

The variables on the next two cards depend on which compressor model is chosen.

Efficiency and Loss Model:

Card 10		FORMAT(8F10.0)	
	VR	Compressor actual clearance volume ratio.	0.06
	EFFMMX	Maximum compressor motor efficiency.	0.82
	ETAISN	Isentropic compressor efficiency.	0.700
	ETAMEC	compressor mechanical efficiency.	0.80
Card 11		FORMAT(I10,7F10.0)	
	MTRCLC	Switch to determine whether compressor full load motor power is specified as input data or if it is calculated, =0, compressor full load motor power is specified as input, =1, compressor full load motor power is calculated.	0
	FLMOT	Compressor motor output at full load, i.e. (0.7457 kW/hp)x(brake hp at rated load), used only if MTRCLC=0 (kW).	2.149
	QHILO	Heat transfer rate from the compressor discharge line to the inlet gas, used if HILOFC=0.0 (Btu/h).	300.0
	HILOFC	Switch to control method of specifying QHILO =0.0, to specify QHILO explicitly, <1.0, to set QHILO=HILOFAC * compressor power, =1.0, to set QHILO=0.03 * compressor power.	0.0

Map-Based Compressor Model:

Card 10		FORMAT(8E10.3)	
	CPOW(1)	Coefficient for the second order term in condensing temperature for the compressor power consumption.	-1.509E-04
	CPOW(2)	Coefficient for the linear term in condensing temperature for the compressor power consumption.	4.089E-02
	CPOW(3)	Coefficient for the second order term in evaporating temperature for the compressor power consumption.	-1.338E-04
	CPOW(4)	Coefficient for the linear term in evaporating temperature for the compressor power consumption.	5.860E-04
	CPOW(5)	Coefficient for the cross-term in condensing and evaporating temperature for the compressor power consumption.	3.638E-04

	CPOW(6)	Constant term in the fit to compressor power consumption as a function of condensing and evaporating temperatures.	9.759E-05
	DISPLB	Base displacement for the compressor map (cu in).	4.520
	SUPERB	Base superheat for the compressor map, use the negative of the return gas temperature to specify a fixed suction temperature, e.g. -65.0 (F).	20.0
Card 11		FORMAT(8E10.3)	
	CXMR(1)	Coefficient for the second order term in condensing temperature for the fit to refrigerant mass flow rate.	-2.675E-02
	CXMR(2)	Coefficient for the linear term in condensing temperature for the fit to refrigerant mass flow rate.	4.633E+00
	CXMR(3)	Coefficient for the second order term in evaporating temperature for the fit to refrigerant mass flow rate.	4.703E-02
	CXMR(4)	Coefficient for the linear term in evaporating temperature for the fit to refrigerant mass flow rate.	9.640E+00
	CXMR(5)	Coefficient for the cross-term in condensing and evaporating temperatures for the fit to refrigerant mass flow rate.	-1.868E-02
	CXMR(6)	Constant term in the fit to refrigerant mass flow rate as a quadratic function in both the condensing and evaporating temperatures.	1.207E-04

INDOOR COIL DATA

Card 12		FORMAT(7F10.6)	
	FINTY	Switch to specify the type of fins, =1.0, for smooth fins, =2.0, for wavy fins, =3.0, for louvered fins.	2.0
	DEA	Outside diameter of the tubes in the indoor coil (in).	0.400
	DER	Inside diameter of the tubes in the indoor coil (in).	0.336
	DELTA	Thickness of the fins in the indoor coil (in).	0.00636
	FP	Fin pitch for the indoor coil (fins/in).	14.00
	XKF	Thermal conductivity of the fins in the indoor coil (Btu/h-ft-F).	128.00
	AAF	Frontal area of the indoor coil (sq ft).	3.1667
Card 13		FORMAT(2F10.0)	
	NT	Number of row of tubes in the indoor coil in the direction of the air flow.	3.0
	NSECT	Number of parallel refrigerant circuits in the indoor coil.	3.0

Card 14		FORMAT(3F10.5)	
	HCONT	Contact conductance between fins and tubes for the indoor coil (Btu/h-sq ft-F).	30000.0
	ST	The vertical spacing of tube passes (in).	1.00
	WT	The spacing of tube rows in the direction of air flow (in).	0.875
Card 15		FORMAT(5F10.4)	
	QA	Air flow rate for the indoor coil (cfm).	1200.0
	TAI	Inlet air temperature for the indoor coil (F).	70.0
	RH	Relative humidity of the inlet air for the indoor coil.	0.50
	RTB	The number of return bends in the indoor coil.	72.00
	FANEF	Combined fan and fan motor efficiency for the indoor coil.	0.200

OUTDOOR COIL DATA

Card 16		FORMAT(7F10.6)	
	FINTY	Switch to specify the type of fins, =1.0, for smooth fins, =2.0, for wavy fins, =3.0, for louvered fins.	2.0
	DEA	Outside diameter of tubes in the outdoor coil (in).	0.400
	DER	Inside diameter of the tubes in the outdoor coil (in).	0.336
	DELTA	The thickness of the fins in the outdoor coil (in).	0.00636
	FP	The fin pitch for the outdoor coil (fins/in).	14.00
	XKF	The thermal conductivity of the fins in the outdoor coil (Btu/h-ft-F).	128.00
	AAF	The frontal area of the outdoor coil (sq ft).	5.040
Card 17		FORMAT(2F10.0)	
	NT	The number of rows of tubes in the outdoor coil in the direction of air flow.	3.0
	NSECT	The number of parallel refrigerant circuits in the outdoor coil.	4.0
Card 18		FORMAT(3F10.5)	
	HCONT	The contact conductance between the fins and tubes for the outdoor coil (Btu/h-sq ft-F).	30000.0
	ST	The vertical spacing of tube passes for the outdoor coil (in).	1.00
	WT	The spacing of tube rows in the direction of air flow for the outdoor coil (in).	0.875
Card 19		FORMAT(5F10.5)	
	QA	The air flow rate for the outdoor coil (cfm).	2300.0
	TAI	The inlet air temperature for the outdoor coil (F).	47.0
	RH	The relative humidity of the air entering the outdoor coil.	0.70
	RTB	The number of return bends in the outdoor coil.	64.00
	FANEF	The combined fan and fan motor efficiency for the outdoor coil, not used if MFANFT=1 on Card 3.	0.160

Appendix B: Sample Input and Output Data

```
SAMPLE DATA SET FOR ORNL HEAT PUMP DESIGN MODEL -- @ 47.0F AMBIENT
   15000.0      8.00     10.00
         2         1         1         2         1         0
         0     45.0
     0.1900    30.40   2000.00    300.00    200.00
     0.6800     6.00    0.5550     30.40
     0.6800     2.00    0.5550      2.00
      30.00   130.00     400.0
         2     4.520   3450.00       0.0     0.350
-1.509E-04 4.089E-02-1.338E-04 5.860E-04 3.638E-04 9.759E-05  4.52E+00  20.0E+00
-2.675E-02 4.633E+00 4.703E-02 9.640E+00-1.868E-02 1.207E-04
       2.0    0.4000    0.3360   0.00636      14.0     128.0    3.1667
     3.000     3.000
  30000.00      1.00     0.875
    1200.0      70.0     0.500     72.00     0.200
       2.0    0.4000    0.3360   0.00636      14.0     128.0    5.0400
     3.000     4.000
  30000.00       1.0     0.875
    2300.0     47.00     0.700     64.00     0.160


***** INPUT DATA *****

        SAMPLE DATA SET FOR ORNL HEAT PUMP DESIGN MODEL -- @ 47.0F AMBIENT
        HEATING MODE OF OPERATION (NCORH=2)

        THE HOUSE LOAD IS  15000. BTU/H
        DIAMETER OF 6 EQUIVALENT DUCTS- 8.000 IN
        COMPRESSOR CAN HEAT LOSS ADDED TO AIR BEFORE CROSSING THE OUTDOOR COIL.
        POWER TO THE INDOOR FAN ADDED TO AIR AFTER CROSSING THE COIL.
        POWER TO THE OUTDOOR FAN ADDED TO AIR BEFORE CROSSING THE COIL.
        CONDENSER SUBCOOLING IS HELD FIXED AT  45.00 F
        EVAPORATOR SUPERHEAT IS HELD FIXED AT  10.00 F

        DESCRIPTION OF CONNECTING TUBING:
          LIQUID LINE FROM INDOOR TO OUTDOOR HEAT EXCHANGER
              ID                        0.19000 IN
              EQUIVALENT LENGTH           30.40 FT
          FROM INDOOR COIL TO REVERSING VALVE            FROM OUTDOOR COIL TO REVERSING VALVE
              ID                        0.55500 IN             ID                        0.68000 IN
              EQUIVALENT LENGTH           30.40 FT             EQUIVALENT LENGTH           6.00 FT
          FROM REVERSING VALVE TO COMPRESSOR INLET       FROM REVERSING VALVE TO COMPRESSOR OUTLET
              ID                        0.68000 IN             ID                        0.55500 IN
              EQUIVALENT LENGTH           2.00 FT              EQUIVALENT LENGTH           2.00 FT

          HEAT LOSS IN DISCHARGE LINE    2000.0 BTU/H
          HEAT GAIN IN SUCTION LINE       300.0 BTU/H
          HEAT LOSS IN LIQUID LINE        200.0 BTU/H

        ESTIMATE OF:
          REFRIGERANT MASS FLOW RATE                  400.000 LBM/H
          SATURATION TEMPERATURE INTO CONDENSER       130.000 F
          SATURATION TEMPERATURE OUT OF EVAPORATOR     30.000 F

        COMPRESSOR CHARACTERISTICS:
          TOTAL DISPLACEMENT         4.520 CUBIC INCHES
          SYNCHRONOUS MOTOR SPEED 3450.000 RPMS

        MAP-BASED COMPRESSOR INPUT:
          POWER CONSUMPTION=    -1.509E-04*CONDENSING  TEMPERATURE**2 +  4.089E-02*CONDENSING  TEMPERATURE
                              + -1.338E-04*EVAPORATING TEMPERATURE**2 +  5.860E-04*EVAPORATING TEMPERATURE
                              +  3.638E-04*CONDENSING  TEMPERATURE*EVAPORATING TEMPERATURE +  9.759E-05

          MASS FLOW RATE=       -2.675E-02*CONDENSING  TEMPERATURE**2 +  4.633E+00*CONDENSING  TEMPERATURE
                              +  4.703E-02*EVAPORATING TEMPERATURE**2 +  9.640E+00*EVAPORATING TEMPERATURE
                              + -1.868E-02*CONDENSING  TEMPERATURE*EVAPORATING TEMPERATURE +  1.207E-04

          CORRECTION FACTOR FOR SUCTION GAS              0.330
          CORRECTION FACTOR FOR VOLUMETRIC EFFICIENCY    0.750
          BASE SUPERHEAT FOR COMPRESSOR MAP             20.000 F
          BASE DISPLACEMENT FOR COMPRESSOR MAP           4.520 CU IN

          HEAT REJECTED FROM COMPRESSOR SHELL IS 0.35 TIMES THE COMPRESSOR POWER
```

INDOOR UNIT: CONDENSER

OD OF TUBES IN HX	0.40000	IN	FIN THICKNESS	0.00636	IN
ID OF TUBES IN HX	0.33600	IN	FIN PITCH	14.00	FINS/IN
FRONTAL AREA OF HX	3.167	SQ FT	THERMAL CONDUCTIVITY OF FINS	128.000	BTU/H-FT-F
NUMBER OF PARALLEL CIRCUITS	3.00		CONTACT CONDUCTANCE	30000.0	BTU/H-SQ FT-F
NUMBER OF TUBES IN DIRECTION OF AIR FLOW	3.00		HORIZONTAL TUBE SPACING	0.875	IN
NUMBER OF RETURN BENDS	72.00		VERTICAL TUBE SPACING	1.000	IN
AIR FLOW RATE	1200.00	CFM	FAN EFFICIENCY	0.20000	
INLET AIR TEMPERATURE	70.000	F	RELATIVE HUMIDITY	0.50000	
WAVY FINS					

OUTDOOR UNIT: EVAPORATOR

OD OF TUBES IN HX	0.40000	IN	FIN THICKNESS	0.00636	IN
ID OF TUBES IN HX	0.33600	IN	FIN PITCH	14.00	FINS/IN
FRONTAL AREA OF HX	5.040	SQ FT	THERMAL CONDUCTIVITY OF FINS	128.000	BTU/H-FT-F
NUMBER OF PARALLEL CIRCUITS	4.00		CONTACT CONDUCTANCE	30000.0	BTU/H-SQ FT-F
NUMBER OF TUBES IN DIRECTION OF AIR FLOW	3.00		HORIZONTAL TUBE SPACING	0.875	IN
NUMBER OF RETURN BENDS	64.00		VERTICAL TUBE SPACING	1.000	IN
AIR FLOW RATE	2300.00	CFM	FAN EFFICIENCY	0.16000	
INLET AIR TEMPERATURE	47.000	F	RELATIVE HUMIDITY	0.70000	
WAVY FINS					

***** CALCULATED HEAT PUMP PERFORMANCE *****

COMPRESSOR OPERATING CONDITIONS:

		EFFICIENCY	
COMPRESSOR POWER	4.011 KW	VOLUMETRIC	0.6311
MOTOR SPEED	3450.000 RPM	OVERALL	0.5053

REFRIGERANT MASS FLOW RATE	413.828 LBM/H	POWER PER UNIT MASS FLOW	33.38864 BTU/LBM
COMPRESSOR SHELL HEAT LOSS	4791.414 BTU/H	POWER CORRECTION FACTOR	0.9996
		MASS FLOW RATE CORRECTION FACTOR	1.0089

SYSTEM SUMMARY	REFRIGERANT TEMPERATURE	SATURATION TEMPERATURE	REFRIGERANT ENTHALPY	REFRIGERANT QUALITY	REFRIGERANT PRESSURE	AIR TEMPERATURE
COMPRESSOR SUCTION LINE INLET	39.470 F	29.577 F	108.958 BTU/LBM	1.0000	69.054 PSIA	
SHELL INLET	43.687	29.263	109.683	1.0000	68.660	
SHELL OUTLET	206.498	126.899	131.185	1.0000	299.682	
CONDENSER INLET	183.889 F	126.558 F	126.352 BTU/LBM	1.0000	298.411 PSIA	70.000 F
OUTLET	81.217	126.196	33.477	0.0	297.060	100.147
EXPANSION DEVICE	79.607 F	120.765 F	32.994 BTU/LBM	0.0	277.316 PSIA	
EVAPORATOR INLET	34.916 F	34.916 F	32.994 BTU/LBM	0.1483	76.055 PSIA	47.000 F
OUTLET	39.470	29.577	108.958	1.0000	69.054	38.908

PERFORMANCE OF EACH CIRCUIT IN THE CONDENSER

INLET AIR TEMPERATURE	70.000 F
OUTLET AIR TEMPERATURE	100.147 F
HEAT LOSS FROM FAN	1257.1 BTU/H
AIR TEMPERATURE CROSSING COIL	99.193 F

TOTAL HEAT EXCHANGER EFFECTIVENESS 0.6949

	SUPERHEATED REGION	TWO-PHASE REGION	SUBCOOLED REGION
NTU	0.0	1.1351	1.9987
HEAT EXCHANGER EFFECTIVENESS	1.0000	0.6786	0.8005
CR/CA	0.0		0.2816
FRACTION OF HEAT EXCHANGER	0.0	0.6453	0.3547
HEAT TRANSFER RATE	0.0 BTU/H	10838.4 BTU/H	1973.0 BTU/H
OUTLET AIR TEMPERATURE	70.000 F	108.270 F	82.676 F

AIR SIDE:		REFRIGERANT SIDE:	
MASS FLOW RATE	1798.1 LBM/H	MASS FLOW RATE	137.9 LBM/H
PRESSURE DROP	0.5224 IN H2O	PRESSURE DROP	1.351 PSI
HEAT TRANSFER COEFFICIENT	13.136 BTU/H-SQ FT-F	HEAT TRANSFER COEFFICIENT	
		VAPOR REGION	102.905 BTU/H-SQ FT-F
		TWO PHASE REGION	453.291 BTU/H-SQ FT-F
		SUBCOOLED REGION	110.787 BTU/H-SQ FT-F

UA VALUES:

VAPOR REGION (BTU/H-F)		TWO PHASE REGION (BTU/H-F)		SUBCOOLED REGION (BTU/H-F)	
REFRIGERANT SIDE	0.0	REFRIGERANT SIDE	2933.419	REFRIGERANT SIDE	394.035
AIR SIDE	0.0	AIR SIDE	1436.706	AIR SIDE	789.615
COMBINED	0.0	COMBINED	964.380	COMBINED	262.862

FLOW CONTROL DEVICE - CONDENSER SUBCOOLING IS SPECIFIED AS 45.000 F

CORRESPONDING TXV RATING PARAMETERS:		CORRESPONDING CAPILLARY TUBE PARAMETERS:		CORRESPONDING ORIFICE PARAMETER:	
RATED OPERATING SUPERHEAT	11.000 F	NUMBER OF CAPILLARY TUBES	1	ORIFICE DIAMETER	0.0544 IN
STATIC SUPERHEAT RATING	6.000 F	CAPILLARY TUBE FLOW FACTOR	2.626		
PERMANENT BLEED FACTOR	1.150				
TXV CAPACITY RATING INCLUDING NOZZLE AND TUBES	1.880 TONS				

PERFORMANCE OF EACH CIRCUIT IN THE EVAPORATOR

INLET AIR TEMPERATURE	47.000 F
HEAT LOSS FROM COMPRESSOR	4791.4 BTU/H
HEAT LOSS FROM FAN	2274.5 BTU/H
AIR TEMPERATURE CROSSING COIL	49.696 F
OUTLET AIR TEMPERATURE	38.908 F

MOISTURE REMOVAL OCCURS

SUMMARY OF DEHUMIDIFICATION PERFORMANCE (TWO-PHASE REGION)

	LEADING EDGE OF COIL AIR	POINT WHERE MOISTURE REMOVAL BEGINS AIR	POINT WHERE MOISTURE REMOVAL BEGINS WALL	LEAVING EDGE OF COIL AIR	LEAVING EDGE OF COIL WALL
DRY BULB TEMPERATURE	49.696 F	44.912 F	37.740 F	38.400 F	35.434 F
HUMIDITY RATIO	0.00475	0.00475	0.00475	0.00446	0.00433
ENTHALPY	17.090 BTU/LBM	15.930 BTU/LBM	14.191 BTU/LBM	14.036 BTU/LBM	13.183 BTU/LBM

RATE OF MOISTURE REMOVAL	0.7345 LBM/H
FRACTION OF EVAPORATOR THAT IS WET	0.6941
LATENT HEAT TRANSFER RATE IN TWO-PHASE REGION	789. BTU/H
SENSIBLE HEAT TRANSFER RATE IN TWO-PHASE REGION	6896. BTU/H
SENSIBLE TO TOTAL HEAT TRANSFER RATIO FOR TWO-PHASE REGION	0.8974

OVERALL SENSIBLE TO TOTAL HEAT TRANSFER RATIO 0.8996

OVERALL CONDITIONS ACROSS COIL

	ENTERING AIR	EXITING AIR
DRY BULB TEMPERATURE	49.696 F	38.908 F
WET BULB TEMPERATURE	43.924 F	37.659 F
RELATIVE HUMIDITY	0.633	0.901
HUMIDITY RATIO	0.00475	0.00448

TOTAL HEAT EXCHANGER EFFECTIVENESS (SENSIBLE) 0.6476

	SUPERHEATED REGION	TWO-PHASE REGION
NTU	0.7608	1.0590
HEAT EXCHANGER EFFECTIVENESS	0.4834	0.6532
CR/CA	0.4025	
FRACTION OF HEAT EXCHANGER	0.0682	0.9318
HEAT TRANSFER RATE	172.2 BTU/H	7684.9 BTU/H
AIR MASS FLOW RATE	184.36 LBM/H	2517.70 LBM/H
OUTLET AIR TEMPERATURE	45.845 F	38.400 F

AIR SIDE		REFRIGERANT SIDE	
MASS FLOW RATE	2702.1 LBM/H	MASS FLOW RATE	103.5 LBM/H
PRESSURE DROP	0.395 IN H2O	PRESSURE DROP	7.005 PSI
HEAT TRANSFER COEFFICIENT		HEAT TRANSFER COEFFICIENT	
DRY COIL	14.462 BTU/H-SQ FT-F	VAPOR REGION	63.625 BTU/H-SQ FT-F
WET COIL	16.803 BTU/H-SQ FT-F	TWO PHASE REGION	631.979 BTU/H-SQ FT-F

DRY FIN EFFICIENCY	0.791
WET FIN EFFICIENCY	0.763

UA VALUES:	VAPOR REGION	TWO PHASE REGION	
REFRIGERANT SIDE	69.286	9398.352	BTU/H-F
AIR SIDE			
DRY COIL	261.250	1091.526	BTU/H-F
WET COIL		2772.596	BTU/H-F
COMBINED			
DRY COIL	54.763	791.186	BTU/H-F
WET COIL		1945.610	BTU/H-F

SUMMARY OF ENERGY INPUT AND OUTPUT:

SAMPLE DATA SET FOR ORNL HEAT PUMP DESIGN MODEL -- @ 47.0F AMBIENT

AIR TEMPERATURE INTO EVAPORATOR	47.00	F
HEAT FROM CONDENSER TO AIR	38434.	BTU/H
HEAT TO EVAPORATOR FROM AIR	31428.	BTU/H
POWER TO INDOOR FAN	1257.	BTU/H
POWER TO OUTDOOR FAN	2275.	BTU/H
POWER TO COMPRESSOR MOTOR	13690.	BTU/H
COMPRESSOR SHELL HEAT LOSS	4791.	BTU/H
TOTAL HEAT TO/FROM INDOOR AIR	39691.	BTU/H

SYSTEM EFFICIENCY:		HEAT OUTPUT:	
COP (HEATING)	2.305	HEAT FROM HEAT PUMP	39691.29 BTU/H
COP (WITH RESISTANCE HEAT)	2.305	RESISTANCE HEAT	0.0 BTU/H
		HOUSE LOAD	15000.00 BTU/H

Appendix C — Definitions of Constants Assigned in BLOCK DATA Subroutine

A number of variables and constants are used by the Heat Pump Design Model that are unlikely to be changed very often, and consequently they are simply assigned values rather than being specified with each set of input data. They have been brought together in the BLOCK DATA subroutine and given values which are in turn passed to the subroutines where they are used via common blocks. These data are divided into several categories determined by use; they are defined in that "natural" order.

Physical Air-Side Parameters

AFILTR — cross-sectional area of filter on indoor unit, 2.78 ft^2

AHEATR — cross-sectional area of resistance heaters in indoor unit, 1.28 ft^2

PA — atmospheric pressure, 14.7 lbf/in^2

RACKS — number of resistance heater racks, 3.0

RAU — universial gas constant, 53.34 ft-lbf/lbm-°R

Refrigerant Tubing Parameter

E — roughness of interior tube walls, 5×10^{-6} ft

Compressor Motor Efficiency

CETAM — coefficients for the 0th through 5th order terms of the fit of the compressor motor efficiency as a function of the fractional motor load (Eq. 4.29), 0.4088, 2.5138, -4.6289, 4.5884, -2.3666, and 0.48324

RPMSLR — slope of linear fit for fraction of no-load compressor motor speed as a function of fraction of full load power, -0.042 (see Eq. 4.24)

Data for Outdoor Fan Efficiency

COFAN constant term for the fit of outdoor fan static efficiency to fan specific speed, -3.993

C1FAN coefficient for the linear term of the fit of outdoor fan static efficiency to the fan specific speed, 4.266

C2FAN coefficient for the quadratic term of the fit of outdoor fan static efficiency to fan specific speed, -1.024

EFFMOT constant motor efficiency for the outdoor fan, 0.55

RPMFAN constant motor speed for the outdoor fan, 825 rpm

Tolerance Parameters

AMBCON convergence parameter for the outdoor ambient air interation, 0.20 F°.

CMPCON convergence parameter for the Δh iteration in the compressor calculations, 0.05 Btu/lbm

CNDCON convergence parameter for iterations on condenser subcooling and refrigerant temperature at the flow control device, 0.20 0.20 F°

CONMST tolerance parameter for the iterations on evaporator tube wall temperatures, 0.003 F°

EVPCON tolerance parameter for iterations on evaporator superheat, 0.50°F.

FLOCON convergence criteria for iterations on refrigerant mass flow rate through the expansion device, 0.2 lbm/h

TOLH tolerance parameter used in calculating properties of superheated vapor when enthalpy is known, 10^{-3}

TOLS tolerance parameter used in calculating properties of superheated vapor when entropy is known, 10^{-4}

Refrigerant Specification

NR refrigerant number, 22

Refrigerant-Side Heat Transfer Correlation for Single-Phase Regions

C1R, C3R, and C5R coefficients for single-phase heat transfer coefficient (Eq. 6.2), 1.10647, 3.5194×10^{-7}, and 0.01080

C2R, C4R, and C6R exponents for single-phase heat transfer coefficient (Eq. 6.3), -0.78992, 1.03804, and -0.13750

ULR lower limit for the Reynolds number for turbulent flow of refrigerant, 6,000

XLLR upper limit on the Reynolds number for laminar flow of refrigerant, 3,500

Thermostatic Expansion Valve Constants

BLEEDF bypass or bleed factor coefficient used to compute TXV parameters when condenser subcooling is held fixed, 1.15

DPRAT rated pressure drop across the TXV at the design conditions, 100 psi for R-22 and R-502, 50 psi for R-12

NZTBOP switch to bypass nozzle and distributor tube pressure drop calculations when calculating TXV parameters if the condenser subcooling is held fixed, 0

STATIC static superheat setting used to compute the TXV parameters when the condenser subcooling is held fixed, 6.0 F°

SUPRAT rated operating superheat used to compute the TXV parameters when the condenser subcooling is held fixed, 11.0 F°

TERAT rated evaporating temperature for the TXV, 40.0°F

TLQRAT rated liquid refrigerant temperature at the inlet to the TXV, 100.0°F

Capillary Tube Parameter

NCAP number of capillary tubes used to compute capillary tube flow factor, ϕ, when condenser subcooling is held fixed, 1

Compressor Efficiency Parameters

ETAVLA intercept of the fit of theoretical minus actual compressor volumetric efficiencies as a linear function of the correlating parameter of Davis and Scott, -0.0933

ETAVLB slope of the fit of theoretical minus actual compressor volumetric efficiencies as a linear function of the correlating parameter of Davis and Scott, 0.733

SUCFAC suction gas heating factor F_{sh} used in Eq. 4.6, 0.33

VOLFAC volumetric efficiency correction factor F_v used in Eq. 4.4, 0.75

Appendix D: Definitions of Variables in Common Blocks

Variable	Definition	Common
A	constant used in a first order approximation of the saturation temperature in the logarithm of the refrigerant pressure. assigned a value in TABLES and used in TSAT.	SUPER
AAFC	the frontal area of the condenser, read by DATAIN, used by CALC and COND (sq ft).	CONDEN
AAFE	the frontal area of the evaporator, read by DATAIN, used by CALC and EVAPR (sq ft).	EVAPOR
ACV,BCV,...,FCV	constants used in calculating refrigerant heat capacity with temperature and specific volume, assigned values in TABLES and used in SATPRP.	OTHER
AFILTR	frontal area of filter for the indoor unit, assigned a value in BLOCK DATA and used in PDAIR (sq ft).	AIR
AHEATR	cross-sectional area of the resistance heaters, assigned a value in BLOCK DATA and used in PDAIR (sq ft).	AIR
AL.BL,...,GL	coefficients for expressing density of the liquid refrigerant as a function of absolute temperature (R), assigned values in TABLES and used in SATPRP (lbm/cu ft).	DENSIT
ALFAAC	ration of the air-side heat transfer area for the condenser to the total volume of the condenser, calculated in CALC, used by COND, EFFCT, and EXCH (/ft).	CONDEN
AALFE	ratio of the air-side heat transfer area for the evaporator to the total volume of the evaporator, calculated in CALC, used by EVAP and EVAPR (/ft).	EVAPOR
ALFARC	ratio of the total refrigerant-side heat transfer area for the condenser to the volume of the condenser, calculated in CALC, used by COND, EFFCT, and EXCH (/ft).	CONDEN
ALFARE	ratio of the total refrigerant side heat transfer area for the evaporator to the volume of the evaporator, calculated in CALC, used by EVAP and EVAPR (/ft).	EVAPOR
ALPHA	constant used in refrigerant equation of state correlating pressure with temperature and specific volume, assigned a value in TABLES, used by SATPRP, SPVOL, and VAPOR.	STATEQ
AMBCON	tolerance parameter for the ambient air temperature iteration in the main program, assigned a value in BLOCK DATA and used in the main program (F).	MPASS
ARFTC	inside cross-sectional area of the tubes in the condenser calculated in CALC and used in COND (ft).	CONDEN

ARFTE	inside cross-sectional area of the tubes in the evaporator calculated in CALC and used by EVAPR (sq ft).	EVAPOR
ARHTC	total refrigerant-side heat transfer area for each circuit in the condenser, calculated and used in CALC, used by COND, EFFCT, and EXCH (sq ft).	CONDEN
ARHTC	total refrigerant side heat transfer area for each circuit in the evaporator, calculated and used in CALC, used by EVAP and EVAPR (sq ft).	EVAPOR
AVP,BVP,...,FVP	constants used in correlating refrigerant vapor pressure with absolute temperature (R), assigned values in TABLES, used in SATPRP and TSAT.	SAT
A2,B2,C2	constants used in refrigerant equations of state correlating pressure with temperature and specific volume, assigned values in TABLES, used by SATPRP, SPVOL, and VAPOR.	STATEQ
A3,B3,C3	constants used in refrigerant equations of state correlating pressure with temperature and specific volume, assigned values in TABLES, used by SATPRP, SPVOL, and VAPOR.	STATEQ
A4,B4,C4	constants used in refrigerant equations of state correlating pressure with temperature and specific volume, assigned values in TABLES, used by SATPRP, SPVOL, and VAPOR.	STATEQ
A5,B5,C5	constants used in refrigerant equations of state correlating pressure with temperature and specific volume, assigned values in TABLES, used by SATPRP, SPVOL, and VAPOR.	STATEQ
A6,B6,C6	constants used in refrigerant equations of state correlating pressure with temperature and specific volume, assigned values in TABLES, used by SATPRP, SPVOL, and VAPOR.	STATEQ
B	constant used in a first order approximation to the refrigerant saturation temperature as a function of the logarithm of the saturation pressure, assigned value in TABLES and used in TSAT.	SUPER
BLEEDF	by-pass or bleed factor coefficient for the thermostatic expansion valve, assigned a value by BLOCK DATA or read by DATAIN, used by TXV.	TXVDAT
B1	constant used in refrigerant equation of state correlating pressure with temperature and specific volume, assigned a value in TABLES, used by SATPRP, SPVOL, and VAPOR.	STATEQ

CA	air-side heat capacity rate for the superheated portion of the of the condenser, calculated in EFFCT, used by EXCH (Btu/h-F).	EFFARG
CANFAC	factor used to express compressor shell heat rejection as a fraction of compressor power consumption, read by DATAIN and used by COMP.	COMPR
CAP	capacity of the evaporator at the operating conditions with an assumed 10 F of superheat at the evaporator exit, calculated in and used in TXV, printed by OUTPUT (Btu/hr).	TXVDAT
CAPFLO	capillary tube flow factor, default value assigned in BLOCK DATA, read by DATAIN if capillary tube submodel is used, calculated or used by CAPTUB, printed by OUTPUT.	FLOWBA
CAPNOZ	heating capacity of the nozzle of the thermostatic expansion valve, calculated and used in TXV, printed by OUTPUT (Btu/hr).	TXVDAT
CAPTUB	heating capacity of each tube from the thermostatic expansion valve to the evaporator, calculated and used in TXV, printed in OUTPUT (Btu/hr).	TXVDAT
CARC	ratio of the fin heat transfer area to the contact area between the fins and the tubes in the condenser, calculated in CALC and used in COND.	CONDEN
CARE	ratio of the fin heat transfer area to the contact area between the fins and the tubes in the evaporator, calculated in CALC and used by EVAP.	EVAPOR
CETAM	coefficients for a fit to the motor efficiency as a function of the fraction of full load power output, assigned values in BLOCK DATA and used by COMP.	CMPMOT
CLCXMR	refrigerant mass flow rate through each capillary tube, calculated in CAPTUB, used by FLOBAL, and printed in OUTPUT (lbm/hr).	PRNT2
CMPCON	tolerance parameter for the iteration on the enthalpy entering the compressor suction port in COMP, assigned a value in BLOCK DATA (Btu/h-F).	MPASS
CNDCON	tolerance parameter for the condenser subcooling iterations in the main program and in COND, and the refrigerant temperature at the flow control device in FLOBAL, assigned a value in BLOCK DATA, used in the main program, COND, and FLOBAL (F).	MPASS
COIL	evaporator coil resistance to heat transfer, calculated and used in EVAP, used by TWISOL.	TWI

CONMST	tolerance parameter for the iterations on the tube wall temperature in EVAP, assigned a value in BLOCK DATA and used in EVAP (F).	MPASS
COP	operating coefficient of performance for the heat pump with any necessary resistance heat, calculated in the main program and printed by OUTPUT.	PRNT8
COPHP	operating coefficient of performance for the heat pump, does not include any resistance heat, calculated by the main program and printed in OUTPUT.	PRNT8
CPA	specific heat of dry air, calculated COND and EVAPR, used by COND, EVAPR, XMOIST, and WBF (Btu/lbm-F).	AIR
CPM	specific heat of moist air, calculated by COND and EVAPR and used by COND, EFFCT, EVAP, and EXCH (Btu/lbm-F).	AIR
CPOW	coefficients for compressor power consumption as a function of the condensing and evaporating temperatures, read by DATAIN if the map-based model is used and used by CMPMAP.	MAPFIT
CPR	constant used in refrigerant equation of state correlating pressure with temperature and specific volume, assigned a value in TABLES, used by SATPRP, SPVOL, and VAPOR.	STATEQ
CPSCC	specific heat for the subcooled refrigerant in the condenser, calculated by MUKCP and EXCH, used by COND, EFFCT, EXCH, and SPHTC (Btu/lbm-F).	CONDS
CPSP	specific heat for the superheated refrigerant in the condenser calculated in COND, modified in EXCH, and used by COND, EFFCT, and EXCH (Btu/lbm-F).	CONDS
CPSPC	specific heat for the condensing superheated refrigerant in the condenser, calculated in COND and used by COND and EXCH (Btu/lbm-F).	CONDS
CPSPE	specific heat for the superheated refrigerant in the evaporator calculated and used by EVAPR (Btu/lbm-F).	EVAPS
CR	refrigerant-side heat capacity rate for the superheated region of the condenser, calculated in EFFCT and used in EXCH (Btu/hr-F).	EFFARG
CSCOOL	ratio of refrigerant to air-side heat capacity rates for the subcooled region of the condenser, calculated in EXCH and printed in OUTPUT.	PRNT4
CSUPER	ratio of the refrigerant to air-side heat capacity rates for the superheated region of the evaporator, calculated in EVAP and printed in OUTPUT.	PRNT5

CUASC	overall thermal conductance times the heat transfer area (UA) for the subcooled region of the condenser, calculated in COND and printed in OUTPUT (Btu/hr-F).	UAS
CUASCA	air-side thermal conductance times the heat transfer area (UA) for the subcooled region of the condenser, calculated in COND and printed in OUTPUT (Btu/hr-F).	UAS
CUASCR	refrigerant-side thermal conductance times the heat transfer area (UA) for the subcooled region of the condenser, calculated in COND and printed in OUTPUT (Btu/hr-F).	UAS
CUATP	overall thermal conductance times heat transfer area (UA) for the two-phase region of the condenser, calculated in COND and printed in OUTPUT (Btu/hr-F).	UAS
CUATPA	air-side thermal conductance times the heat transfer area (UA) for the two-phase region of the condenser, calculated in COND and printed in OUTPUT (Btu/hr-F).	UAS
CUATPR	refrigerant-side thermal conductance times the heat transfer area (UA) for the two-phase region of the condenser, calcuated in COND and printed in OUTPUT (Btu/hr-F).	UAS
CUAV	overall thermal conductance times the heat transfer area for the vapor region of the condenser, calculated in COND and printed in OUTPUT (Btu/hr-F).	UAS
CUAVA	air-side thermal conductance times the heat transfer area (UA) for the vapor region of the condenser, calculated in COND and printed in OUTPUT (Btu/hr-F).	UAS
CUAVR	refrigerant-side thermal conductance times heat transfer area for the superheated region of the condenser, calculated in COND and printed in OUTPUT (Btu/hr-F).	UAS
CXMR	coefficients for the refrigerant mass flow rate as a function of the condensing and evaporating temperatures, read by DATAIN, if the map-based compressor model is chosen, and used by CMPMAP.	MAPFIT
COFAN,C1FAN,C2FAN	coefficients for the fan static efficiency for the outdoor heat exchanger as a function of the static speed of the fan, assigned values in BLOCK DATA and used by FANFIT.	FANMOT
C1R,C2R,...,C6R	coefficients and exponents for fit to single-phase heat transfer coefficient as a function of refrigerant Reynolds and Prandtl numbers, assigned values in BLOCK DATA and used in SPHTC.	VAPHTC

DDL	inside diameter of the compressor discharge line from the reversing valve to the condenser, assigned a value by DATAIN and used by COMP (ft).	LINES
DDLRV	inside diameter of the line from the compressor discharge port to the reversing valve, read by DATAIN and used by COMP (ft).	LINES
DDUCT	diameter of each of 6 identical air ducts with equivalent lengths of 100 ft, read by DATAIN and used by COND and EVAPR (ft).	BLANK
DEAC	outside diameter of the tubes in the condenser, read by DATAIN, used by CALC and COND (ft).	CONDEN
DEAE	outside diameter of the tubes in the evaporator, read by DATAIN, used by CALC, EVAP and EVAPR (ft).	EVAPOR
DELTAC	thickness of the fins in the condenser, read by DATAIN, used by CALC and COND (ft).	CONDEN
DELTAE	thickness of the fins in the evaporator, read by DATAIN, used by CALC and EVAPR (ft).	EVAPOR
DERC	inside diameter of the refrigerant tubes in the condenser, read by DATAIN, used by CALC and COND (ft).	CONDEN
DERE	inside diameter of the refrigerant tubes in the evaporator, read by DATAIN, used by CALC and EVAPR (ft).	EVAPOR
DISPL	total compressor piston displacement, read by DATAIN and used by COMP (cu in).	COMPR
DLL	inside diameter of the liquid line connecting the indoor and outdoor heat exchangers, read by DATAIN and used by FLOBAL (ft).	LINES
DP	air-side pressure drop across the outdoor coil, calculated in FANFIT and printed by OUTPUT (inches of water).	PRNT8
DPDL	pressure drop in the compressor discharge line from the discharge port to the condenser, calculated and used by COMP (psi).	LINES
DPLL	pressure drop in the liquid line connecting the heat exchangers, calculated and used in FLOBAL (psi).	LINES
DPNOZ	pressure drop in the nozzle for the thermostatic expansion valve, calculated and used in TXV, print in OUTPUT (psi).	TXVDAT
DPRAT	rated pressure drop across the thermostatic expansion valve at the design conditions, assigned a value in BLOCK DATA and used by TXV (psi).	TXVDAT

DPSL	pressure drop in the suction line connecting the evaporator and compressor, calculated and used in COMP (psi).	LINES
DPTUBE	pressure drop across the tubes from the thermostatic expansion valve to the evaporator, calculated and used in TXV, printed in OUTPUT (psi).	TXVDAT
DPTXV	pressure drop across the valve of the thermostatic expansion valve (does not include nozzle and tube losses), calculated and used in TXV, printed in OUTPUT (psi).	TXVDAT
DSL	inside diameter of the suction line from the evaporator to the reversing valve, read by DATAIN and used by COMP (ft).	LINES
DSLRV	inside diameter of the line from the compressor suction port to the reversing valve, read by DATAIN and used by COMP (ft).	LINES
DTROC	specified condenser subcooling, read by DATAIN used by CNDNSR, FLOBAL, and FLODEV, and printed by OUTPUT (F).	FLOWBA
DZC	equivalent length of the refrigerant tubing in the condenser, calculated in CALC and used by COND.	CONDEN
DZE	equivalent length of the refrigerant tubing in the evaporator, calculated in CALC and used by EVAPR.	EVAPOR
E	roughness factor for all of the refrigerant lines, assigned a value in BLOCK DATA, used by COMP, COND, EVAPR, and FLOBAL (ft).	LINES
EFFMMX	product of the maximum motor efficiency and the mechanical efficiency for the compressor, read by DATAIN and used by COMP.	COMPR
EFFMOT	fan motor efficiency for the outdoor fan, assigned a value in BLOCK DATA and used in FANFIT.	FANMOT
EINDF	rate of power consumption for the indoor fan, calculated in COND or EVAPR, used by the main program, printed by OUTPUT (Btu/hr).	PRNT8
EOUTF	rate of power consumption for the outdoor fan, calculated in COND or EVAPR, used by the main program, printed by OUTPUT (Btu/hr).	PRNT8
ETAISN	isentropic efficiency from the suction port to the discharge port of the compressor, read by DATAIN and used by COMP, printed and used by OUTPUT.	COMPR

ETAMEC	mechanical efficiency of the compressor, read by DATAIN and used by COMP.	COMPR
ETAMOT	operating motor efficiency for the PRNT1essor, calculated and used in COMP, used and printed by OUTPUT.	COMPR
ETASUP	compressor suction gas heating efficiency, calculated by COMP and printed by OUTPUT.	PRNT1
ETATOT	compressor overall isentropic efficiency from the shell inlet to the shell outlet, calculated by COMP, used and printed by OUTPUT.	PRNT1
ETAVLA	intercept of the fit of theoretical minus actual compressor volumetric efficiency as a linear function of the correlating parameter of Davis and Scott, assigned in BLOCK DATA and used in COMP.	COMPR
ETAVLB	slope of the fit of theoretical minus actual compressor volumetric efficiency as a linear function of the correlating parameter of Davis and Scott, assigned in BLOCK DATA and used in COMP.	COMPR
ETAVOL	volumetric efficiency of the compressor based on the shell inlet conditions, calculated and used in COMP, printed by OUTPUT.	PRNT1
ETP	heat exchanger effectiveness for the two-phase region of the condenser, calculated and used in EXCH, used and printed in OUTPUT.	PRNT4
ETPE	heat exchanger effectiveness for the two-phase region of the evaporator, calculated and used in EVAP, printed by OUTPUT.	PRNT5
EUATP	overall thermal conductance times heat transfer area (UA) for the two-phase region of the evaporator, calculated in EVAPR, printed in OUTPUT (Btu/hr-F).	UAS
EUATPA	air-side thermal conductance times the heat transfer area (UA) for the two-phase region of the evaporator, calculated in EVAPR and printed in OUTPUT (Btu/hr-F).	UAS
EUATPR	refrigerant-side thermal conductance times the heat transfer area (UA) for the two-phase region of the evaporator, calculated in EVAPR and printed in OUTPUT (Btu/hr-F).	UAS
EUAV	overall thermal conductance times the heat transfer area (UA) for the superheated region of the evaporator, calculated in EVAPR and printed in OUTPUT (Btu/hr-F).	UAS
EUAVA	air-side thermal conductance times the heat transfer area (UA) for the superheated region of the evaporator, calculated in EVAPR and printed in OUTPUT (Btu/hr-F).	UAS

EUAVR	refrigerant-side thermal conductance times the heat transfer area (UA) for the superheated region of the evaporator, calculated in EVAPR and printed in OUTPUT (Btu/hr-F).	UAS
EVPCON	tolerance parameter for the iteration on evaporator superheat in the main program and in EVAPR, assigned a value in BLOCK DATA and used in the main program and EVAPR (F).	MPASS
EXFR	heat exchanger effectiveness for the subcooled region of the condenser based on effectiveness-NTU correlations for cross-flow heat exchangers, calculated and used in EXCH.	EFFARG
EXFRC	heat exchanger effectiveness for the subcooled region of the condenser, assigned a value in EXCH, used and printed in OUTPUT.	PRNT4
EXFRE	heat exchanger effectiveness for the superheated region of the evaporator, calculated and used in EVAP, printed by OUTPUT.	PRNT5
EXFS	heat exchanger effectiveness for the superheated region of the condenser based on heat capacity rates and delta T's, calculated in EFFCT and used by EXCH.	EFFARG
EXFSC	heat exchanger effectiveness for the superheated region of the condenser, assigned a value in EXCH, used and printed in OUTPUT.	PRNT4
FANEFC	the combined fan-fan motor efficiency for the condenser, the value is either read by DATAIN or calculated by FANFIT, used by COND.	CONDEN
FANEFE	the combined fan-fan motor efficiency for the evaporator, the value is either read by DATAIN or calculated by FANFIT, used by COND.	EVAPOR
FANOUT	combined operating efficiency of the outdoor fan-fan motor, calculated in FANFIT, printed by OUTPUT.	PRNT8
FARC	ratio of the fin heat transfer area for the condenser to the total heat transfer area on the air side, calculated in CALC and used in COND.	CONDEN
FARE	ratio of the fin heat transfer area for the evaporator to the total heat transfer area, calculated in CALC, used by EVAP and EVAPR.	EVAPOR
FINTYC	switch to specify the type of fins in the condenser (smooth, wavy, or louvered), read by DATAIN, used by HAIR and PDAIR.	CONDEN

FINTYE	switch to specify the type of fins in the evaporator (smooth, wavy, or louvered), read by DATAIN, used by HAIR and PDAIR.	EVAPOR
FIXCAP	specified heating load for the heat pump, read by DATAIN and used by the main program (Btu/hr).	BLANK
FLMOT	full load motor power for the compressor, either read by DATAIN or calculated in COMP, used by COMP and printed by OUTPUT (kW).	COMPR
FLOCON	relative tolerance parameter used in the refrigerant mass flow rate iteration in the main program, assigned a value in BLOCK DATA and used in the main program.	MPASS
FMOIST	fraction of the evaporator where moisture removal from the air occurs, calculated and used in EVAP, used in EVAPR and printed in OUTPUT.	EVAPRS
FPC	the fin pitch for the condenser, read by DATAIN and used by CALC and COND (fins/ft).	CONDEN
FPE	the fin pitch for the evaporator, read by DATAIN and used by CALC and EVAPR (fins/ft).	EVAPOR
FSCC	fraction of each circuit in the condenser which is subcooled calculated in EXCH, used by COND and EXCH, printed in OUTPUT.	CONDS
FSPC	fraction of each circuit in the condenser that is superheated, calculated and used in EXCH, used in COND, and printed in OUTPUT.	CONDS
FSPE	fraction of each circuit in the evaporator that is superheated, calculated and used in EVAP, used in EVAPR, and printed in OUTPUT.	EVAPS
FTPC	fraction of each circuit in the condenser which is in two-phase flow, calculated and used in EXCH, used in COND, and printed in OUTPUT.	CONDS
FTPE	fraction of each circuit in the evaporator which is in two-phase flow, calculated and used in EVAP, used in EVAPR, and printed by OUTPUT.	EVAPS
HAC	air-side heat transfer coefficient for the condenser, calculated by HAIR, used by COND, EFFCT, EXCH, and SEFF, printed by OUTPUT (Btu/hr-sq ft-F).	CONDS
HAE	air-side heat transfer coefficient for the evaporator, calculated and used by EVAPR, used by EVAP, and printed by OUTPUT (Btu/hr-sq ft-F).	EVAPS

HAIRI	enthalpy of the moist air entering the evaporator, calculated and used in EVAP, used by TWISOL, and printed by OUTPUT (Btu/lbm).	TWI
HAIRO	enthalpy of the air leaving the evaporator, calculated and used in EVAP, printed by OUTPUT (Btu/lbm).	PRNT5
HAIR1	enthalpy of the air in the evaporator at the point where moisture removal begins, calculated and used in EVAP, printed by OUTPUT (Btu/lbm).	PRNT5
HAW	air-side heat transfer coefficient for the wetted surface of the evaporator, calculated in EVAPR, used by EVAP and EVAPR, printed by OUTPUT (Btu/h-sq ft-F).	EVAPRS
HCONTC	contact conductance between the fins and tubes in the condenser, read by DATAIN and used by COND (Btu/hr-sq ft-F).	CONDEN
HCONTE	contact conductance between the fins and the tubes in the evaporator, read by DATAIN, used by EVAP (Btu/hr-sq ft-F).	EVAPOR
HIC	enthalpy of the refrigerant entering the condenser, calculated in COMP, modified by DESUPR, used by COMP and FLOBAL, printed by OUTPUT (Btu/lbm-F).	CONDSR
HIE	enthalpy of the refrigerant entering the evaporator, calculated in the main program, used by EVAPR, then calculated and used by FLOBAL, used by TXV, and printed by OUTPUT (Btu/lbm-F).	EVAPTR
HILOFC	factor used to express the internal compressor heat transfer from the high side discharge line to the low side suction line as a fraction of compressor power, read by DATAIN and used by COMP.	COMPR
HINCMP	enthalpy of the refrigerant at the compressor shell inlet calculated and used in COMP or CMPMAP, printed in OUTPUT (Btu/lbm).	CMPRSR
HOC	enthalpy of the refrigerant leaving the condenser, calculated in COND and FLOBAL, used by the main program, COND, and FLOBAL, printed by OUTPUT (Btu/lbm-F).	CONDSR
HOE	enthalpy of the refrigerant leaving the evaporator, calculated and used by COMP, used by FLOBAL, and printed by OUTPUT (Btu/lbm-F).	EVAPTR
HOUCMP	enthalpy of the refrigerant at the compressor shell outlet calculated and used in COMP or CMPMAP, printed in OUTPUT (Btu/lbm).	CMPRSR

HSCC	refrigerant-side heat transfer coefficient for the subcooled region of the condenser, calculated in SPHTC, used by CHTC, COND, and EXCH, printed by OUTPUT (Btu/hr-sq ft-F).	CONDS
HSPC	refrigerant-side heat transfer coefficient for the superheated region of the condenser, calculated by SPHTC, used by COND, EFFCT, and EXCH, printed by OUTPUT (Btu/hr-sq ft-F).	CONDS
HSPE	refrigerant-side heat transfer coefficient for the superheated region of the evaporator, calculated and used by EVAPR, also used by EVAP, printed by OUTPUT (Btu/hr-sq ft-F).	EVAPS
HTPC	refrigerant-side heat transfer coefficient for the two-phase region of the condenser, calculated in CHTC, adjusted by COND, used by COND and EXCH, printed by OUTPUT (Btu/hr-sq ft-F).	CONDS
HTPE	refrigerant-side heat transfer coefficient for the two-phase region in the evaporator, calculated and used by EVAPR, also used by EVAP, printed by OUTPUT (Btu/hr-sq ft-F).	EVAPS
HWALLI	enthalpy of the air at the tube walls on the leading edge of the evaporator where moisture removal begins, calculated in EVAP, calculated and used in TWISOL, printed in OUTPUT (Btu/lbm-F).	TWI
HWALLO	enthalpy of the air at the tube walls on the leaving edge of the evaporator, calculated and used in EVAP, printed in OUTPUT (Btu/lbm-F).	PRNT5
ICOMP	switch to specify which compressor model is used, read by DATAIN and used by FLOBAL.	FLOWBA
IREFC	switch to specify type of flow control device, read by DATAIN, used by the main program, CAPTUB, FLOBAL, OUTPUT, and TXV.	FLOWBA
ITITLE	descriptive title for labelling output, read by DATAIN and printed by OUTPUT.	BLANK
J	constant used in correlating refrigerant heat capacity at a constant volume with temperature and specific volume, assigned a value in TABLES and used in SATPRP.	OTHER

K	constant used in refrigeration equations of state correlating pressure with temperature and specific volume, assigned a value in TABLES, used by SATPRP, SPVOL, and VAPOR.	STATEQ
LE10	multiplication constant used to convert logarithms base ten to natural logarithms, assigned a value in TABLES, used by SATPRP and TSAT.	SUPER
LPRINT	switch to control levels of printed output, read by DATAIN, used by the main program, COMP, COND, EVAP, EVAPR, and FLOBAL.	MPASS
L10E	multiplicative constant used to convert natural logarithms to logarithms base ten, assigned a value in TABLES, used in SATPRP.	SUPER
MCMPOP	switch to specify option for adding heat from the compressor shell to the air-stream, read by DATAIN, used by COND, EVAPR, and OUTPUT.	MPASS
MFANFT	switch to specify whether or not to use efficiency curve for the outdoor fan, read by DATAIN, used by the main program, COND, EVAPR, and OUTPUT.	MPASS
MFANIN	switch to specify option for adding heat loss from the indoor fan to the air-stream, read by DATAIN, used by COND, EVAPR, and OUTPUT.	MPASS
MFANOU	switch to specify option for adding heat loss from the outdoor fan to the air-stream, read by DATAIN, used by COND, EVAPR, and OUTPUT.	MPASS
MTRCLC	switch used to specify whether or not to calculate the compressor motor speed, read by DATAIN, used by COMP.	COMPR
MUNITC	switch to specify whether the condenser is the indoor or the outdoor heat exchanger, assigned a value by DATAIN and used by COND.	CONDEN
MUNITE	switch to specify whether the evaporator is the indoor or the outdoor heat exchanger, assigned a value by DATAIN and used by EVAPR.	EVAPOR

NCAP	number of capillary tubes used, default value assigned in BLOCK DATA, optionally read by DATAIN if capillary tube submodel is used, used by CAPTUB and printed by OUTPUT.	FLOWBA
NCORH	switch to specify heating or cooling mode of operation, read by DATAIN, used by the main program, COND, EVAPR, and OUTPUT.	MPASS
NR	refrigerant number, assigned a value in BLOCK DATA, used by the main program, MUKCP, SATPRP, TSAT, TXV, and VAPOR.	REFRIG
NSECTC	the number of equivalent parallel refrigerant circuits in the condenser, read by DATAIN, used by OUTPUT, CALC, and COND.	CONDEN
NSECTE	the number of equivalent parallel refrigerant circuits in the evaporator, read by DATAIN, used by EVAPR and OUTPUT.	EVAPOR
NTC	the number of tubes in the direction of the air flow in the condenser, read by DATAIN, used by CALC and COND.	CONDEN
NTE	the number of tubes in the direction of the air flow in the evaporator, read by DATAIN, used by CALC and EVAPR.	EVAPOR
NZTBOP	switch to bypass the nozzle and distributor tube pressure drop calculations for the thermostatic expansion valve, assigned a value in BLOCK DATA or read by DATAIN, used by TXV.	TXVDAT
ORIFD	diameter of the orifice or short tube, read by DATAIN or calculated by ORIFIC, used by ORIFIC and printed by OUTPUT (ft).	FLOWBA
PA	the atmospheric pressure, assigned a value in BLOCK DATA, used by COND, EVAP, EVAPR, and XMOIST (psia).	AIR
PC	inside perimeter of each tube in the condenser, calculated and used in CALC, used in COND (ft).	CONDEN
PCTFL	fraction of the full-load compressor motor power, calculated and used in COMP, printed in OUTPUT.	PRNT1
PDAIRC	air-side pressure drop for the condenser, calculated by PDAIR and used by COND and FANFIT, printed by OUTPUT (psi).	CONDS

PDAIRE	air-side pressure drop for the evaporator, initialized to 0 in the main program, calculated by PDAIR, used by EVAPR, and printed by OUTPUT (psi).	EVAPS
PDC	refrigerant-side pressure drop for the condenser, calculated by PDROP in calls from FLOBAL and COND, used by FLOBAL and COND, printed by OUTPUT (psi).	CONDS
PDE	refrigerant-side pressure drop for each circuit in the evaporator, calculated and used by EVAPR, printed by OUTPUT (psi).	EVAPS
PE	inside perimeter of each tube in the evaporator, calculated and used by CALC, used by EVAPR (ft).	EVAPOR
PFLODV	pressure of the refrigerant entering the flow control device, calculated and used in FLOBAL, printed in OUTPUT (psia).	PRNT2
PIC	pressure of the refrigerant entering the condenser, calculated in COMP, modified by DESUPR and FLOBAL, used by COMP and COND, printed by OUTPUT (psia).	CONDSR
PIE	pressure of the refrigerant entering the evaporator, calculated and used by EVAPR, also calculated and used by TXV, printed by OUTPUT (psia).	EVAPTR
PINCMP	pressure of the refrigerant at the compressor shell inlet calculated and used in COMP or CMPMAP, printed in OUTPUT (psia).	CMPRSR
POC	pressure of the refrigerant leaving the condenser, calculated in COND and FLOBAL, used by COND and FLOBAL, printed by OUTPUT (psia).	CONDSR
POE	pressure of the refrigerant leaving the evaporator, calculated and used by COMP, used by EVAPR and TXV, printed by OUTPUT (psia).	EVAPTR
POUCMP	pressure of the refrigerant at the compressor shell outlet calculated and used in COMP or CMPMAP, printed in OUTPUT (psia).	CMPRSR
POW	compressor power consumption, computed and used in COMP, used in the main program, printed by OUTPUT (kW).	COMPR
POW2	rate of power consumption by the compressor, calculated and used by the main program, printed by OUTPUT (Btu/hr).	PRNT8
PRA	Prandtl number of air, calculated and used by COND and EVAPR.	AIR
PRINT	logical variable to control the output of intermediate calculations, set to TRUE or FALSE in the main program depending on the value of LPRINT.	A1

QAC	air flow rate through the condenser, read by DATAIN, used by COND (cfm).	CONDEN
QAE	air flow rate through the evaporator, read by DATAIN, used by EVAPR (cfm).	EVAPOR
QAIR	rate of heat transfer to or from the air, includes heat transfered from the coil and the indoor fan, calculated and used by the main program, printed by OUTPUT (Btu/hr).	PRNT8
QC	rate of heat transfer from the condenser to the air, calculated in COND and used by the main program, printed by OUTPUT (Btu/hr).	CONDS
QCAN	rate of heat rejection from the compressor shell, read by DATAIN, optionally computed and used in COMP, used in COND and EVAPR, printed in OUTPUT (Btu/hr).	COMPR
QDISLN	heat loss rate in the compressor discharge line, read by DATAIN, used by COMP (Btu/hr).	LINES
QE	total rate of heat transfer for the evaporator, calculated in EVAPR, used by the main program, and printed by OUTPUT (Btu/hr).	EVAPS
QFANC	heat loss from the condensor fan motor, calculated by COND, printed by OUTPUT (Btu/hr).	PRNT3
QFANE	rate of heat loss from the evaporator fan, calculated in EVAPR and printed in OUTPUT (Btu/hr).	PRNT7
QHILO	internal heat transfer rate from the discharge line of the compressor to the suction line, read by DATAIN, optionally calculated and used by COMP, and printed by OUTPUT (Btu/hr).	COMPR
QLIQLN	rate of heat loss in the liquid line, read by DATAIN, used by the main program and FLOBAL (Btu/hr).	LINES
QMTPL	latent heat transfer rate for the two-phase region of the evaporator, calculated and used by EVAP, printed by OUTPUT (Btu/hr).	PRNT5
QSCC	rate of heat transfer for the subcooled region of each circuit in the condenser, calculated in EXCH, used by COND and EXCH, and printed and used by OUTPUT (Btu/hr).	CONDS
QSPC	rate of heat transfer for the superheated region of each circuit in the condenser, calculated in EXCH, used by COND and EXCH, andp printed by OUTPUT (Btu/hr).	CONDS
QSPE	rate of heat transfer for the superheated region of each circuit of the evaporator, calculated and used by EVAP, also used by EVAPR, printed and used by OUTPUT (Btu/hr).	EVAPS

QSTPT	sensible heat transfer rate for the two-phase region of the evaporator, calculated and used in EVAP, printed by OUTPUT (Btu/hr).	PRNT5
QSUCLN	rate of heat gain in the suctin line between the evaporator and the compressor, read by DATAIN and used by either CMPMAP or COMP (Btu/hr).	LINES
QTPC	rate of heat transfer for the two-phase region of each circuit in the condenser, calculated and used in EXCH, used by COND, printed by OUTPUT (Btu/hr).	CONDS
QTPE	rate of heat transfer for the two-phase region of each circuit of the evaporator, calculated and used by EVAP, also assigned a value and used by EVAPR, printed by OUTPUT (Btu/hr).	EVAPS
R	constant used in refrigerant equations of state correlating pressure with temperature and specific volume, assigned a value in TABLES, used by SATPRP, SPVOL, and VAPOR.	STATEQ
RACKS	number of racks of resistance heaters, assigned a value in BLOCK DATA and used in PDAIR.	AIR
RAU	universal gas constant for air, assigned a value in BLOCK DATA, used by COND and EVAPR (ft-lbf/lbm-R).	AIR
RESIST	amount of resistance heat required to meet the house load, calculated and used in the main program, printed by OUTPUT (Btu/hr).	PRNT8
RHI	the relative humidity of the air entering the evaporator coil, calculated and used in EVAP, printed in OUTPUT.	PRNT5
RHIC	the relative humidity of the air entering the condenser unit, read by DATAIN and used in COND and EXCH.	CONDEN
RHIE	the relative humidity of the air entering the evaporator unit, read by DATAIN, used by EVAP and EVAPR.	EVAPOR
RHO	relative humidity of the air at the leaving edge of the evaporator, calculated and used by EVAP, printed by OUTPUT.	PRNT5
RHTERM	constant in dehumidification solution, calculated in EVAP and used in TWOSOL.	TWO
RPM	actual compressor motor speed, assigned a value and used in COMP, printed by OUTPUT (rpm's).	PRNT1

RPMFAN	motor speed for the outdoor fan, assigned a value in BLOCK DATA, used by FANFIT (rpm's).	FANMOT
RPMSLP	slope of the linear fit to the fraction of no-load compressor motor speed as a function of fraction of full-load power, assigned a value in BLOCK DATA and used in COMP.	CMPMOT
RTBCND	the number of return bends in the condenser, read by DATAIN, scaled and used by CALC.	CONDEN
RTBEVP	the number of return bends in the evaporator, read by DATAIN, scaled and used by CALC.	EVAPOR
RTOT	overall resistance to heat transfer for the superheated region of the condenser (1/UA), calculated in EFFCT and used by EXCH (hr-F/Btu).	EFFARG
SEFFD	overall surface efficiency for hexagonal fins (staggered tubes) in the evaporator, calculated and used in EVAP, used by EVAPR, and printed by OUTPUT.	EVAPRS
SEFFWA	average surface efficiency for the portion of the evaporator where moisture removal occurs, calculated and used in EVAP, used in EVAPR, and printed in OUTPUT.	EVAPRS
SEFFXC	overall surface efficiency for the condenser, calculated in SEFF, and used by COND, EFFCT, and EXCH.	CONDS
SIGAC	ratio of the free flow frontal area of the condenser to the total frontal area, calculated in CALC and used in COND.	CONDEN
SIGAE	ratio of the free flow frontal area of the evaporator to the total frontal area, calculated in CALC and used in EVAPR.	EVAPOR
SS	specific speed of the outdoor fan, calculated in FANFIT and printed by OUTPUT.	PRNT8
STATIC	static superheat setting for the thermostatic expansion TXVDAT valve, assigned a value in BLOCK DATA or read by DATAIN, used by TXV and printed by OUTPUT (F).	
STC	vertical spacing between tube passes in the condenser, read by DATAIN, used by CALC and COND (ft).	CONDEN
STE	vertical spacing between tube passes in the evaporator, read by DATAIN, used by CALC, EVAP, and EVAPR (ft).	EVAPOR
STRTOT	ratio of the sensible to total heat transfer rates for the evaporator, calculated in EVAP, printed by OUTPUT.	PRNT5

STRTP	ratio of the sensible to total heat transfer rates for the two-phase region of the evaporator, calculated in EVAP and printed in OUTPUT.	PRNT5
SUCFAC	correction factor for suction gas heating in the compressor, assigned a value in BLOCK DATA and used in CMPMAP.	MAPFIT
SUPER	specified superheat of the refrigerant leaving the evaporator read by DATAIN, used by COMP, EVPTR, OUTPUT, and TXV (F).	FLOWBA
SUPERB	base superheat value for the compressor map, read by DATAIN and used by CMPMAP (F).	MAPFIT
SUPRAT	rated operating superheat for the thermostatic expansion valve, assigned a value in BLOCK DATA or read by DATAIN, used by TXV, and printed by OUTPUT (F).	TXVDAT
SYNC	synchronous or actual compressor motor speed depending on whether or not the full load motor power is calculated, read in DATAIN and used in COMP (rpm's).	COMPR
TACI	temperature of the air at the point where moisture removal begins, calculated and used in EVAP, printed in OUTPUT (F).	PRNT5
TAIC	temperature of the air crossing the condenser, includes any heat losses from the fan motor or compressor, calculated in COND and printed in OUTPUT (F).	PRNT3
TAIE	air temperature crossing the evaporator coil, inlet air temperature with any additions due to fan motor and compressor heat losses, calculated in EVAPR and printed in OUTPUT (F).	PRNT7
TAIIC	air temperature entering the condenser, read by DATAIN, used by COND and EFFCT, printed by OUTPUT (F).	CONDSR
TAIIE	air temperature entering the evaporator which corresponds to the current values of TSATEI and TSATEO, the desired value for the ambient air temperature is read by DATAIN, current value is calculated and used by the main program, also used by EVAPR, EVPTR, and OUTPUT, printed by OUTPUT (F).	EVAPTR
TAOC	air temperature after it passes over the condenser coil, calculated in EXCH, used by COND, and printed in OUTPUT (F).	CONDSR
TAOE	air temperature leaving the evaporator with any additions for compressor and fan motor heat losses, calculated and used by EVAP, used by EVAPR, and printed by OUTPUT (F).	EVAPTR

TAOOC	air temperature leaving the condenser, includes any heat losses from the compressor and fan motors, calculated in COND and printed in OUTPUT (F).	PRNT3
TAOOE	air temperature leaving the evaporator, includes any additions due to heat losses from the fan and compressor motors, calculated in EVAPR and printed in OUTPUT (F).	PRNT7
TAOSC	outlet air temperature from the subcooled region of the condenser, calculated in EXCH, printed in OUTPUT (F).	PRNT4
TAOSPC	outlet air temperature from the superheated region of the condenser, calculated in EXCH, printed in OUTPUT (F).	PRNT4
TAOSPE	outlet air temperature from the superheated region of the evaporator, calculated and used in EVAP, printed in OUTPUT (F).	PRNT5
TAOTPC	outlet air temperature from the two-phase region of the condendser, calculated in EXCH, printed in OUTPUT (F).	PRNT4
TAOTPE	outlet air temperature from the two-phase region of the evaporator, calculated and used in EVAP, printed in OUTPUT (F).	PRNT5
TC	critical temperature for the refrigerant, assigned a value in TABLES, used in SATPRP, SPVOL, and VAPOR (R).	SUPER
TERAT	evaporating temperature used for rating the thermostatic expansion valve, assigned a value in BLOCK DATA, used in TXV (F).	TXVDAT
TFLODV	refrigerant temperature entering the flow control device, calculated and used in FLOBAL, printed in OUTPUT (F).	PRNT2
TFR	constant used to convert from Farenheit to absolute temperature when using correlations for refrigerant properties (i.e. the value assumed by researcher deriving the correlation), assigned a value in TABLES, used by SATPRP, SPVOL, TSAT, and VAPOR (F).	SUPER
TIC	temperature of the refrigerant entering the condenser, initialized by COMP, calculated in DESUPR and COMP, used by COND, DESUPR, EFFCT, and EXCH, printed by OUTPUT (F).	CONDSR
TIE	temperature of the refrigerant entering the evaporator, calculated by EVAPR and printed by OUTPUT (F).	EVAPTR
TLQCOR	correction factor to adjust tube and nozzle pressure drops in the thermostatic expansion valve for liquid temperatures entering the valve other than the rating temperature, calculated and used in TXV, printed in OUTPUT.	TXVDAT

TLQRAT	rating temperature of the liquid refrigerant at the inlet to the thermostatic expansion valve, assigned a value in BLOCK DATA and used in TXV (F).	TXVDAT
TOLH	tolerance parameter used to calculate superheated vapor properties when the two known properties are the pressure and enthalpy, assigned a value in BLOCK DATA, used by COMP.	MPASS
TOLS	tolerance parameter used to calculate superheated vapor properties when the two known properties are pressure and entropy, assigned a value in BLOCK DATA and used by COMP.	MPASS
TRICMP	temperature of the refrigerant at the compressor shell inlet calculated and used in COMP or CMPMAP, printed in OUTPUT (F).	CMPRSR
TROC	temperature of the refrigerant at the condenser exit, estimated in FLOBAL, calculated in EXCH, used by CNDNSR, COND, FLOBAL, and FLODEV, printed in OUTPUT (F).	CONDSR
TROCMP	temperature of the refrigerant at the compressor shell outlet calculated in COMP or CMPMAP, printed in OUTPUT (F).	CMPRSR
TROE	temperature of the refrigerant leaving the evaporator, calculated and used in EVAP, used by EVAPR and EVPTR, printed by OUTPUT (F).	EVAPTR
TRVDS	refrigerant temperature at the end of the desuperheating region in the condenser, initialized in COND, calculated by EXCH, and used by COND, EFFCT, and EXCH (F).	CONDS
TSATCI	saturation temperature of the refrigerant entering the condenser, initial guess read by DATAIN, calculated in the main program, used by COMP, FLOBAL, COND, EXCH, and DESUPR, printed by OUTPUT (F).	CONDSR
TSATCO	saturation temperature of the refrigerant leaving the condenser calculated in COND and FLOBAL, used by CNDNSR, COND, EXCH, FLOBAL, and FLODEV, printed in OUTPUT (F).	CONDSR
TSATEI	saturation temperature of the refrigerant entering the evaporator, initialized in the main program, calculated and used by EVAPR and TXV, printed by OUTPUT (F).	EVAPTR
TSATEO	saturation temperature of the refrigerant leaving the evaporator, initial guess read by DATAIN, calculated and used by the main program, used by COMP, EVAPR, EVPTR, FLOBAL, and TXV, printed by OUTPUT (F).	EVAPTR
TSATFL	saturation temperature of the refrigerant entering the flow control device, calculated and used in FLOBAL, printed in OUTPUT (F).	PRNT2

TSATR1	average saturation temperature in the evaporator, assigned a value in EVAP, used in TWISOL (F).	TWI
TSATR2	average saturation temperature in the evaporator, assigned a value in EVAP, used by TWOSOL (F).	TWO
TSICMP	saturation temperature of the refrigerant at the compressor shell inlet calculated and used in COMP or CMPMAP, printed in OUTPUT (F).	CMPRSR
TSOCMP	saturatin temperature of the refrigerant at the compressor shell outlet calculated in COMP or CMPMAP, printed in OUTPUT (F).	CMPRSR
TWALLI	tube wall temperature at the leading edge of the evaporator where moisture removal begins, calculated and used in EVAP, used by TWOSOL, printed in OUTPUT (F).	TWO
TWALLO	air temperature at the tube walls on the leaving edge of the evaporator, calculated and used in EVAP, printed in OUTPUT (F).	PRNT5
TWBI	wet bulb temperature of the air entering the evaporator, calculated in EVAP, printed in OUTPUT (F).	PRNT5
TWBO	wet bulb temperature of the air at the leaving edge of the evaporator, calculated in EVAP, printed in OUTPUT (F).	PRNT5
TXVRAT	rated capacity of the thermostatic expansion valve, assigned a value in BLOCK DATA and used in TXV (tons).	TXVDAT
UATPAW	air-side thermal conductance times the heat transfer area (UA) for the portion of the two-phase region of the evaporator which is wetted due to dehumidification, calculated in EVAPR, and printed in OUTPUT (Btu/hr-F).	UAS
UATPW	refrigerant-side thermal conductance times the heat transfer area (UA) for that portion of the two-phase region of the evaporator whose outside surface is wetted due to dehumidification, calculated in EVAPR and printed in OUTPUT (Btu/hr-F).	UAS
ULA	upper limit on the Reynold's number for laminar flow of the refrigerant, assigned a value in BLOCK DATA and used in SPHTC.	VAPHTC
V	constant in dehumidification solution, calculated in EVAP and used in TAOSOL and TWOSOL.	TWO

VOLFAC	correction factor for the compressor volumetric efficiency, assigned value in BLOCK DATA and used in CMPMAP.	MAPFIT
VR	compressor clearance volume ratio, read by DATAIN and used by COMP.	COMPR
W	constant in dehumidification solution, calculated in EVAP and used in TAOSOL and TWOSOL.	TWO
WAIRI	humidity ratio of the air at the leading edge of the evaporator calculated and used in EVAP, printed in OUTPUT.	PRNT5
WAIRO	humidity ratio of the air leaving the evaporator, calculated and used in EVAP, printed in OUTPUT.	PRNT5
WOUT	humidity ratio of the air at the leaving edge of the evaporator, calculated and used by EVAP, printed by OUTPUT.	PRNT5
WTC	spacing of the tubes in the condenser in the direction of air flow, read by DATAIN, used by CALC and COND (ft).	CONDEN
WTE	spacing of the tubes in the evaporator in the direction of the air flow, read by DATAIN, used by EVAP and EVAPR (ft).	EVAPOR
WWALLI	humidity ratio at the tube walls on the leading edge of the evaporator where moisture removal begins, calculated and used in EVAP, calculated in TWISOL, printed in OUTPUT.	TWI
WWALLO	humidity ratio of the air at the tube walls on the leaving edge of the evaporator, calculated and used in EVAP, printed in OUTPUT.	PRNT5
X	constant used in correlating enthalpy of refrigerant vapor with temperature and specific volume, assigned a value in TABLES and used in SATPRP.	OTHER
XFLODV	vapor quality of the refrigerant entering the flow control device, calculated in FLOBAL and printed in OUTPUT.	PRNT2
XIC	refrigerant vapor quality entering the condenser, set to 1.0 in FLOBAL, modified in DESUPR, used by COND and EXCH, printed in OUTPUT.	CONDSR
XIE	refrigerant vapor quality entering the evaporator, calculated and used in EVAPR and printed in OUTPUT.	EVAPTR

XINCMP	refrigerant vapor quality at the compressor shell inlet calculated and used in COMP or CMPMAP, printed in OUTPUT.	CMPRSR
XKFC	thermal conductivity of the fins in the condenser, read by DATAIN, used by CALC and COND (Btu/hrFt-F).	CONDEN
XKFE	thermal conductivity of the fins in the evaporator, read by DATAIN, used by CALC and EVAP (Btu/hr-ft-F).	EVAPOR
XLCORR	correction factor for the pressure drop in distributor tubes of the thermostatic expansion valve for tubes of lengths other than the rated length, calculated and used in TXV, printed in OUTPUT.	TXVDAT
XLLR	lower limit on the Reynold's number for laminar flow of the refrigerant, assigned a value in BLOCK DATAand used in SPHTC.	VAPHTC
XLEQDL	equivalent length of the compressor discharge line from the reversing valve to the condenser, read by DATAIN and used by COMP (ft).	LINES
XLEQHP	equivalent length of the high pressure line from the compressor discharge port to the reversing valve, read by DATAIN and used by COMP (ft).	LINES
XLEQLL	equivalent length of the liquid line connecting the indoor and outdoor heat exchangers, read by DATAIN and used by FLOBAL (ft).	LINES
XLEQLP	equivalent length of the low pressure line from the compressor suction port to the reversing valve, read by DATAIN and used by COMP (ft).	LINES
XLEQSL	equivalent length of the suction line from the evaporator to the reversing valve, read by DATAIN and used by COMP (ft).	LINES
XMAC	mass flow rate of air across each parallel circuit in the condenser, calculated in COND, used by EFFCT and EXCH, printed in OUTPUT (lbm/hr).	CONDS
XMAE	mass flow rate of air across each parallel circuit in the evaporator, calculated in EVAPR and used in EVAP, printed in OUTPUT (lbm/hr).	EVAPS
XMASP	mass flow rate of the air across the superheated region of each circuit in the evaporator, calculated and used in EVAP, printed in OUTPUT (lbm/hr).	PRNT5
XMATP	mass flow rate of the air across the two-phase region of each circuit in the evaporator, calculated and used in EVAP, printed in OUTPUT (lbm/hr).	PRNT5
XMM	rate of moisture removal from the air, calculated in EVAP and printed in OUTPUT (lbm/hr).	PRNT5

XMR	refrigerant mass flow rate, initial guess or estimate read by DATAIN, calculated in COMP, used by the main program, COND, EFFCT, EVAPR, FLOBAL, and the flow control device subroutines, printed and used by OUTPUT (lbm/hr).	FLOBAL
XMUA	viscosity of air, calculated and used by COND and EVAPR (lbm/hr-ft).	AIR
XNTUSC	number of transfer units for the subcooled region of the condenser, calculated in EXCH, printed in OUTPUT.	PRNT4
XNTUSP	number of heat transfer units for the superheated region of the condenser, calculated and used in EXCH, printed in OUTPUT.	PRNT4
XNTUSU	number of heat transfer units for the superheated region of the evaporator, calculated and used in EVAP, printed in OUTPUT.	PRNT5
XNTUTP	number of heat transfer units for the two-phase region of the condenser, calculated and used in EXCH, printed in OUTPUT.	PRNT4
XNTUTP	number of heat transfer units for the two-phase region of the evaporator, calculated and used in EVAP, printed in OUTPUT.	PRNT5
XOC	refrigerant vapor quality leaving the condenser, initialized in COND, calculated in EXCH, used by CNDNSR, COND, EXCH, FLOBAL, and FLODEV, printed in OUTPUT.	CONDSR
XOE	vapor quality of the refrigerant leaving the evaporator, calculated and used in EVAPR, used in EVPTR and COMP, and printed in OUTPUT.	EVAPTR
XOUCMP	refrigerant vapor quality at the compressor shell outlet calculated in COMP or CMPMAP and printed in OUTPUT.	CMPRSR
Y	constant used in correlating entropy of refrigerant vapor with temperature and specific volume, assigned a value in TABLES and used in SATPRP.	OTHER

Appendix E — Cross-Reference of Common Blocks

The common blocks listed in the rows of Table 1 are used to transmit data to or from the subroutines identified by the columns with the "X" marks.

Table E.1

COMMON BLOCKS	MAIN PROG	BLOCK DATA	CALC	CAPTUB	CMPMAP	CNDNSR	COMP	COND	DATAIN	EFFCT	EVAP	EVAPR	EVPTR	EXCH	FANFIT	FLOBAL	MUKCP	ORIFIC	OUTPUT	SATPRP	SPFHT	SPFHTC	SPVOL	TABLES	TSAT	TWISOL	TWOSOL	TXV	VAPOR	XMOIST
	SUBROUTINES																													
AIR		X						X		X	X	X		X																X
A1	X		X	X	X	X	X	X			X	X	X	X		X		X										X		
BLANK	X							X	X			X							X											
CMPMOT		X					X																							
CMPRSR					X		X												X											
COMPR	X	X			X	X	X		X				X						X											
CONDEN	X		X					X	X	X				X																
CONDS	X							X		X				X					X											
CONDSR	X				X	X	X	X	X	X				X		X			X											
DENSIT																				X				X						
EFFARG										X				X																
EVAPOR	X		X			X			X		X	X																		
EVAPRS											X	X							X											
EVAPS	X										X	X							X											
EVAPTR	X				X		X		X		X	X	X			X			X									X		
FANMOT		X													X															
FLOWBA	X	X		X	X	X	X		X				X			X		X	X									X		
LINES		X			X		X	X	X			X				X														
MAPFIT		X			X				X										X											
MPASS	X	X				X		X	X		X	X	X			X			X											
OTHER																				X	X			X					X	
PRNT1					X		X												X											
PRNT2																X			X											
PRNT3								X											X											
PRNT4														X					X											
PRNT5											X								X											
PRNT7												X							X											
PRNT8	X							X				X			X				X											
REFRIG	X	X															X			X	X			X			X	X		
SAT																				X				X	X					
STATEQ																				X	X		X	X				X		
SUPER																				X	X		X	X	X			X		
TWI											X								X						X					
TWO											X								X							X				
TXVDAT		X							X										X								X			
UAS								X				X							X											
VAPHTC		X																				X								

Appendix F — Subroutine Descriptions and Cross-Reference of Subroutine Calls

Subroutine Descriptions

Main Program — serves as driving program for high- and low-side computations and contains iterative loop converging on evaporator inlet air temperature

BLOCK DATA — assigns values to constants and infrequently changed parameters

CALC — calculates geometric constants for both heat exchangers

CAPTUB — submodel for capillary tube flow rate

CHTC — calculates refrigerant-side heat transfer coefficient for the two-phase region of the condenser

CMPMAP — computes refrigerant mass flow and compressor power consumption from compressor map data

CNDNSR — serves as driving routine for COMP, COND and FLOBAL and returns the difference between the calculated and specified condenser subcooling or between the compressor and expansion device refrigerant mass flow rates

COMP — computes refrigerant mass flow rate and compressor power consumption from efficiency and loss parameters

COND — calculates total condenser heat transfer rate, air and refrigerant properties and refrigerant and air-side pressure drops for fixed inlet refrigerant conditions

DPF — determines an approximate dew-point temperature for a given vapor pressure of moist air

DPFSOL — calculates the difference between the known saturation pressure of water vapor at the tube wall and the saturation pressure corresponding to an estimated, or given tube wall temperature

DPLINE — determines the single-phase pressure drop in the refrigerant lines

EFFCT — computes the difference in condenser effectiveness values between the general effectiveness equation and the specific cross-flow effectiveness equation as a function of the fraction of the coil, f_v, containing superheated refrigerant vapor

EHTC — calculates refrigerant-side heat transfer coefficient for the two-phase region of the evaporator

EVAP	determines the heat transfer, moisture removal, and outlet air temperatures and humidities from one circuit of the evaporator for given heat transfer coefficients and saturation temperatures at the beginning and end of the two-phase region
EVAPR	calculates evaporator heat transfer rate, air and refrigerant properties, and refrigerant and air-side pressure drops for fixed exit refrigerant conditions
EVPTR	serves as a driving routine for EVAPR and returns the difference between the specified evaporator superheat and the calculated value
EXCH	determines the heat transfer and outlet temperatures for one circuit of the condenser for given heat transfer coefficients and saturation temperatures at the beginning and end of the two-phase region
EXF	determines the effectiveness of a cross-flow heat exchanger using the effectiveness — NTU method
FANFIT	calculates combined fan-fan motor efficiency given air-side pressure drop and volumetric air-flow rate
FLOBAL	determines refrigerant conditions at the inlet to the flow control device and drives the expansion device models
FRICT	computes the general Moody friction factor for single phase flow in tubes
GUESS2	brackets a solution prior to using a root finder by shifting end points by factors of 10
GUESS3	brackets a solution prior to using a root finder by shifting end points by constant step
INTER	interpolate in a single dimension using Lagrangian polynomial
HAIR	computes air-side heat transfer coefficient for smooth fin and tube geometry
MUKCP	calculates viscosity, thermal conductivity, and specific heat of 13 refrigerants
MUKCPA	calculates viscosity, thermal conductivity, and specific heat of air
ORIFIC	computes refrigerant mass flow rate through a short-tube orifice
OUTPUT	prints a detailed summary of output data

PDAIR	calculates air-side pressure drop for smooth, wavy, or louvered fin and tube heat exchangers
PDROP	determines single- and two-phase pressure drops for flow in heat exchanger tubes
PVSF	calculates partial pressure of water vapor in saturated air
SATPRP	evaluates the saturation thermodynamic properties of a specified refrigerant
SEFF	determines surface efficiency for a hexagonal shaped fin surface
SLAG	computes single precision Lagrangian interpolation in two dimensions from tabulated data
SPFHT	calculates refrigerant specific heats at constant pressure and volume and specific heat ratio
SPHTC	computes single-phase heat transfer coefficient for laminar, transition, or turbulent gas flow from an abrupt contraction entrance
SPHTC2	computes single-phase heat transfer coefficient for fully developed liquid or gas flow
SPVOL	evaluates specific volume of superheated refrigerant
SUPCOR	calculates power and mass flow correction factors for map-based compressor model to correct for superheat level
TABLES	assigns constants for refrigerant thermodynamic property subroutines
TAOSOL	computes the exit air temperature from the region of the evaporator where moisture removal occurs
TRIAL	determines thermodynamic properties of superheated refrigerant vapor given two known properties
TSAT	calculates saturation temperature of refrigerant given saturation pressure
TWISOL	used to compute the wall temperature at which moisture removal begins on the leading edge of the evaporator
TWOSOL	used to compute the wall temperature at the exit from the evaporator
TXV	computes the refrigerant mass flow rate through a thermostatic expansion valve

VAPOR	determines thermodynamic properties of superheated refrigerant vapor given temperature and pressure
WBF	determines wet-bulb temperature of moist air
WTSFIT	computes coefficients for a quadratic fit of wall temperature to enthalpy of moist air
XMOIST	calculates dew point temperature, humidity ratio enthalpy, and wet-bulb temperature or relative humidity of moist air
ZERO's	each of these routines solves for the root, or zero, of a function from two points which bracket the solution using bi-section and Newton's method

The subroutines listed in the columns of Table F.1 are called from the subprograms listed in the rows of Table F.1 which are indicated by "X's".

Table F.1

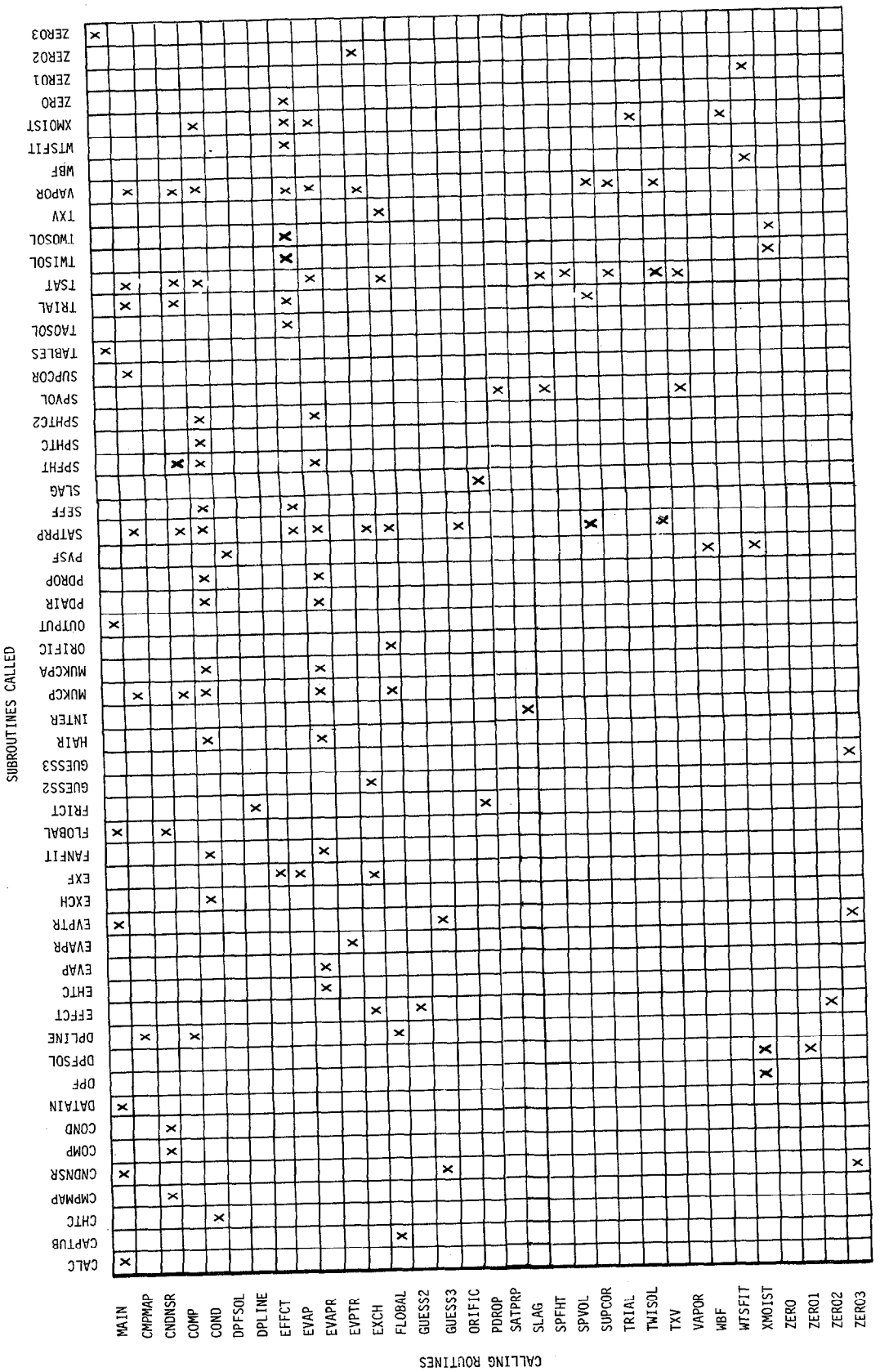
SUBROUTINES CALLED
CALLING ROUTINES
CALC
CAPTUB
CHTC
CMPMAP
CNDNSR
COMP
COND
DATAIN
DPF
DPFSOL
DPLINE
EFFCT
EHTC
EVAP
EVAPR
EXCH
EXF
FANFIT
FLOBAL
FRICT
GUESS2
GUESS3
HAIR
INTER
MUKCP
MUKCPA
ORIFIC
OUTPUT
PDAIR
PDROP
PYSF
SATPRP
SEFF
SLAG
SPFHT
SPHTC
SPHTC2
SPVOL
SUPCOR
TABLES
TAOSOL
TRIAL
TSAT
TWISOL
TWOSOL
TXV
VAPOR
WBF
WTSFIT
XMOIST
ZERO
ZERO1
ZERO2
ZERO3
MAIN
CMPMAP
CNDNSR
COMP
COND
DPFSOL
DPLINE
EFFCT
EVAP
EVAPR
EVPTR
EXCH
FLOBAL
GUESS2
GUESS3
ORIFIC
PDROP
SATPRP
SLAG
SPFHT
SPVOL
SUPCOR
TRIAL
TWISOL
TXV
VAPOR
WBF
WTSFIT
XMOIST
ZERO
ZERO1
ZERO2
ZERO3

Appendix G — Algebraic Notation

A	frontal area of heat exchanger
a	intercept of a linear fit to data which is determined by context
A_a	air-side fin and tube heat transfer area
$A_{contact}$	total contact area between fins and tubes
A_f	air-side fin heat transfer area
A_{filter}	frontal area of filter on indoor unit
A_{ft}	air-side fin and tube heat transfer area
A_{heater}	cross-sectional area of the resistance heater section
A_{min}	ratio of total air-side heat transfer area to the minimum free-flow area
$A_{orifice}$	cross-sectional area of the short tube orifice
A_r	total refrigerant-side heat transfer area
A_{rh}	refrigerant-side heat transfer area for each parellel circuit
A_{side}	heat transfer area of each side of each fin
A_{tubes}	total exposed surface area of tubes in heat exchanger
A_o	refrigerant-side heat transfer area per unit air flow rate
b	slope of a linear fit to data which is determined by context
b_{fac}	bypass or bleed factor for a thermostatic expansion valve
C	compressor piston clearance volume ratio or expansion device flow area coefficient or Dittus-Boetter exponent
C_a	heat capacity rate of air ($\dot{m}_a c_{pa}$)
C_{fac}	ratio of humidity ratio gradient to the temperature gradient
C_{max}	maximum of the heat capacity rates for the air and the refrigerant
C_{min}	minimum of the heat capacity rates for the air and the refrigerant

C_r	heat capacity rate of refrigerant ($\dot{m}_r c_p$)
c	constant in Eq. 6.15
c_p	specific heat of the refrigerant
c_{pa}	specific heat of air
c_{pm}	specific heat of moist air
C_r	heat capacity rate of the refrigerant
C_o	correction factor to the air-side heat transfer coefficient for wavy and louvered fins
D	total compressor piston displacement or refrigerant tube diameter depending on context
d	depth of heat exchanger
D_a	air-side or outer diameter of heat exchanger tubes
D_{ducts}	diameter of air ducts
D_r	refrigerant-side or inner diameter of heat exchanger tubes
f	fraction of rated value, fraction of coil, or friction factor determined by context
F_a	fin heat transfer area per unit total air-side heat transfer area
F_{moist}	fraction of that part of the evaporator which is in two-phase flow that is wetted due to dehumidification
F_p	fin pitch
F_{sh}	compressor suction gas heating factor
f_{tot}	combined wet and dry friction factor for the evaporator
F_w	fraction of the evaporator that is wetted due to dehumidification
f_{wet}	friction factor for the region of the evaporator which is wetted due to dehumidification
F_v	compressor volumetric efficiency correction factor
$F(X_{tt})$	correlating function for the refrigerant-side two-phase heat transfer coefficient

F_2	correlating parameter
G	mass flux
g_c	gravitational acceleration constant
h	enthalpy of refrigerant or height of heat exchanger
$h_{a,s}$	enthalpy of saturated air at wall surface temperature
$h_{a,\infty}$	enthalpy of moist air at freestream conditions
h_{fg}	latent heat of vaporization
h'_{fg}	driving enthalpy difference in the condenser
h	air or refrigerant heat transfer coefficient (determined by subscript or context)
h_{ave}	average condensation heat transfer coefficient
h_d	mass transfer coefficient
h_{tp}	average condensing or evaporating heat transfer coefficient (condensation value includes an adjustment due to Rohsenow)
h_w	sensible heat transfer coefficient for a wetted surface
h_w^*	effective heat transfer coefficient for a wet surface
h_1	local evaporation heat transfer coefficient using Chaddock-Noerager correlation
h_2	local evaporation heat transfer coefficient for the dry-out region using nonlinear interpolation between the Chaddock-Noerager value at x_{do} and the value for saturated vapor
k	thermal conductivity
L	equivalent length of refrigerant pipes
ℓ	length of tubes in heat exchangers
$\ell_{exposed}$	length of tubes in heat exchanges exposed to the air
ℓ_{tubes}	equivalent length of distributor tubes in thermostatic expansion valve
$\dot{m}$	mass flow rate
$\dot{m}'$	mass flow rate at "standardized" test or rating conditions

N_{cap}	number of parallel capillary tubes
$N_{circuits}$	number of equivalent parallel refrigerant circuits in the heat exchanger
N_f	total number of fins in the heat exchanger
N_{Le}	Lewis number
N_{pr}	Prandtl number
N_{Re}	Reynolds number
N_T	number of tube rows in the heat exchanger in the direction of the air flow
N_{tot}	total number of tubes in the heat exchanger
N_{tu}	number of heat transfer units
N_v	number of tubes stacked vertically in the heat exchanger
P	pressure
$\dot{Q}$	heat transfer rate
$\dot{Q}_{can}$	rate of heat rejection from the compressor shell
$\dot{Q}_{cooling}$	rate of heat transfer from the compressor and compressor motor to the suction gas
$\dot{Q}_{hilo}$	rate of heat transfer from the compressor discharge line to the suction gas
$\dot{Q}$	volumetric air flow rate
R	thermal resistance per unit of refrigerant side-area
r	ratio of UA values used in Eq. 6.11
r_1	ratio of UA values used in Eq. 6.23
S	motor speed
s	heat exchanger coil characteristic
S_{oper}	actual or operating motor speed
S_s	specific speed of the fan for the outdoor heat exchanger
S_{sync}	synchoronous speed of compressor motor

S_T	vertical spacing between tubes in heat exchanger
T	air or refrigerant temperature (determined by context)
T_{aid}	evaporator inlet air temperature for which dehumidification would occur at the finned tube surface
T_{aie}	temperature of the air entering the evaporator
$T_{v,ds}$	bulk refrigerant vapor temperature at the start of the desuperheating region of the condenser
T_{sat}	refrigerant saturation temperature
U	thermal conductance
V_{hx}	volume of space occupied by heat exchanger
W	humidity ratio
$\dot{W}$	work performed or energy input
$W_{a,\infty}$	humidity ratio of air at freestream conditions
$\dot{W}_{fan}$	fan motor power consumption
$\dot{W}_{s,fl}$	compressor-motor full load shaft power
W_T	spacing of heat exchanger tubes in the direction of air flow
x	refrigerant vapor quality
X_{tt}	correlating parameter for two-phase heat transfer coefficient
α_a	total air-side heat transfer area per unit heat exchanger volume
α_{can}	fraction of the compressor power consumption which is rejected from the shell to the ambient air
α_{corr}	correction factor for liquid refrigerant temperatures at the inlet to a thermostatic expansion valve other than 100°F
α_{hilo}	fraction of compressor power consumption transferred from the discharge line to the suction line
α_r	total refrigerant-side heat transfer area per unit heat exchanger volume
α_{racks}	correction factor to adjust air-side pressure drop for the number of resistant heater racks

β_{corr}	correction factor for TXV distributor tube lengths other than 30 inches
γ	ratio of specific heat at constant pressure to specific heat at constant volume
δ	fin thickness
Δh	enthalpy change
ΔP	pressure drop
ΔP_{H_2O}	pressure drop measured in inches of water
ΔT	temperature difference, level of subcooling, or level of superheat depending on context
ε	heat exchanger effectiveness
ε_{cf}	effectiveness of a counter-flow heat exchanger
η	compressor efficiency or heat exchanger overall surface effectiveness
μ	viscosity
ν	specific volume
ρ	density
ϕ	capillary tube flow factor
σ_a	free-flow frontal area per unit total frontal area of heat exchanger

Subscripts

a	air
actual	at modeled operating conditions
ave	average
cm	compressor
d	dry
do	dry-out point in the evaporator where there is no longer a liquid film on the tube wall
dp	dew point

eff	effective
evap	evaporator
f	fin
fl	compressor motor full load
frict	friction
ft	fin and tube
i	heat exchanger inlet
in	entering
inlet	compressor shell inlet
isen	isentropic
ℓ	liquid
loc	local
m	mean
map	from compressor map
max	maximum
mech	mechanical
mom	momentum
noz	TXV nozzle
o	heat exchanger outlet
oper	at modeled operating conditions
out	exiting
outlet	compressor shell outlet
r	refrigerant
rated	at rating conditions
rb	return bends
s	compressor shaft

sat	saturation
sh	suction gas heating
static	static fan efficiency or static superheat value of a thermostatic expansion valve
t	tube
tp	two-phase
tubes	heat exchanger or TXV distributor tubes
TXV	thermostatic expansion valve
v	vapor
vol	volumetric
w	region wetted due to dehumidification
∞	freestream condition

Appendix H — Derivation of Dehumidification Solution

H.1 Introduction

A method is described in this section for computing the performance of an air-to-refrigerant evaporator under dehumidification conditions. The method represents an assimilation and/or expansion of the work of Goodman [H.1], McElgin and Wiley [H.2], Hiller and Glicksman [H.3], Threlkeld [H.4], and McQuiston [H.5, H.6], and uses wet heat transfer coefficients derived from dry heat transfer values via the equation of Myers [H.7] as noted in Section 6.

H.2 Heat Transfer Equations — Air to Wall

The local driving force for simultaneous heat and mass transfer can be described, using simplifying assumptions, by Eq. H.1 [H.6]

$$d\dot{Q} = h_d \, (h_{a,\infty} - h_{a,s}) dA_s \tag{H.1}$$

where

- $d\dot{Q}$ - a differential quantity of local heat and mass transfer
- h_d - the mass transfer coefficient
- $h_{a,\infty}$ - the enthalpy of humid air at the freestream condition
- $h_{a,s}$ - the enthalpy of saturated air at the wall surface temperature
- dA_s - a differential element of wetted surface area.

Equation H.1 contains the assumption that the Colburn analogy, given by Eq. H.2 [H.6],

$$\frac{h_w}{c_{pm} h_d} = N_{Le}^{2/3} \tag{H.2}$$

where

h_w - sensible heat transfer coefficient for a wetted surface

c_{pm} - moist air specific heat, $c_{pm} = c_{pa} + .444\ W_{a,\infty}$

$W_{a,\infty}$ - humidity ratio of air, and

N_{Le} - Lewis number,

holds and that $(N_{Le})^{2/3} \simeq 1$. Also, the energy content of the condensate is neglected and the effect of the water film thickness is ignored (except for the effect on the sensible heat transfer coefficient for a wetted surface). There are analyses in the literature by Threlkeld [H.4] and Elmahdy [H.8] which do not require some or all of these assumptions; however, these analyses were judged too complicated for use with the simplified heat exchanger routines in the heat pump model.

Equation H.1 is strictly applicable for describing heat and mass transfer rates for situations such as humid air flowing between two parallel flat plates. For a fin-and-tube heat exchanger, an appropriate equation presented by McQuiston [H.5, H.6] is

$$d\dot{Q} = h_d\, \eta_{w,ft}(h_{a,\infty} - h_t)dA_{ft} \qquad (H.3)$$

where the subscripts "t" and "ft" refer to tube and total fin-and-tube surface, respectively. The overall wet surface effectiveness, $\eta_{w,ft}$, in Eq. H.3 is defined as

$$\eta_{w,ft} = 1 - \frac{A_f}{A_{ft}}(1 - \eta_{w,f}) \qquad (H.4)$$

where the subscript "f" refers to fin surface. The term $\eta_{w,f}$ in Eq. H.4 is a wet fin efficiency which is defined by McQuiston [H.5] in a manner similar to usual fin efficiency equations except that the usual parameter "m", where

$$m = \left(\frac{2h}{k\delta}\right)^{1/2},$$

is replaced by M, i.e.,

$$M = \left[\left(\frac{2h_w}{k_f \delta}\right)\left(1 + \frac{C_{fac} h_{fg}}{c_{pm}}\right)\right]^{1/2} = \left[\frac{2h^*_w}{k_f \delta}\right]^{1/2} \qquad (H.5)$$

where

- h - sensible heat transfer coefficient for a dry surface
- h_w - sensible heat transfer coefficient for a wet surface
- h^*_w - effective heat transfer coefficient for a wet surface
- k_f - thermal conductivity of the fin,
- δ - fin thickness
- h_{fg} - enthalpy of vaporization of the water vapor,

and

- C_{fac} - ratio of humidity ratio gradient to temperature gradient, (specifically defined in Appendix I).

Since C_{fac} in Eq. H.5 is dependent on the ratio of latent to sensible heat gradients, the value of wet fin efficiency will be dependent on the dehumidification rate.

H.3 Heat Transfer Equations — Air to Mean Surface Conditions

Equation H.3 contains h_t -- the enthalpy of saturated air evaluated at the tube wall temperature. Since the tube surface is only a small portion of the external heat transfer surface, a better variable for use in determining when both the fin and tube start to condense water vapor is the mean temperature of the fin-and-tube combination (the effective surface temperature). From Threlkeld [H.4], it is shown that for a dry surface

$$\eta_{d,f} = \frac{T_{a,\infty} - T_{f,m}}{T_{a,\infty} - T_t} \qquad (H.6)$$

where the subscript "f,m" refers to a mean fin value. Similarly, for a wet surface, since McQuiston's solution for $\eta_{m,f}$ is in terms of T_t and $T_{a,\infty}$, it follows that

$$\eta_{w,f} = \frac{T_{a,\infty} - T_{f,m}}{T_{a,\infty} - T_t} \tag{H.7}$$

and

$$\eta_{w,ft} = \frac{T_{a,\infty} - T_{ft,m}}{T_{a,\infty} - T_t} \quad . \tag{H.8}$$

Next, using a relationship implied in the derivation of $\eta_{w,f}$, i.e.,

$$h_{a,\infty} - h_{ft,m} = (1 + C_{fac})(T_{a,\infty} - T_{ft,m}) \tag{H.9}$$

the overall wet surface effectiveness $\eta_{w,ft}$ can also be written as

$$\eta_{w,ft} = \frac{h_{a,\infty} - h_{ft,m}}{h_{a,\infty} - h_t} \quad . \tag{H.10}$$

Substitution of Eq. H.10 into Eq. H.3 yields

$$d\dot{Q} = h_d(h_{a,\infty} - h_{ft,m})dA_{ft} \quad . \tag{H.11}$$

H.4 Heat Transfer Equations — Mean Surface to Refrigerant Conditions

Next, a relationship is needed between conditions at the mean fin and tube temperature, $T_{ft,m}$, and the refrigerant temperature, T_r.

Using McQuiston's definition of $\eta_{w,ft}$, the total heat flow can be written in two ways, i.e.,

$$d\dot{Q} = h^*_w \eta_{w,ft}(T_{a,\infty} - T_t)dA_{ft} \tag{H.12}$$

$$d\dot{Q} = h^*_w(T_{a,\infty} - T_{ft,m})dA_{ft} \tag{H.13}$$

Combination of Eqs. H.12 and H.13 to eliminate $T_{a,\infty}$ yields

$$d\dot{Q} = \frac{h^*_w \eta_{w,ft}(T_{ft,m} - T_t)dA_{ft}}{1 - \eta_{w,ft}} \tag{H.14}$$

The total heat flow from the tube to the refrigerant is given by

$$d\dot{Q} = h_r(T_t - T_r)dA_r \tag{H.15}$$

Using Eqs. H.14 and H.15 to eliminate T_t yields

$$d\dot{Q} = (T_{ft,m} - T_r)/\left(\frac{1 - \eta_{w,ft}}{\eta_{w,ft} h^*_w dA_{ft}} + \frac{1}{h_r dA_r}\right) \tag{H.16}$$

H.5 Derivation of the Coil Characteristic and Total Heat Flow Equation

Equations H.16 and H.11 are next combined to arrive at a relationship between $[h_{a,\infty} - h_{ft,m}]$ and $[T_{ft,m} - T_r]$. This relationship is known as the coil characteristic, s, and is given here by

$$s = \frac{T_{ft,m} - T_r}{h_{a,\infty} - h_{ft,m}} = \frac{1}{c_{pm}}\left[\frac{(1 - \eta_{w,ft})}{\eta_{w,ft}} \quad \frac{h_w}{h^*_w} + \frac{h_w}{h_r}\frac{dA_{ft}}{dA_r}\right] \tag{H.17}$$

where h_d in Eq. H.11 has been replaced by h_w/c_{pm}.

Assuming that

$$\frac{dA_{ft}}{dA_r} = \frac{A_{ft}}{A_r}$$

and using the relationship

$$h^*_w = h_w\left(1 + \frac{C_{fac}}{c_{pm}}\, h_{fg}\right) \quad ,$$

Eq. H.17 can be written as

$$s = \frac{T_{ft,m} - T_r}{h_{a,\infty} - h_{ft,m}} = \frac{(1 - \eta_{w,ft})}{\eta_{w,ft}(c_{pm} + C_{fac}\, h_{fg})} + \frac{h_w}{h_r c_{pm}}\,\frac{A_{ft}}{A_r} \qquad (H.18)$$

At this point, we have a local relationship between $h_{a,\infty}$ and T_r at one cross-sectional element in the air flow direction. Equation H.19 gives the relation between the local cross-sectional heat flow and the change in energy content of the air stream, that is,

$$\dot{m}_a dh_{a,\infty} = -h_d(h_{a,\infty} - h_{ft,m})dA_{ft} \qquad (H.19)$$

where $\dot{m}_a$ is the mass flow rate of air.

Equations H.18 and H.19 can be combined to give a differential equation in $T_{ft,m}$ which can then be integrated to solve for the value of $T_{ft,m}$ at x_o, the exit of the heat exchanger coil. With $T_{ft,m}(x_o)$ evaluated, Eq. H.17 can be used to evaluate $h_{a,\infty}(x_o)$. A sensible heat transfer equation from $T_{a,\infty}$ to $T_{ft,m}$ can also be written and used with Eq. H.17 and H.18 to solve for $T_{a,\infty}(x_o)$. The derivation of the solution for $T_{ft,m}(x_o)$ follows, after which the derivation of the solution for $T_{a,\infty}(x_o)$ is given.

H.6 Derivation of the Solution for the Exit Effective Surface Temperature, $T_{ft,m}(x_o)$

First, Eq. H.18 is written in differential form, i.e.,

$$dT_{ft,m} - dT_r = s(dh_{a,\infty} - dh_{ft,m}) \tag{H.20}$$

For a direct expansion coil, $dT_r = 0$, and Eq. H.20 becomes

$$dT_{ft,m} = s(dh_{a,\infty} - dh_{ft,m}) \tag{H.21}$$

Next, a relationship between $h_{ft,m}$ and $T_{ft,m}$ (between h and T on the saturation line of the psychrometric chart) is required. The conventional assumption is that

$$h_{ft,m} = a^* + b^* T_{ft,m} \tag{H.22}$$

However, since this relationship is only valid within a very small range of $T_{ft,m}$, a sequential solution has typically been recommended (see McElgin and Wiley [H.2] and Hiller and Glicksman [H.3]) where the coil calculations are broken into two sections in the air flow direction and the second section uses new values of "a" and "b" derived from the exit conditions of the first section. This sectionalization can be avoided if instead, $h_{ft,m}$ is related to $T_{ft,m}$ by a quadratic expression, i.e.,

$$h_{ft,m} = a + bT_{ft,m} + cT_{ft,m}^2 \tag{H.23}$$

Differentiation of Eq. H.23 yields

$$dh_{ft,m} = dT_{ft,m}(b + 2cT_{ft,m}) \tag{H.24}$$

Using Eq. H.24, Eq. H.21 becomes

$$dT_{ft,m} = s\,[dh_{a,\infty} - dT_{f,m}(b + 2cT_{ft,m})] \qquad (H.25)$$

Solving Eq. H.25 for $dh_{a,\infty}$ yields

$$dh_{a,\infty} = dT_{ft,m}\left(\frac{1}{s} + b + 2cT_{ft,m}\right) \qquad (H.26)$$

Equation H.19 is now solved for $dh_{a,\infty}$ and the term $[h_{a,\infty} - h_{ft,m}]$ is replaced by $[T_{ft,m} - T_r]/s$, i.e.,

$$dh_{a,\infty} = \frac{-h_d}{\dot{m}_a}\,\frac{(T_{ft,m} - T_r)\,dA_{ft}}{s} \qquad (H.27)$$

Equating Eqs. H.26 and H.27 yields

$$\left(\frac{1}{s} + b + 2cT_{ft,m}\right)dT_{ft,m} = \frac{-h_d}{\dot{m}_a}\,\frac{(T_{ft,m} - T_r)dA_{ft}}{s} \qquad (H.28)$$

Collecting like terms on each side of the equation yields

$$\frac{(u + vT_{ft,m})dT_{ft,m}}{T_{ft,m} - T_r} = \frac{-h_d}{\dot{m}_a}\,dA_{ft} \qquad (H.29)$$

where $u = 1 + bs$ and

$v = 2cs$.

Integration of Eq. H.29 from $T_{ft,m}(x_i)$ to $T_{ft,m}(x_o)$, where x_i and x_o are the beginning and end of the wet coil region in the air flow direction, yields

$$\left\{(u + vT_r)\,\ell n[T_{ft,m}(x) - T_r] + v(T_{ft,m}(x) - T_r)\right\}\Bigg|_{T_{ft,m}(x_i)}^{T_{ft,m}(x_o)} = \frac{-h_d A_{ft} F_{moist}}{\dot{m}_a} \qquad (H.30)$$

where F_{moist} is the fraction of the coil depth that is wetted. The value of $T_{ft,m}(x_i)$ is calculated from Eq. H.18 and F_{moist} is known from the calculation of the point at which dehumidification first occurs (described in Appendix I). Therefore, the only unknown in Eq. H.30 is $T_{ft,m}(x_o)$. Rearrangement of Eq. H.30 to collect all knowns on one side of the equation gives

$$(u + vT_r)\ \ell n[T_{ft,m}(x_o) - T_r] + v[T_{ft,m}(x_o) - T_r] =$$

$$(u + vT_r)\ \ell n[T_{ft,m}(x_i) - T_r] + v[T_{ft,m}(x_i) - T_r] - \frac{h_d A_{ft} F_{moist}}{\dot{m}_a} \qquad (H.31)$$

Since Eq. H.31 is a transcendental equation it must be solved iteratively for $T_{ft,m}(x_o)$.

Once $T_{ft,m}(x_o)$ has been evaluated, Eq. H.18 is used in conjunction with the psychrometric routines to calculate $h_{a,\infty}(x_o)$. With $h_{a,\infty}(x_o)$ evaluated, the total heat flow from the air to the refrigerant can be computed from

$$\dot{Q} = \dot{m}_a[T_{a,\infty}(0) - T_{a,\infty}(x_i)] + \dot{m}_a[h_{a,\infty}(x_i) - h_{a,\infty}(x_o)] \qquad (H.32)$$

where the first term on the right side of Eq. H.31 represents total heat transfer (sensible) in the dry coil section and the second term is the total heat transfer (sensible and latent) in the wet coil region.

However, the equations to this point do not provide for a separation of the sensible and latent heat transfer rates in the wet coil region and thus the exit air dry bulb temperature and humidity ratio are not known. An additional solution for either the air dry bulb temperature or humidity ratio at the exit of the coil is required to obtain this extra information. The solution used in the Heat Pump Model is in terms of the exit air dry bulb temperature and is derived in a manner consistent with, and dependent on, the preceding equations as follows.

H.7 Derivation of the Solution for the Exit Air Dry Bulb Temperature, $T_{a,\infty}(x_o)$

The sensible heat transfer from the air to the fin-and-tube surface at a cross-section in the air flow direction can be written as

$$d\dot{Q}_s = h_w \eta_{w,ft} (T_{a,\infty} - T_t) dA_{ft} \tag{H.33}$$

or, alternatively, using Eq. H.7, as

$$d\dot{Q}_s = h_w (T_{a,\infty} - T_{ft,m}) dA_{ft} \tag{H.34}$$

Equations H.33 and H.34 contain the assumption that the wet fin efficiency for sensible heat transfer is the same as that for total heat transfer. It has been shown by O'Brien and Turner [H.9] that the wet fin efficiency for sensible heat transfer is slightly lower than that for total heat transfer. Based on their results, Eqs. H.33 and H.34 will slightly overestimate the sensible heat transfer rate in proportion to the total heat transfer rate. However, this effect is ignored in McQuiston's analysis [H.5] and here as well to avoid the necessity of a numerical solution.

By equating the local sensible heat gain at the fin-and-tube surface to the change in sensible energy content of the air stream, i.e.,

$$\dot{m}_a c_p dT_{a,\infty} = -h_w (T_{a,\infty} - T_{ft,m}) dA_{ft} \tag{H.35}$$

the basic governing equation for the sensible transfer rate is obtained. When transforming Eq. H.35 into a integrable form, Eq. H.29 is used to eliminate the term "dA_{ft}" from Eq. H.35, i.e.,

$$\dot{m}_a c_p dT_{a,\infty} = -h_w (T_{a,\infty} - T_{ft,m}) \left[\frac{-\dot{m}_a (u + v T_{ft,m}) dT_{ft,m}}{h_d (T_{ft,m} - T_r)} \right] \tag{H.36}$$

Cancellation of terms yields

$$dT_{a,\infty} = \frac{(T_{a,\infty} - T_{ft,m})}{(T_{ft,m} - T_r)} \; (u + vT_{ft,m}) \; dT_{ft,m} \tag{H.37}$$

Since T_r is a constant, Eq. H.37 can be rewritten in terms of $(T - T_r)$'s to give

$$\frac{d(T_{a,\infty} - T_r)}{d(T_{ft,m} - T_r)} - \frac{(T_{a,\infty} - T_r)\,[u + v(T_{ft,m} - T_r) + vT_r]}{T_{ft,m} - T_r} =$$

$$-[u + v(T_{ft,m} - T_r) + vT_r] \tag{H.38}$$

Equation H.38 is of the form

$$\frac{dy}{dz} + yP(z) = Q(z) \tag{H.39}$$

where

z - $T_{ft,m} - T_r$

y - $T_{a,\infty} - T_r$

$P(z)$ - $-(u + vT_r + vz)/z$

$Q(z)$ - $-(u + vT_r + vz)$

The solution to Eq. H.39 can be written as:

$$ye^{\int P dz} = \int Qe^{\int P dz} dz + \text{constant} \tag{H.40}$$

Evaluating the innermost integral,

$$\int P dz = -\int \frac{(u + vT_r + vz)dz}{z} \quad \text{, and}$$

$$\int P dz = -[(u + vT_r)\ell n(z) + vz] \tag{H.41}$$

Then

$$e^{\int P dz} = z^{-(u + vT_r)} e^{vz} \tag{H.42}$$

Next, the outer integral becomes

$$\int Q e^{\int P dz} dz = -\int (u + vT_r + vz)\, z^{-(u + vT_r)}\, e^{-vz}\, dz \tag{H.43}$$

Let $w = u + vT_r$. Equation H.43 becomes

$$\int Q e^{\int P dz} dz = -\int (w + vz) z^{-w}\, e^{-vz}\, dz \tag{H.44}$$

An exponential series expansion is used to integrate Eq. H.44, i.e.,

$$e^{-vz} = 1 - vz + \frac{vz^2}{2!} - \frac{vz^3}{3!} + \frac{vz^4}{4!} + \ldots \tag{H.45}$$

Substitution of Eq. H.45 into Eq. H.44 yields an integrable form, with the result

$$\int Qe^{\int Pdz}\,dz = \left[\frac{wz^{(1-w)}}{1-w} + \frac{vz^{(2-w)}}{2-w} - v\left(\frac{wz^{(2-w)}}{2-w} + \frac{vz^{(3-w)}}{3-w}\right) + \frac{v^2}{2!}\left(\frac{wz^{(3-w)}}{3-w} + \frac{vz^{(4-w)}}{4-w}\right) - \frac{v^3}{3!}\left(\frac{wz^{(4-w)}}{4-w} + \frac{vz^{(5-w)}}{5-w}\right) + \ldots \right. \tag{H.46}$$

Equation H.46 can be written in summation form as

$$\int Qe \int Pdz_{dz} = -\sum_{i=1}^{n} \frac{-v^{(i-1)}}{(i-1)!}\left(\frac{wz^{(i-w)}}{i-w} + \frac{vz^{[(i+1)-w]}}{(i+1)-w}\right) \tag{H.47}$$

where "n" is the number of terms which gives acceptable convergence of the series expansion solution. Substituting Eq. H.47 and H.42 into Eq. H.40 gives

$$y(z^{-w}\, e^{-vz}) = -\sum_{i=1}^{n} \frac{-v^{(i-1)}}{(i-1)!}\left(\frac{wz^{(i-w)}}{i-w} + \frac{vz^{[(i+1)-w]}}{(i+1)-w}\right) + C \tag{H.48}$$

Equation H.48 can be written in shorthand form as

$$yF_1(z) = F_2(z) + C \tag{H.49}$$

The known conditions at the beginning of the dehumidification region are used to evaluate the constant C in Eq. H.49, i.e.,

$$C = y_i \, F_1(z_i) - F_2(z_i) \tag{H.50}$$

Use of Eq. H.50 in Eq. H.49 yields the solution for the exit conditions, i.e.,

$$y_o = \frac{1}{F_1(z_o)} \left[F_2(z_o) + y_i \, F_1(z_i) - F_2(z_i)\right] \tag{H.51}$$

Expanding z and y back to their original representations yields

$$T_{a,\infty}(x_o) - T_r = \frac{1}{F_1[T_{ft,m}(x_o) - T_r]} \left\{F_2[T_{ft,m}(x_o) - T_r] + [T_{a,}(x_i) - T_r] \, F_1(T_{ft,m}(x_i) - T_r) - F_2(T_{ft,m}(x_i) - T_r)\right\} \tag{H.52}$$

Once $T_{a,\infty}(x_o)$ has been evaluated from Eq. H.52, the humidity ratio of the exit air $W_{a,\infty}$ is calculated from the equation

$$W_{a,\infty}(x_o) = \left[h_{a,\infty}(x_o) - c_p T_{a,\infty}(x_o)\right] / \left[1061.2 + 0.444 * T_{a,\infty}(x_o)\right] \tag{H.53}$$

The sensible heat transfer rate $\dot{Q}_s$ and the rate of water condensation on the coil, $\dot{m}_w$, are obtained from Eqs. H.54 and H.55, using the computed values of $T_{a,\infty}(x_o)$ and $W_{a,\infty}(x_o)$:

$$\dot{Q}_s = \dot{m}_a \left[T_{a,\infty}(x_i) - T_{a,\infty}(x_o)\right] \tag{H.54}$$

and

$$\dot{m}_w = \dot{m}_a \left[W_{a,\infty}(x_i) - W_{a,\infty}(x_o)\right] \tag{H.55}$$

The calculations described in this appendix are performed in the heat pump model only for the region of the coil where the refrigerant is in a two-phase state. If a fraction of the coil contains superheated refrigerant vapor, the air flow rate $\dot{m}_a$ is multiplied by f_{tp}, the fraction of the coil in a two-phase state, for use in the calculation of the heat transfer rates and exit air conditions in the two-phase region.

References for Appendix H

H.1 W. Goodman, "Dehumidification of Air with Coils," *Refrigerating Engineering*, October, 1936, p. 225-274.

H.2 J. McElgin and D. C. Wiley, "Calculation of Coil Surface Areas for Air Cooling and Dehumidification," *Heating, Piping, and Air Conditioning*, March, 1940, pp. 195-201.

H.3 C. C. Hiller and L. R. Glicksman, *Improving Heat Pump Performance via Compressor Capacity Control – Analysis and Test*, Report No. 24525-96, Heat Transfer Laboratory, Massachusetts Institute of Technology (1976).

H.4 J. L. Threlkeld, *Thermal Environmental Engineering*, Prentice-Hall, Inc., Englewood Cliffs, New Jersey, 1970.

H.5 F. C. McQuiston, "Fin Efficiency with Combined Heat and Mass Transfer," *ASHRAE Transactions*, Vol. 81, Pt. 1, 1975.

H.6 F. C. McQuiston and J. D. Parker, *Heating, Ventilating, and Air Conditioning Analysis and Design*, Wiley, New York, 1977.

H.7 R. J. Myers, "The Effect of Dehumidification on the Air Side Heat Transfer Coefficient for a Finned Tube Coil," Master's Thesis, University of Minnesota, 1967.

H.8 A. H. Elmahdy and R. C. Biggs, "Performance Simulation of Multi-Row Dry (and/or Wet) Heat Exchangers", *Sixth International Heat Transfer Conference*, Toronto, Aug 7-11, 1978, pp. 327-332.

H.9 N. G. O'Brien and R. L. Turner, "Fin Thermal Efficiency During Simultaneous Heat and Mass Transfer," *AICHE Journal*, May 1965, pp. 546-548.

Appendix I — Description of the Dehumidification Algorithm

The calculational scheme used in the moisture removal section of the evaporator routine (as shown in Fig. 6.4 of the text) is described in this appendix. The solutions for $T_{ft,m}(x_o)$ and $T_{a,\infty}(x_o)$ (the mean fin-and-tube surface temperature and air dry bulb temperature, respectively, at the trailing edge of the evaporator) derived in Appendix H form the basis for the calculational procedure discussed here.

A flow diagram of the dehumidification algorithm is shown in Fig. I.1. The algorithm is used only if the air temperature, T_{aid}, at which dehumidification would occur at the fin-tube surface is greater than the exit air temperature $T_{a,\infty,sens}(x_o)$ from the two-phase region that is calculated assuming only sensible heat transfer. If this condition occurs, T_{aid} is then compared to the evaporator inlet air temperature, T_{aie}. If T_{aie} is greater than T_{aid}, moisture removal does not occur on the leading edge of the coil and the fraction of the coil depth which has only sensible heat transfer, F_{sens}, is computed from the equation

$$F_{sens} = \ell n \left[(T_{aie} - T_r)(T_{aid} - T_r)\right] / N_{tu,tp} \qquad (I.1)$$

Equation I.1 is obtained from the standard effectiveness equation for $C_{min}/C_{max} = 0$, i.e.,

$$\varepsilon_{tp} = 1 - e^{-N_{tu,tp}} \qquad (I.2)$$

by using

$$\varepsilon = \frac{T_{aie} - T_{aid}}{T_{aie} - T_r} \qquad (I.3)$$

ORNL-DWG 81-4746R

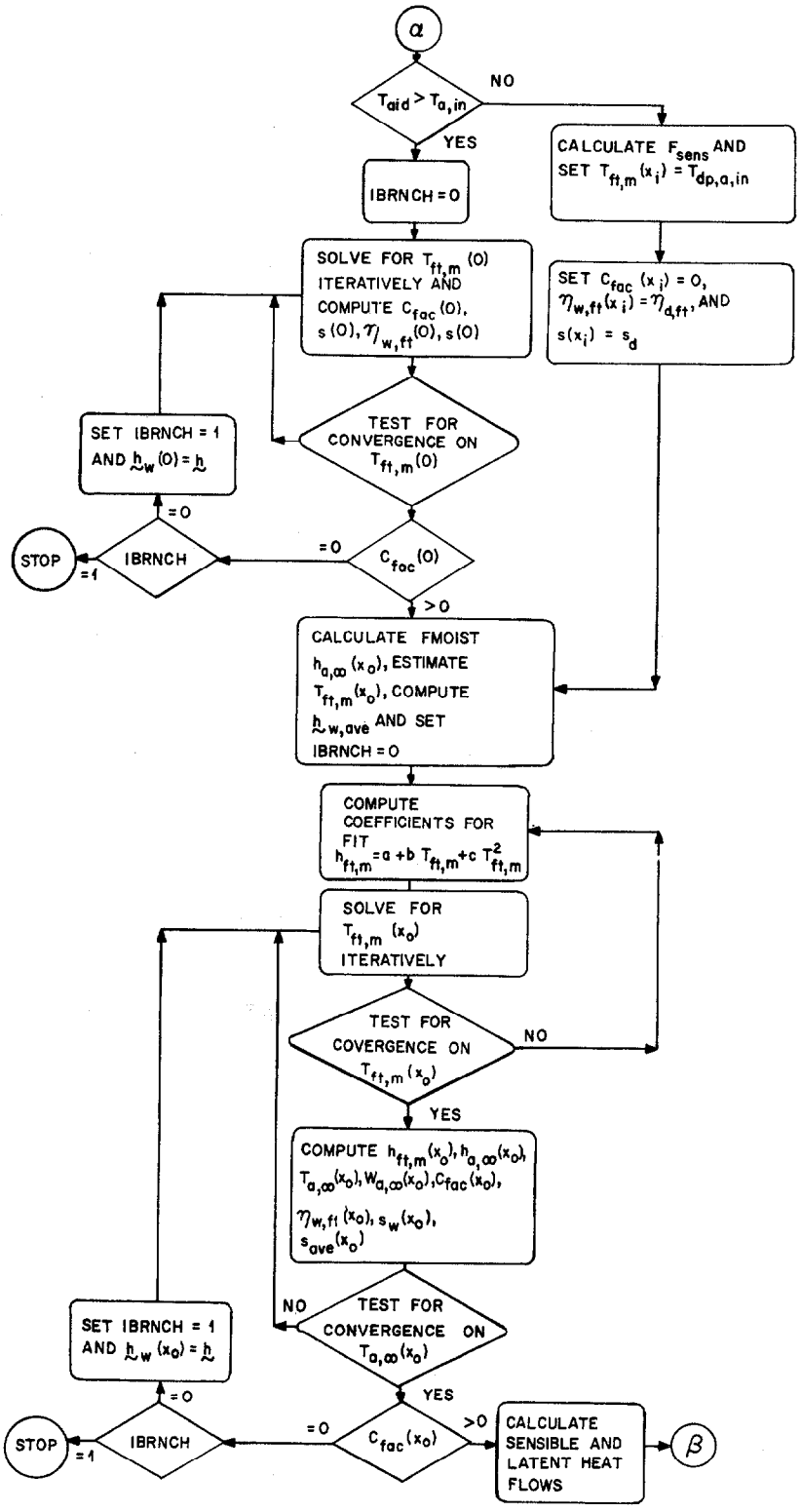

Fig. I.1 Block Diagram of the Dehumidification Algorithm

and replacing $N_{tu,tp}$ by $F_{sens}\, N_{tu,tp}$. The value of the effective surface temperature, $T_{ft,m}$, at the transition point from dry to wet coil, x_i, is equal to the dew point temperature of the entering air, i.e.,

$$T_{ft,m}(x_i) = T_{dp,a,in} \tag{I.4}$$

Values for $C_{fac}(x_i)$, $\eta_{w,ft}(x_i)$, and $s(x_i)$ are computed next. $C_{fac}(x)$ is defined by the equation [I.1]

$$C_{fac}(x) = \frac{W_{a,\infty}(x) - W_{ft,m}(x)}{T_{a,\infty}(x) - T_{ft,m}(x)} \quad . \tag{I.5}$$

It follows from Eq. I.4 that when the first part of the coil is dry, $W_{a,\infty}(x_i) = W_{ft,m}(x_i)$ and, from Eq. I.5, $C_{fac}(x_i) = 0.0$. It is not appropriate to use the wet heat transfer coefficient h_w at x_i since dehumidification is just beginning at this point. Were h_w used to replace h at x_i, the transition point would shift further into the coil because of an increase in the effective surface temperature due to the increase in the air-side heat transfer coefficient. A situation could occur where moisture removal was predicted when h was used, but not predicted when h_w was used. Thus, h is used at the transition point in place of h_w in the calculation of fin effectiveness $\eta_{w,ft}(x_i)$ and the coil characteristic $s(x_i)$. Note that since $C_{fac}(x_i) = 0$, it follows from Eq. H.5 that $h^*_w = h_w$. Therefore,

$$\eta_{w,ft}(x_i) = \eta_{d,ft}(x_i) \tag{I.6}$$

and

$$s(x_i) = s_d \tag{I.7}$$

at the transition point.

One feature of this procedure needs to be explained before proceeding to discuss the case where dehumidification occurs at the leading edge. In the derivation of the solutions for $T_{ft,m}(x_o)$ and $T_{a,\infty}(x_o)$ in Appendix H, the integrations over the coil depth, represented by the variable "x", were carried out assuming that the coil characteristic s (and from Eq. H.16, h_w, h^*_w, and $\eta_{w,ft}$) was constant. That assumption is handled by using average values of h_w, h^*_w, $\eta_{w,ft}$, and s over the region of integration. Local values of these parameters (at the entrance and exit of the moisture removal region) as denoted by f(0), $f(x_i)$, and $f(x_o)$ are used to obtain the average values and to calculate the local entrance and exit conditions more exactly.

Returning to Fig. I.1, when T_{aid} is greater than T_{aie}, dehumidification occurs on the leading edge of the coil. In this case, the temperature at the fin-tube surface $T_{ft,m}(0)$ is below the dew point temperature of the entering air. The value of $T_{ft,m}(0)$ must be found iteratively using the coil characteristic equation from Appendix H evaluated at leading edge conditions, i.e.,

$$\frac{T_{ft,m}(0) - T_r}{h_{a,\infty}(0) - h_{ft,m}(0)} = \frac{1 - \eta_{w,ft}(0)}{\eta_{w,ft}(0)\left[c_{p,m} + C_{fac}(0)\right]} + \frac{h_w(0)}{h_r c_{pm}} \frac{A_{ft}}{A_r} \qquad (I.8)$$

which simplified is

$$s(0) = s_w(0) \qquad (I.9)$$

For the first evaluation of $T_{ft,m}(0)$, s(0) is not known because $C_{fac}(0)$ and $h_{fg}(0)$ in Eq. I.8 are not known where $C_{fac}(0)$ is given by Eq. I.5 and $h_{fg}(0)$ is given by

$$h_{fg}(0) = 1061.2 + 0.444\, T_{ft,m}(0) + h_\ell(0) \qquad (I.10)$$

and

$$h_\ell(0) = \begin{cases} T_{ft,m} - 32, & \text{if } T_{ft,m} \geq 32 \\ 0, & \text{if } T_{ft,m} < 32 \end{cases} \qquad (I.11)$$

The initial evaluation of $T_{ft,m}(0)$ is made assuming

$$s(0) = s_d \tag{I.12}$$

Equation I.9 is then used with the psychrometric routines [to relate $h_{ft,m}(0)$ to $T_{ft,m}(0)$] to solve iteratively for $T_{ft,m}(0)$. Once an initial value for $T_{ft,m}(0)$ has been found, $C_{fac}(0)$, $h_{fg}(0)$, and $s(0)$ are calculated and a new value for $T_{ft,m}(0)$ is computed. This process is repeated until the difference in the value of $T_{ft,m}(0)$ from one iteration to the next is smaller than a prescribed tolerance.

The value of $C_{fac}(0)$ is then checked to see if it is positive, that is, to see if the humidity ratio difference from freestream to surface is positive. If $C_{fac}(0)$ is equal to zero, the switch from a dry coil heat transfer coefficient to a wet coil coefficient [in $s(0)$] has caused the surface temperature to rise above the dew point of the entering air. If such has occurred, the wet coefficient is replaced by the dry coefficient and the calculation of $T_{ft,m}(0)$ is repeated. If $C_{fac}(0)$ is not positive at the end of the second series of calculations, an error message is printed and the program execution is stopped.

Once $T_{ft,m}(0)$ has been evaluated at the leading edge of the coil or $T_{ft,m}(x_i)$ has been found at the transition point from dry to wet conditions, the fraction of the coil depth that is wetted, F_{moist}, and the enthalpy of the air at the transition point, $h_{a,\infty}(x_i)$, are evaluated. If dehumidification occurs at the leading edge, $F_{moist} = 1$ and $x_i = 0$.

The coefficients for the quadratic fit of $h_{ft,m}(x)$ as a function of $T_{ft,m}(x)$ (as assumed in Appendix H) can be estimated once the initial conditions at the start of the dehumidification region have been obtained. The coefficients are determined using $T_{ft,m}(x_i)$, an estimate of $T_{ft,m}(x_o)$ $[T_{ft,m}(x_i) - 5]$, and an equation relating $h_{ft,m}$ to $T_{ft,m}$ and $W_{ft,m}$, i.e.,

$$h_{ft,m}(x) = 0.24T_{ft,m}(x) + W_{ft,m}(x)\,[1061.2 + 0.444T_{ft,m}(x)] \tag{I.13}$$

The saturation curve on the standard ASHRAE psychrometric chart represents $W_{ft,m}$ as a function of $T_{ft,m}$. This curve is most closely approximated by a quadratic equation; however, we will assume that a linear equation derived from $T_{ft,m}(x_i)$ and $T_{ft,m}(x_o)$ will be adequate, i.e.,

$$W_{ft,m}(x) = a' + b'T_{ft,m}(x) \tag{I.14}$$

where

$$a' = W_{ft,m}(x_i) - b' T_{ft,m}(x_i) \tag{I.15}$$

and

$$b' = [W_{ft,m}(x_i) - W_{ft,m}(x_o)]/[T_{ft,m}(x_i) - T_{ft,m}(x_o)] \tag{I.16}$$

Substitution of Eq. I.14 into Eq. I.13 yields

$$h_{ft,m}(x) = a + b\, T_{ft,m}(x) + c\, T^2_{ft,m}(x) \tag{I.17}$$

where

$$a = 1061.2\ a' \tag{I.18}$$

$$b = 0.24 + 1061.2\ b' + 0.444\ a' \tag{I.19}$$

$$c = 0.444\ b' \tag{I.20}$$

Note that the assumption of

$$h_{ft,m}(x) = a^* + b^* T_{ft,m}(x) \tag{I.21}$$

made in simpler analyses implies that

$$W_{ft,m}(x) = a^* \tag{I.22}$$

Once estimates of the coefficients a, b, and c have been calculated, the transcendental solution for $T_{ft,m}(x_o)$ derived in Appendix H is evaluated iteratively until $T_{ft,m}(x_o)$ is obtained. This new value for $T_{ft,m}(x_o)$ is used to evaluate the coefficients a, b, and c more accurately, upon which the calculations are repeated until convergence on $T_{ft,m}(x_o)$ is achieved.

Once $T_{ft,m}(x_o)$ has been evaluated, the psychrometric routines are used to obtain $h_{ft,m}(x_o)$ and an estimate of $s(x_o)$ [s(0) or s_d] is used to obtain a value for $h_{a,\infty}(x_o)$ from a form of Eq. H.17, i.e.,

$$h_{a,\infty}(x_o) = [T_{ft,m}(x_o) - T_r]/s(x_o) + h_{ft,m}(x_o) \tag{I.23}$$

The exit air dry bulb temperature, $T_{a,\infty}(x_o)$ is computed next using the values of $T_{ft,m}(x_o)$, T_r, $s(x_o)$, b and c and the series solution derived in Appendix H. After $T_{a,\infty}(x_o)$ and $h_{a,\infty}(x_o)$ are evaluated, the humidity ratio of the exit air, $W_{a,\infty}$ can be calculated from a rearrangement of Eq. I.13, i.e.,

$$W_{a,\infty}(x_o) = [h_{a,\infty}(x_o) - c_{pa}\, T_{a,\infty}(x_o)]/[1061.2 + 0.444\, T_{a,\infty}(x_o)] \tag{I.24}$$

Values can be calculated for $C_{fac}(x_o)$, $h_{ft}(x_o)$, $\eta_{w,ft}(x_o)$, and $s(x_o)$ using the computed exit surface and air conditions. Arithmetic averages are then computed for h_w and h_w^* from which $\eta_{w,ft,ave}$ and s_{ave} are obtained. The new estimates of s_{ave} and $s(x_o)$ are used to calculate new exit conditions from the coil. This iteration continues until convergence is obtained on $T_{a,\infty}(x_o)$.

The value of $C_{fac}(x_o)$ is checked for a positive value following the iteration on $T_{a,\infty}(x_o)$. If $C_{fac}(x_o)$ is equal to zero, the value of

$h_w(x_o)$ is set equal to h and the iterations repeated starting at the solution of $T_{ft,m}(x_o)$. Such a situation might occur if dehumidification begins near the trailing edge of the coil where the discrete jump from h to $h_w(x_o)$ could cause the wet region to revert to a dry surface.

Upon completion of the calculation of the exit air conditions, the sensible and latent heat transfer rates and the water removal rate in the two-phase region of the evaporator are computed as described in Appendix H.

References for Appendix I

I.1 F. C. McQuiston, "Fin Efficiency with Combined Heat and Mass Transfer," *ASHRAE Transactions*, Vol. 81, Pt. 1, 1975.

Appendix J — Ratios of Geometric Parameters Used in the Heat Exchanger Calculations

The correlations for pressure drops and heat transfer coefficients make use of ratios of air- and refrigerant-side geometric parameters. The need for and use of these terms is discussed elsewhere and is not repeated here. This section is devoted to deriving how these parameters are calculated; in many instances the equations used are not altogether straightforward, and they were obtained by various degrees of algebraic manipulations and cancellation of terms. The input data required for each heat exchanger:

- A - cross-sectional area,
- N_T - number of tubes in the direction of air-flow (horizontally),
- $N_{circuit}$ - number of equivalent, parallel refrigerant circuits,
- S_T - vertical distance between tubes (center-to-center),
- W_T - horizontal distance between tubes (center-to-center),
- D_a - outer, or air-side, diameter of tubes,
- D_r - inner, or refrigerant-side, diameter of tubes,
- F_p - fin pitch, and
- δ - fin thickness,

are sufficient to describe the evaporator and condenser completely. However, there are some basic geometric parameters that are not required as input nor explicitly calculated: (see Fig. J.1)

- h - height of the heat exchanger
- ℓ - length of the heat exchanger
- d - depth of the heat exchanger
- N_v - number of tubes in a row (vertically)

These remaining basic parameters are not computed because all of the geometry-related ratios can be computed by careful use of the given

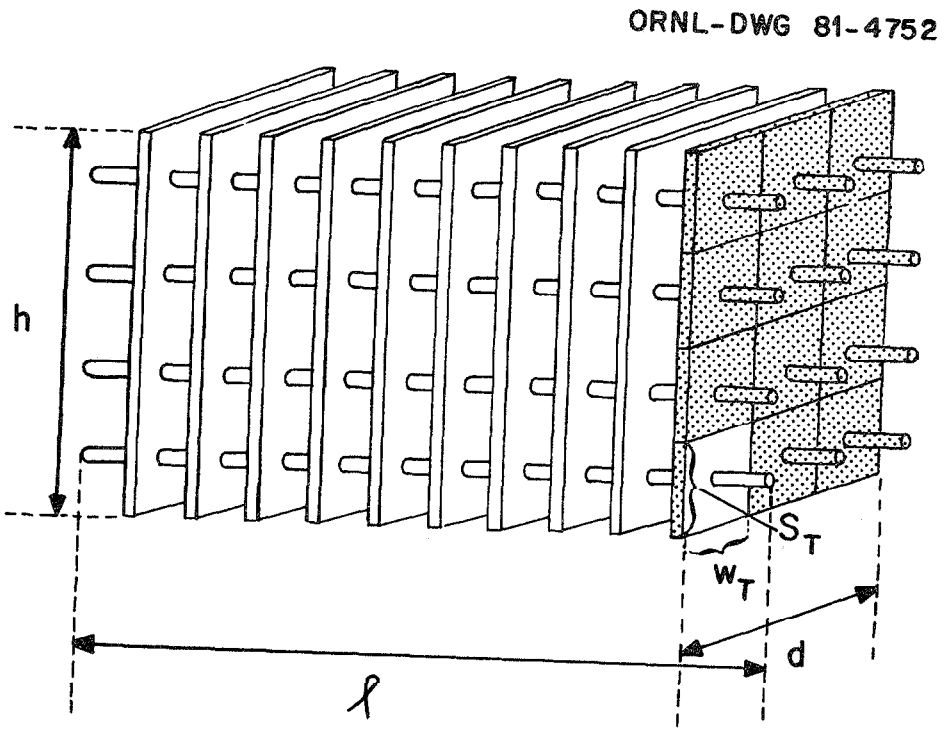

Fig. J.1 Sample Tube-and-Fin Heat Exchanger

input parameters. The following equations are used to compute the geometric ratios used in the Design Model.

N_f = number of fins

$$N_f = \ell \, F_p \tag{J.1}$$

N_{tot} = total number of refrigerant tubes

$$N_{tot} = N_v N_T \tag{J.2}$$

$$d = N_T W_T \tag{J.3}$$

$$h = N_v \, S_T \tag{J.4}$$

$$\ell = \frac{A}{h} = \frac{A}{N_v S_T} \tag{J.5}$$

V_{hx} = volume of heat exchanger

$$V_{hx} = \ell h d = \ell(N_v S_T)(N_T W_T) = N_{tot} \ell S_T W_T \tag{J.6}$$

A_{side} = the area of each side of each fin is

$$A_{side} = hd - \frac{N_{tot} \pi D_a^2}{4} = N_{tot} S_T W_T - N_{tot} \frac{\pi D_a^2}{4}$$

A_f = fin heat transfer area,

$$A_f = 2N_f A_{side} = 2\ell F_p N_{tot} \left[S_T W_T - \frac{\pi D_a^2}{4} \right] \tag{J.7}$$

$A_{contact}$ = contact area between fins and tubes

$$A_{contact} = N_f N_{tot} \pi D_a \delta = \ell F_p N_{tot} \pi D_a \delta \qquad (J.8)$$

A_a = total air-side heat transfer area

$$A_a = A_f + A_{tubes}$$

A_{tubes} = area of *exposed* tube surfaces

$$A_{tubes} = N_{tot} \pi D_a \ell_{exposed} ,$$

where $\ell_{exposed}$ is the length of each tube *not* covered by fins, which can be written using Eq. J.1:

$$\ell_{exposed} = \ell - N_f \delta = \ell(1 - F_p \delta) \qquad (J.9)$$

$$A_a = 2N_{tot} \ell F_p (S_T W_T - \frac{\pi D_a^2}{4}) + N_{tot} D \pi_a \ell (1 - F_p \delta) \qquad (J.10)$$

A_r = refrigerant-side heat transfer area

$$A_r = N_{tot} \ell \pi D_r \qquad (J.11)$$

$A_{free-flow}$ = free-flow frontal area

$$A_{free-flow} = A - A^*_{tubes} - A^*_f$$

where A^*_{tubes} = "projected" area of tubes obstructing air flow

$$A^*_{tubes} = N_v D_a \ell_{exposed}$$

and using Eq. J.9

$$A^*_{tubes} = N_v D_a \ell(1 - F_p\delta)$$

A^*_f = total cross-sectional area of the fins obstructing air-flow

$$A^*_f = N_f h\delta = \ell F_p \delta(N_v S_T)$$

$$\begin{aligned} A_{free\text{-}flow} &= \ell(N_v S_T) - N_v D_a \ell(1 - F_p\delta) - \ell(N_v S_T)F_p\delta \\ &= \ell N_v[S_T - D_a(1 - F_p\delta) - S_T F_p\delta] \\ &= \ell N_v(S_T - D_a)(1 - F_p\delta) \end{aligned} \qquad (J.12)$$

The ratios that are needed by the heat pump model are:

$$C_f = \frac{\text{fin heat transfer area}}{\text{contact area}} = \frac{A_f}{A_{contact}}$$

Substituting Eqs. J.1, J.7, and J.8

$$C_f = \frac{2\ell F_p N_{tot}(S_T W_T - \frac{\pi D_a^2}{4})}{\ell F_p N_{tot} \pi D_a \delta} = \frac{2(S_T W_T - \frac{\pi D_a^2}{4})}{\pi D_a \delta} \qquad (J.13)$$

$$\alpha_a = \frac{\text{total air-side area}}{\text{volume of heat exchanger}} = \frac{A_a}{V_{hx}}$$

Substituting Eq. J.6 and J.10:

$$\alpha_a = \frac{2N_{tot}\ell F_p(S_T W_T - \frac{\pi D_a^2}{4}) + N_{tot}\pi D_a \ell(1 - F_p\delta)}{N_{tot}\ell S_T W_T} =$$

$$\frac{2F_p(S_T W_T - \frac{\pi D_a^2}{4}) + \pi D_a(1 - F_p\delta)}{S_T W_T} \qquad (J.14)$$

$$\alpha_r = \frac{\text{refrigerant-side heat transfer area}}{\text{volume of heat exchanger}}$$

Substituting Eq. J.6 and J.11:

$$\alpha_r = \frac{N_{tot}\ell\pi D_r}{N_{tot}\ell S_T W_T} = \frac{\pi D_r}{S_T W_T} \qquad (J.15)$$

$$F_a = \frac{\text{fin heat transfer area}}{\text{total air-side heat transfer area}}$$

Substituting J.7 and J.10:

$$F_a = \frac{2\ell F_p N_{tot}(S_T W_T - \frac{\pi D_a^2}{4})}{2\ell N_{tot} F_p(S_T W_T - \frac{\pi D_a^2}{4}) + N_{tot}\ell\pi D_a(1 - F_p\delta)} \qquad (J.16)$$

$$\sigma_a = \frac{\text{free-flow frontal area}}{\text{frontal area}}$$

Substituting Eq. J.4 and J.12:

$$\sigma_a = \frac{A_{\text{free-flow}}}{A} \tag{J.17}$$

$$\sigma_a = \frac{\ell N_v (S_T - D_a)(1 - F_p \delta)}{\ell (N_v S_T)} = \frac{(S_T - D_a)(1 - F_p \delta)}{S_T} \tag{J.18}$$

$$A_{rh} = \frac{\text{refrigerant-side heat transfer area}}{\text{number of parallel circuits}}$$

Substituting Eq. J.11 and then Eqs. J.2 and J.5:

$$A_{rh} = \frac{A_r}{N_{\text{circuits}}} = \frac{N_{\text{tot}} \pi D_r \ell}{N_{\text{circuits}}} \tag{J.19}$$

$$= \frac{(N_v N_T) \frac{A}{N_v S_T} \pi D_r}{N_{\text{circuits}}} = \frac{N_T A \pi D_r}{S_T N_{\text{circuits}}} \tag{J.20}$$

$$A_o = \frac{\text{refrigerant-side heat transfer area}}{\text{mass flow rate of air}}$$

$$A_o = \frac{A_r}{\dot{m}_a} = \frac{A_r}{G_a A_{\text{free-flow}}} \tag{J.21}$$

Substituting Eqs. J.2, J.5, J.11, and J.17 into J.21:

$$A_o = \frac{(N_v N_T)(\frac{A}{N_v S_T}) \pi D_r}{G_a A \sigma_a}$$

$$= \frac{N_T \pi D_r}{G_a \sigma_a S_T}$$

$$A_{min} = \frac{\text{total air-side heat transfer area}}{\text{total free-flow frontal area}}$$

$$A_{min} = \frac{A_a}{A_{free\text{-}flow}} \qquad (J.22)$$

Note that

$$A_a = \left(\frac{\alpha_a}{\alpha_r}\right)A_r = \left(\frac{\alpha_a}{\alpha_r}\right)(A_{rh}N_{circuits})$$

and then substituting Eq. J. 17 into J.22:

$$A_{min} = \frac{\alpha_a A_{rh} N_{circuits}}{\alpha_r A \sigma_a}$$

APPENDIX K: AVAILABILITY AND DISTRIBUTION OF THE HEAT PUMP MODEL

The ORNL Heat Pump Model is available to organizations performing heat pump research development. It is customarily distributed in the form of six files on a nine track magnetic tape which consist of:

(1) FORTRAN source of the model set up for batch processing on a computer,

(2) sample input data for the Heat Pump Model,

(3) FORTRAN source of a program to fit a fuction of condensing and evaporating temperatures to compressor map data (this program can be used to generate the coefficients required to use the map-based compressor model described in Section 4.3),

(4) sample input data for the map fitting program in file 3,

(5) FORTRAN source for subroutines that can be used to convert the batch processing version of the Heat Pump Model in file 1 to an interactive program (some of these subroutines are in addition to those in file 1 and others are used to replace subroutines in file 1 that have the same name), and

(6) FORTRAN source for an interactive program that can be used to set up a file of input data for the batch version of the Heat Pump Model.

These files are listed in Appendices L-Q (with cross-references of the FORTRAN source files).

The tapes are written on an IBM computer and:

- can be at 800, 1600, or 6250 BPI,
- can be in ASCII or EBCDIC, and
- can have either labeled or non-labeled files.

After a tape is written it is rewound and the copies of the Heat Pump Model (file 1) and the compressor map fitting program (file 3) that are on the tape are executed using the appropriate data (files 2 and 4). The printed listing of the job that generated the tape and the output from these two computer runs are enclosed when the tape is returned.

People who wish to use the interactive programs need to be aware that they contain system and installation dependent features. The logical units used for input and output can vary from one computer system to another and some of the I/O related subroutines will be different. It is not difficult to identify these differences and it is left to each recipient of the programs to do this for himself.

The interactive input for the programs in files 5 and 6 is organized into seven pages of data. Each page contains related information (e.g., compressor data, parameters for the indoor heat exchanger) and is designed to fit on the screen of a CRT terminal. Examples of these pages are shown in Table K.1. Each data entry on a page is assigned an item number and a default value. Data is changed by first specifying which page it is on and then giving the item number and new value. Once the user has made changes and is satisfied with the results he can:

- save the data for use with the batch version of the model,
- save the data so that it can be read by the interactive model to override or replace the default data values, and/or
- execute the Heat Pump Model and get output listed on the computer terminal.

The user needs to be aware that when he selects from two or more alternatives (e.g., map-based or loss-and-efficiency compressor model, type of flow control device) the last one chosen is what will be used.

The programs that are distributed with the Heat Pump Model are provided as a convenience to the users of the model. They are not formally documented although there should be sufficient comments in them to be understandable.

Table K.1 Sample Pages of Input Data for Interactive Version of Heat Pump Model

```
PAGE #1:  COMPRESSOR DATA (EFFICIENCY & LOSS MODEL)
GEOMETRY:                                    LOSSES:
 1. DISPLACEMENT (CU IN)          4.520      8. HEAT REJECTION RATE FROM
 2. CLEARANCE VOLUME RATIO         .060         COMPRESSOR SHELL (BTU/HR)      0.0
MOTOR:                                                 OR
 3. SPEED (RPM)                   3450.      9. FRACTION OF COMPRESSOR POWER
 4. OUTPUT AT FULL LOAD (KW)      2.149         REJECTED FROM THE SHELL         .350
EFFICIENCIES:
 5. MAXIMUM MOTOR                  .820     10. HEAT TRANSFER RATE FROM HIGH
 6. ISENTROPIC                     .700         SIDE TO LOW SIDE (BTU/HR)    300.0
 7. MECHANICAL                     .800                 OR
                                            11. FRACTION OF COMPRESSOR POWER
                                                TRANSFERED FROM HIGH SIDE
                                                TO LOW SIDE                     .000
NOTES:
  1. ITEM 8 OR 9 IS SPECIFIED, NOT BOTH
  2. ITEM 10 OR 11 IS SPECIFIED, NOT BOTH
  3. IF ITEM 4 IS SET TO 0, THE NECESSARY OUTPUT AT FULL LOAD WILL BE
     CALCULATED AND ITEM 3 IS THE ACTUAL MOTOR SPEED
  4. IF ITEM 4 IS NOT 0, ITEM 3 IS THE SYNCHRONOUS MOTOR SPEED AND THE
     ACTUAL SPEED IS CALCULATED
TYPE "RETURN" TO CONTINUE
```

```
PAGE #2:  COMPRESSOR DATA (MAP-BASED MODEL)
GEOMETRY:                                    LOSSES:
  1. DISPLACEMENT (CU IN)         4.520      6. HEAT REJECTION RATE FROM
  2. BASE DISPLACEMENT FOR                      COMPRESSOR SHELL (BTU/HR)      0.0
     THE MAP (CU IN)              4.520                 OR
MOTOR:                                       7. FRACTION OF COMPRESSOR POWER
  3. RATED SPEED (RPM)            3450.         REJECTED FROM SHELL            .350
SUPERHEAT AT SHELL INLET:
  4. BASE SUPERHEAT FOR MAP (F)  20.00
CURVE FITS FROM COMPRESSOR MAP (AS FUNCTIONS OF CONDENSING & EVAPORATING
                                TEMPERATURES):
  5. POWER CONSUMPTION                       8. REFRIGERANT MASS FLOW RATE
     CONDENSING **2          -1.509E-04         CONDENSING **2          -2.675E-02
     CONDENSING               4.089E-02         CONDENSING               4.633E+00
     EVAPORATING **2         -1.338E-04         EVAPORATING **2          4.703E-02
     EVAPORATING              5.860E-04         EVAPORATING              9.640E+00
     CONDENSING*EVAPORATING   3.638E-04         CONDENSING*EVAPORATING  -1.868E-02
     CONSTANT                 9.759E-05         CONSTANT                 1.207E-04
NOTE:
  1. ITEM 6 OR 7 IS SPECIFIED, NOT BOTH
TYPE "RETURN" TO CONTINUE
```

PAGE #3: INDOOR HEAT EXCHANGER

GEOMETRY:	
1. FRONTAL AREA (SQ FT)	3.167
2. NUMBER OF PARALLEL CIRCUITS	3.0
3. NUMBER OF TUBE ROWS	3.0
4. NUMBER OF RETURN BENDS	72.0
FAN - FAN MOTOR:	
5. COMBINED EFFICIENCY	.200
INLET AIR:	
6. FLOW RATE (CFM)	1200.0
7. TEMPERATURE (F)	70.0
8. RELATIVE HUMIDITY	.500
FINS:	
9. TYPE (1 SMOOTH, 2 WAVY, OR 3 LOUVERED)	2.
10. PITCH (FINS/INCH)	14.0
11. THICKNESS (IN)	.00636
12. THERMAL CONDUCTIVITY (BTU/HR-FT-F)	128.0
13. CONTACT CONDUCTANCE (BTU/HR-FT2-F)	30000.
TUBES:	
14. O.D. (IN)	.400
15. I.D. (IN)	.336
16. VERTICAL SPACING (IN)	1.000
17. HORIZONTAL SPACING (IN)	0.875

TYPE "RETURN" TO CONTINUE

PAGE #4: OUTDOOR HEAT EXCHANGER

GEOMETRY:	
1. FRONTAL AREA (SQ FT)	5.040
2. NUMBER OF PARALLEL CIRCUITS	4.0
3. NUMBER OF TUBE ROWS	3.0
4. NUMBER OF RETURN BENDS	64.0
FAN - FAN MOTOR:	
5. COMBINED EFFICIENCY	.160
INLET AIR:	
6. FLOW RATE (CFM)	2300.0
7. TEMPERATURE (F)	47.0
8. RELATIVE HUMIDITY	.700
FINS:	
9. TYPE (1 SMOOTH, 2 WAVY, OR 3 LOUVERED)	2.
10. PITCH (FINS/INCH)	14.0
11. THICKNESS (IN)	.00636
12. THERMAL CONDUCTIVITY (BTU/HR-FT-F)	128.0
13. CONTACT CONDUCTANCE (BTU/HR-FT2-F)	30000.
TUBES:	
14. O.D. (IN)	.400
15. I.D. (IN)	.336
16. VERTICAL SPACING (IN)	1.000
17. HORIZONTAL SPACING (IN)	0.875

NOTES:

1. IF ITEM #5 IS SET TO 0, THE FAN VS STATIC EFFICIENCY CURVE IS USED WITH A 55% EFFICIENT MOTOR

TYPE "RETURN" TO CONTINUE

Table K.1 (continued)

```
PAGE #5:  FLOW CONTROL DEVICE
FIXED CONDENSOR SUBCOOLING IS BEING USED

SPECIFIED CONDENSER SUBCOOLING:
  1. DESIRED SUBCOOLING (F)        45.00
          OR
CAPILLARY TUBES:
  2. NUMBER OF CAPILLARY TUBES         0
  3. CAPILLARY TUBE FLOW
     FACTOR                        0.000
          OR
SHORT-TUBE ORIFICE:
  4. DIAMETER OF ORIFICE (IN)    .00000
          OR

THERMOSTATIC EXPANSION VALVE:
  5. VALVE CAPACITY RATING (TONS)   .000
  6. STATIC SUPERHEAT (F)           0.0
  7. RATED OPERATING
     SUPERHEAT (F)                  0.0
  8. BLEED FACTOR                   .000
  9. NOZZLE & TUBE PRESSURE
     DROP (1 INCLUDE, 0 EXCLUDE)       0

NOTES:
  1. CATEGORIES ARE MUTUALLY EXCLUSIVE, I.E. SPECIFY 1, OR 2 & 3, OR 4,
     OR 5 - 9
  2. IF CONDENSER SUBCOOLING IS SPECIFIED, THE VALUES OF ITEMS 2-9 THAT
     WOULD PRODUCE THAT LEVEL OF SUBCOOLING ARE COMPUTED
TYPE "RETURN" TO CONTINUE
```

PAGE #6: CONNECTING REFRIGERANT LINES

GEOMETRY:	FROM:	TO:	ID (IN)	EQUIVALENT LENGTH (FT)
LIQUID LINE	INDOOR HX	OUTDOOR HX	1. 0.190	2. 30.4
SUCTION LINE	REVERSING VALVE	COMPRESSOR INLET	3. 0.000	4. 0.0
DISCHARGE LINE	COMPRESSOR OUTLET	REVERSING VALVE	5. 0.000	6. 0.0
VAPOR LINE	REVERSING VALVE	OUTDOOR HX	7. 0.680	8. 6.0
VAPOR LINE	REVERSING VALVE	INDOOR HX	9. 0.556	10. 30.4

RATES OF HIGH SIDE HEAT LOSSES:
11. FROM DISCHARGE LINE (BTU/HR) 2000.
12. FROM LIQUID LINE (BTU/HR) 200.

RATES OF LOW SIDE HEAT GAINS:
13. IN SUCTION LINE (BTU/HR) 300.

NOTE:
1. GAIN & LOSSES IN ITEMS 11-13 CAN BE FOR VALIDATION RUNS OR TO SIMULATE HIGH TO LOW SIDE HEAT EXCHANGERS AND REVERSING VALVES

TYPE "RETURN" TO CONTINUE

PAGE #7: MISC. DATA

1. TITLE:
2. HOUSE LOAD AT OUTDOOR AMBIENT (BTU/HR) 15000.
3. EVAPORATOR SUPERHEAT (F) 10.0
4. DUCT SIZE (IN) 8.0
5. MODE OF OPERATION (1 COOLING, 2 HEATING) 2
6. LEVEL OF OUTPUT (0 SUMMARY, 1 COMPRESSOR, 2 COILS, 3 STANDARD) 1

EFFECTS OF HEAT LOSSES ON INLET AIR:
7. INDOOR FAN (SEE NOTE BELOW) 2
8. OUTDOOR FAN (SEE NOTE BELOW) 1
9. COMPRESSOR (SEE NOTE BELOW) 1

ESTIMATES TO BEGIN ITERATIONS:
10. EVAPORATING TEMPERATURE (F) 30.0
11. CONDENSING TEMPERATURE (F) 115.0
12. REFRIGERANT MASS FLOW RATE (LBM/HR) 400.0

NOTE:
1. HEAT LOSSES FROM THE FANS AND COMPRESSOR CAN BE ADDED TO THE AIRSTREAM EITHER BEFORE OR AFTER IT CROSSES THE COIL (SIMULATE BLOW-THROUGH & DRAW-THROUGH FANS)
SPECIFY 0 TO NEGLECT THE HEAT LOSS
1 TO ADD THE HEAT TO THE AIR BEFORE IT CROSSES THE COIL
2 TO ADD THE HEAT TO THE AIR AFTER IT CROSSES THE COIL

TYPE "RETURN" TO CONTINUE

Appendices L, M, N, O, P, and Q are on microfiche in an envelope attached to the back cover.